ENVIRONMENTAL ENGINEERING
ASSOCIATION OF THAILAND

THAI ENVIRONMENTAL ENGINEERING JOURNAL

Vol. 39 No. 1 January – April 2025
ISSN (PRINT) : 1686 - 2961
ISSN (ONLINE) : 2673 - 0359

Thai Environmental Engineering Journal

Owner
Environmental Engineering Association of Thailand

Enquiries 122/4 Soi Rawadee, Rama IV Rd., Phayathai, Phayathai, Bangkok 10400

ENVIRONMENTAL ENGINEERING
ASSOCIATION OF THAILAND

Thai Environmental Engineering Journal

Vol. 39 No. 1 January – April 2025

ISSN (PRINT) : 1686 - 2961
ISSN (ONLINE) : 2673 - 0359

Thai Environmental Engineering Journal Vol. 39 No. 1 (2025) : 1-11
www.eeat.or.th

Life Cycle Assessment of Plant-Based Milk Incorporating Functional Ingredients

Panusorn Hunsub[1], Kamonthip Nilmat[2], Nut Thephuttee[1], Pitchaya Pothinuch[1], Tarit Apisittiwong[1] and Nattapong Prichapan[1*]

[1]Faculty of Food Technology, College of Agricultural Innovation and Food Technology, Rangsit University, Pathum thani 12000, Thailand
[2]Institute of Biotechnology and Genetic Engineering, Chulalongkorn University, Bangkok 10330, Thailand
[*]E-mail : nattapong.p@rsu.ac.th

Article History; *Received: 30 June 2024, Accepted: 27 January 2025, Published: 30 April 2025*

Abstract

As a sustainable source, the plant-based product has gained popularity in the food industry over the last decade. This study adopted a life cycle assessment (LCA) to evaluate the environmental impacts and identify critical points of plant-based milk incorporating functional ingredients, addressing the existing gap in understanding their incorporation from an environmental perspective. The cradle-to-gate analysis encompassed raw material acquisition, including the agricultural stage, functional ingredient procurement, processing-stage resource consumption (emission, water, steam, and electricity), and waste treatment in manufacturing. Six investigated scenarios were formed by combining three types of plant-based milk (soybean, rice, and pea) with two sources of additional alternative protein (pea protein concentrate and insect powder), mangosteen peel extract as antioxidant, and fructo-oligosaccharide (FOS) as dietary fiber, defining 1 L of milk without packaging as a functional unit (FU). The modeling was conducted using Simapro software 9.0, and the assessment was implemented via the IMPACT 2002+ method. The results showed that pea milk had a lower environmental impact in 8 out of 15 categories, followed by rice and soybean milk in 3 and 4 out of 15 categories. The fortification of plant-based milk with FOS should not be utilized in formulation due to the potential for problem shifting and the occurrence of significant adverse environmental impacts. The major hotspot comes from energy consumption in processing and freeze-drying. The adoption of insect powder exhibited a lower impact than pea protein concentrates in carcinogens, non-carcinogens, aquatic ecotoxicity, terrestrial ecotoxicity, land occupation, aquatic eutrophication, and mineral extraction. The results also indicated that producing functional ingredients, especially FOS, generated a substantial environmental impact. Improvement solutions are also discussed. A large amount of generated biowaste from plant-based milk production could be promising feed to insects due to their residue nutritional value. Therefore, the credits of biowaste for the avoided animal feed mitigated the environmental impact. The incorporation of functional ingredients for nutritional fortification in plant-based milk could be assessed through a comprehensive life cycle assessment to prevent problem shifting.

Keywords : plant-based milk; life cycle assessment; pea protein concentrate; insect powder; mangosteen peel extract

Introduction

The plant-based product and alternative sources of protein play crucial roles in the rapidly expanding global market, as consumers increasingly opt for plant-based alternatives over dairy milk. Mainly, health-conscious consumers prioritize environmental awareness, nutrition, and ethical considerations. Furthermore, there is a growing environmental consciousness and responsibility, aiming to reduce environmental impacts such as eutrophication, ecotoxicity, fossil fuel depletion, and carcinogenicity compared to dairy milk [1]. The market for dairy alternatives is experiencing rapid growth within the plant-based food sector, gaining traction worldwide. It is anticipated to increase by over 439.43 billion THB between 2018 and 2023 [2]. Aligned with sustainable development goals (SDGs), this trend fosters encouragement within the food sector [3].

Plant-based milk originates from diverse sources, including cereals, legumes, nuts, oilseeds, pseudo-cereals, and others [4]. The rise and expansion of plant-based milk can be attributed to several factors, including milk protein allergies, lactose intolerance, and dietary preferences such as veganism and vegetarianism. Generally, plant-based milk exhibits lower protein quality and available calcium, but higher glycemic index values compared to bovine milk. However, it contains various health-beneficial components such as dietary fiber, essential fatty acids, vitamin E, and antioxidants that are lacking in bovine milk [5, 6]. Despite offering certain health benefits and mitigating allergy risks associated with cow's milk protein and lactose intolerance, plant-based milk often lacks essential micronutrients in adequate quantities. Therefore, the nutritional fortification of plant-based milk alternatives presents an effective solution.

The poor nutritional value of plant-based milk, particularly its low protein content, is a significant concern. Therefore, fortification with protein concentrates and isolates could effectively address this issue. However, in terms of nutrition, rice, and pea milk present disadvantages due to its lower protein content compared to soybean milk. The FOS are non-digestible carbohydrates that could be used as a low-calorie alternative sweetener or sugar substitute. It could also improve the texture of food products. For health benefits, FOS exhibits prebiotic activity, boosts immunity, improves mineral absorption, and reduces the absorption of triacylglycerols and cholesterol [7]. The mangosteen peel extract could be utilized to fortify antioxidant and anti-inflammatory properties. Previous studies have demonstrated that it contains xanthones, anthocyanins, tannins, phenolic acids, flavonoids, and other polyphenolic compounds, particularly α-mangostin, at approximately 69% [8]. Furthermore, nutrients in mangosteen peel extract exhibit antibacterial, anti-aging, anti-hyperpigmentation, anti-obesity, antidiabetic, and antitumor activities [9]. Pea is one of the most popular sources of vegetable proteins due to its accessibility, superior returns, and cost-effective manufacturing. Additionally, pea protein is generally considered a non-food allergen with notably high nutritional content and no genetic modification, presenting a clean label for food manufacture. Moreover, pea protein is rich in lysine, which is deficient in cereals [10]. Therefore, rice milk fortified with pea protein could complement the protein quality and balance this deficiency. Finally, cricket powder was used in this research owing to its high protein content, phenolic content, antioxidant, and anti-inflammatory activities. Additionally, cricket protein also exhibits high gastrointestinal digestibility. Moreover, cricket powder is safe, and its production is environmentally sustainable [11]. Therefore, cricket powder is one of the most popular alternative animal protein sources.

The LCA methodology, in accordance with ISO 14040/44 standards, is widely used to evaluate environmental performance and to identify and compare different scenarios for the design of optimally sustainable systems. It consists of the purpose and scope definition, the life cycle inventory, the life cycle impact assessment, and the life cycle interpretation. Furthermore, the term 'cradle-to-gate' encompasses the stages of agricultural production and raw material extraction, transportation to manufacturing facilities, and product processing, including cleaning, grinding, extraction, filtration, pasteurization, and fortification along with energy consumption, emissions, and waste treatment and management [2].

The environmental impacts of milk production have contributed significantly to global warming potential, accounting for 48-65% due to methane emissions, and to acidification potential, accounting for 78-97% due to ammonia volatilization. While transitioning to organic milk production may reduce pesticide use, it is associated with increased land requirements [12]. On another aspect, oat milk demonstrated an 80% reduction in greenhouse gas emissions compared to traditional cow's milk. Additionally, oat milk exhibited significantly lower water consumption compared to almond milk [13]. A comparative LCA of dairy milk and plant-based milk, based on 1 liter of milk, revealed the following impacts: dairy milk exhibited eutrophication potential of more than 0.005 kg N, ecotoxicity of more than 100 comparative toxic units (CTUe), approximately 3 MJ surplus of fossil fuel depletion, 10 liters of water intake, and nearly 40 MJ of cumulative energy demand. In contrast, soy milk showed eutrophication potential of less than 0.0001 kg N, ecotoxicity of less than 10 CTUe, approximately 1.7 MJ surplus of fossil fuel depletion, nearly 10 liters of water intake, and more than 40 MJ of cumulative energy demand. Overall, dairy milk demonstrated the highest impacts on ozone depletion, eutrophication, smog, ecotoxicity, fossil fuel depletion, and carcinogenic potential [1]. In addition, the environmental advantages of plant-based milk, including almond, oat, soy, pea, and coconut milk over dairy milk are evident, with lower levels of global warming potential, land use, eutrophication, ozone depletion, ecotoxicity, and fossil fuel depletion [14]. Notably, as reported by Winans et al. [2], the global warming potentials (GWPs) of dairy milk ranged from 1.80 to 1.97 kg CO_2 equivalent per 48 oz. of milk, which exceeded those of almond, pea, soy, coconut, and oat milk, ranging from 0.39 to 0.58, 0.44, 0.24 to 1.21, 0.58, and 0.54, respectively. Therefore, transitioning to plant-based milk could represent the most effective strategy for reducing greenhouse gas emissions. However, the environmental benefits of incorporating plant-based milk regarding human health, ecosystem quality, global warming, and resource conservation remain uncertain. Further analysis and interpretation of product development are necessary to clarify these aspects and eco-design new products to minimize environmental impact.

Despite the considerable research on plant-based milk, there remains a lack of understanding regarding incorporating functional ingredients from an environmental perspective. Therefore, this study aimed to conduct a comparative assessment of plant-based milk fortified with different functional ingredients using the life cycle assessment (LCA) methodology, focusing on environmental impacts to facilitate further improvements.

Methodology

Production of plant-based milk

For functional ingredients, the insect powder (100% house cricket, *Acheta domesticus* L., containing 70% protein, 10% fat, 2.6% carbohydrate, 3.57-5.10% ash) was supplied by Protanica Co., LTD., Thailand, whereas mangosteen peel (*Garcinia mangostana* L.) powder was purchased from Healthy Hills Farm Co., LTD., Thailand. Pea protein (80% protein, 6.9% fat, 5.6% carbohydrate, 4.4% dietary fiber) and FOS (90% dietary fiber) were purchased from Krungthepchemi, Thailand.

Plant-based milks were prepared using the following methods: dry soybeans or rice were soaked separately in water for 6 hours, drained, and washed. Subsequently, soybeans, rice, or peas were blended with water at a ratio of 1:7 using a blender for 5 minutes, followed by filtration through a straining cloth. The plant-based milks were then boiled at 90°C for 10 minutes. Next, 5% pea protein concentrate, or cricket powder, was added to the plant-based milk, followed by 5% FOS. The resulting plant-based milk was homogenized using the IKA T25 ULTRA-TURRAX® homogenizer for 5 minutes. Afterward, the plant-based milks were boiled at 72°C for 10 minutes. Additionally, 0.5% mangosteen peel extract obtained through hot water extraction was added to the plant-based milk. Finally, the plant-based milks were cooled down for approximately 30 ± 5 minutes in an ice-water bath and stored at 4°C.

Life cycle assessment

The LCA study was conducted following ISO 14040/44. The goal of this study is to investigate and compare the environmental impacts associated with each plant-based milk production incorporating functional ingredients from cradle-to-gate. The system encompasses the life cycle stages, including the agricultural production of raw materials (soybean, rice, and pea), the production of pea protein concentrate, insect powder, FOS, and mangosteen peel extract as functional ingredients, transportation to the processing facility, and the manufacturing of plant-based milk. This includes processes such as raw material utilization, water consumption, energy use, emissions, and waste treatment. For waste management, seed residue waste was treated as biowaste, and wastewater from the production chain was subjected to wastewater treatment. The analysis was conducted within a cradle-to-gate system boundary, as illustrated in Figure 1. The boundary excludes milk packaging, transportation to retail stores, consumer use, end-of-life disposal, facility construction, capital equipment, and infrastructure from the life cycle. The functional unit (FU) is defined as 1 L in (a) soybean milk, (b) rice milk, and (c) pea with functional ingredients in various scenarios associated with the production. The fortification comprised FOS as a prebiotic, an antioxidant agent, and an alternative protein. Data were collected from experimental data, used in the Ecoinvent 3.5 database by using the cut-off system model, Agri-footprint 4.0 database, and compiled from existing literature presented in Table 1. Inventory data for each scenario is shown in Table 2.

The modeling was conducted using the LCA SimaPro 9.0 software, employing the IMPACT 2002+ methodology. It included the following four damage categories: human health, ecosystem quality, climate change, and resource depletion. Midpoint categories consisted of carcinogens (CG), non-carcinogens (NCG), respiratory inorganics (RI), ionizing radiation (IR), ozone layer depletion (OLD), respiratory organics (RO), aquatic ecotoxicity (AEC), terrestrial ecotoxicity (TE), terrestrial acid/nutrition (TA), land occupation (LO), aquatic acidification (AA), aquatic eutrophication (AE), global warming (GWP), non-renewable energy (NRE), and mineral extraction (ME) that all aligned with the comprehensive impact of the food industry. The drying data of mangosteen peels was obtained from García et al. [8], and Rodríguez-Meizoso et al. [16]. The LCI of FOS was obtained from Gerbino et al. [15]. Briefly, the production used yacon potato with autohydrolysis without allocation. The 100% Cricket powder (*Acheta Domesticus*) was harvested from 1,176.5 tons/ 10,000 m^3 of farmland. The Life cycle inventory data of 1 L of each plant-based milk production is shown in Table 2.

Results and Discussion

Life cycle assessment

For interpretation, the process comprises seven steps: soaking, extraction (using a disintegrator), separation (via a filter press), formulation, nutrient fortification, homogenization, and heat treatment, which are discussed in detail below for each stage. The environmental impact of the materials, as assessed by the IMPACT 2002+ method, is depicted in Figure 2.

In agricultural production, when comparing the same amount of rice, soybeans, and peas, it was found that peas exhibited the lowest contribution to 7 out of the 15 midpoint impacts, including CG, RI, IR, OLD, RO, LO, AE, and GWP. For endpoints, peas showed the lowest impact on human health and climate change, while soybeans exhibited the lowest impact on resource depletion. The environmental impact of 1 kg of pea seed includes; (1) human health: 66.2% of the impact is attributed to pea production processes such as combined harvesting, application of phosphate fertilizer (P_2O_5), and harrowing tillage, with an additional 11.6% attributed to transport via sea transoceanic ship, (2) ecosystem quality: this is influenced by activities related to pea seed for sowing, application of plant production via field sprayer, and combined harvesting, (3) climate change: 67.9% of the impact arises from pea production activities, including combined harvesting, application of phosphate fertilizer, and pea seed for sowing, with an additional 10.4% attributed to freight transportation, (4) resource: 59.4% of the impact is due to pea production processes and freight transportation. On the other hand, the environmental impact of 1 kg of soybeans includes; (1) human health: arising from land use change in annual crops due to land tenure

and diesel burned in building machine processing, (2) ecosystem quality: influenced by activities related to seed for sowing, application of plant production via field sprayer, and combined harvesting, (3) climate change: stemming from land use change in annual crops due to land tenure, (4) resources: resulting from combined harvesting and freight transportation. In contrast, the environmental impact of 1 kg of rice is primarily attributed to irrigation processing and drying of the grain. This stage typically requires high quantities of water and electricity consumption.

In terms of functional ingredients are depicted in Figure 3, focusing on sustainable sources. FOS, as a prebiotic, resulted in climate change from freeze-drying and extracting processes [15]. The freezing of the supernatant for storage emerged as the primary hotspot, making the highest contribution to 10 out of the 15 midpoint impacts, followed by substrate extraction, which contributed to 4 out of the 15 midpoint impacts, along with RO in the purification stage due to freeze-dried in water solution. Moreover, antioxidant extract was extracted and analyzed for LCA, as described in [8]. Using agricultural waste as a raw material would not contribute to environmental burdens in the cultivation stage and previous stage. Therefore, more attention should be paid to leaves and peels [16]. The result in Figure 3 (b) shows that electricity for drying mangosteen peels could be the main environmental impact.

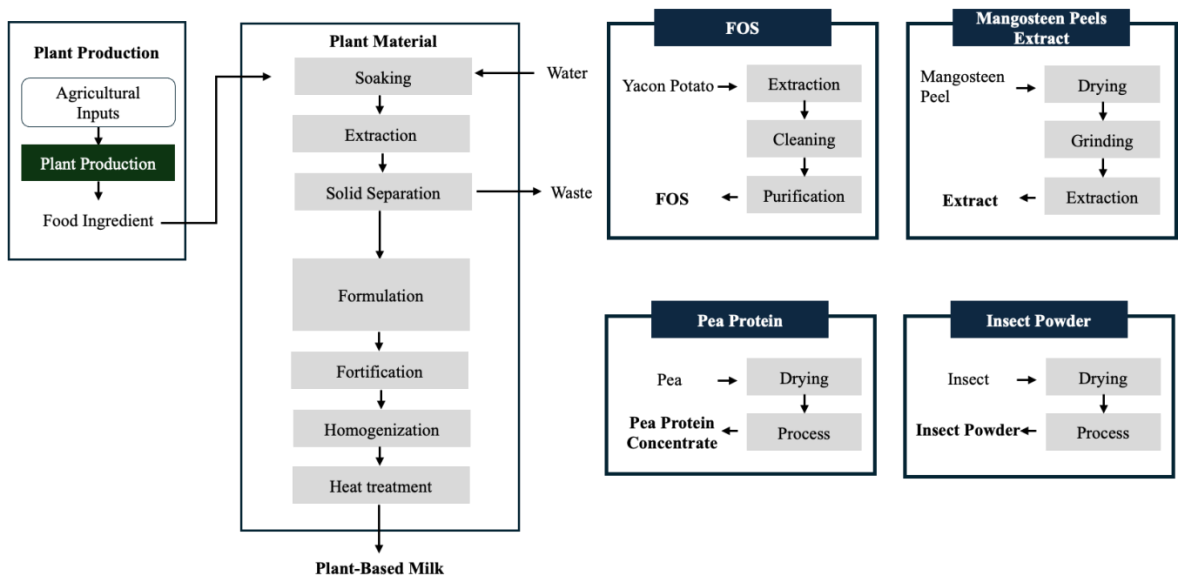

Figure 1 System Boundary

Table 1 Functional ingredients used for fortification

Name	Specification	Reference
1. FOS	Prebiotics, fiber, and alternative sweeteners	[15]
2. Mangosteen peel extract	Antioxidant and anti-inflammatory activities	[8, 16]
3. Protein		
a) Pea protein concentrate	75% protein, 5% fat, and 3% carbohydrate	Agri-footprint
b) Insect powder	70% protein, 10% fat, <10% carbohydrate, 0.3% Cholesterol, and 0.4% Sodium	[17]

Table 2 Life cycle inventory of 1 L of plant-based milk production

		Soybean milk (S1)		Rice milk (S2)		Pea milk (S3)	
Inputs	**Unit**	**Pea protein concentrate (S1.1)**	**Insect powder (S1.2)**	**Pea protein concentrate (S2.1)**	**Insect powder (S2.2)**	**Pea protein concentrate (S3.1)**	**Insect powder (S3.2)**
- Seeds	g	336.28	340.14	342.17	339.07	186.22	181.87
- Tap Water	L	2.35	2.38	2.40	2.37	1.30	1.27
- Electricity	kWh	0.0583	0.0583	0.0583	0.0583	0.0583	0.0583
- Steam [a]	kg	0.30	0.30	0.30	0.30	0.30	0.30
- FOS	g	67.3	68.0	59.88	59.34	50.55	49.36
- Pea protein concentrate	g	67.3	-	59.88	-	50.55	-
- Insect powder	g	-	68.0	-	59.34	-	49.36
- Extract	g	6.7	6.8	5.99	5.93	5.05	4.94
Outputs							
- Product	L	1.00	1.00	1.00	1.00	1.00	1.00
- Solid waste (Biowaste) [b]	g	768.64	777.45	1075.40	1065.66	292.63	285.79
- Wastewater [c]	cm^3	955.47	967.66	975.79	963.60	528.56	516.36

Note: (a) data from Ecoinvent database, (b) Biowaste {RoW}| market for | Cut-off, U, and (c) Wastewater, average {RoW}| market for wastewater, average | Cut-off, U

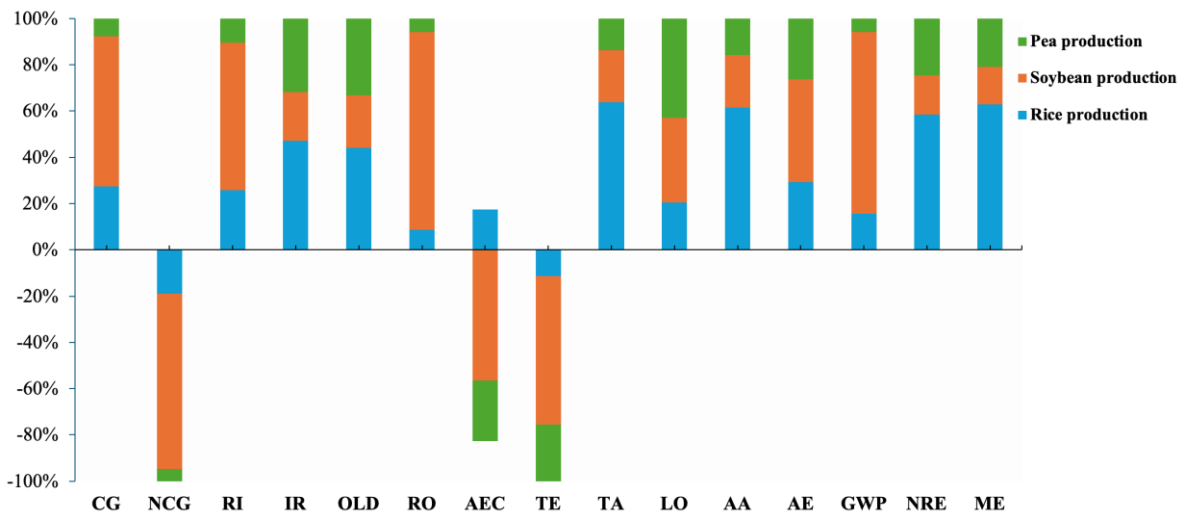

Figure 2 Environmental Impact of Materials

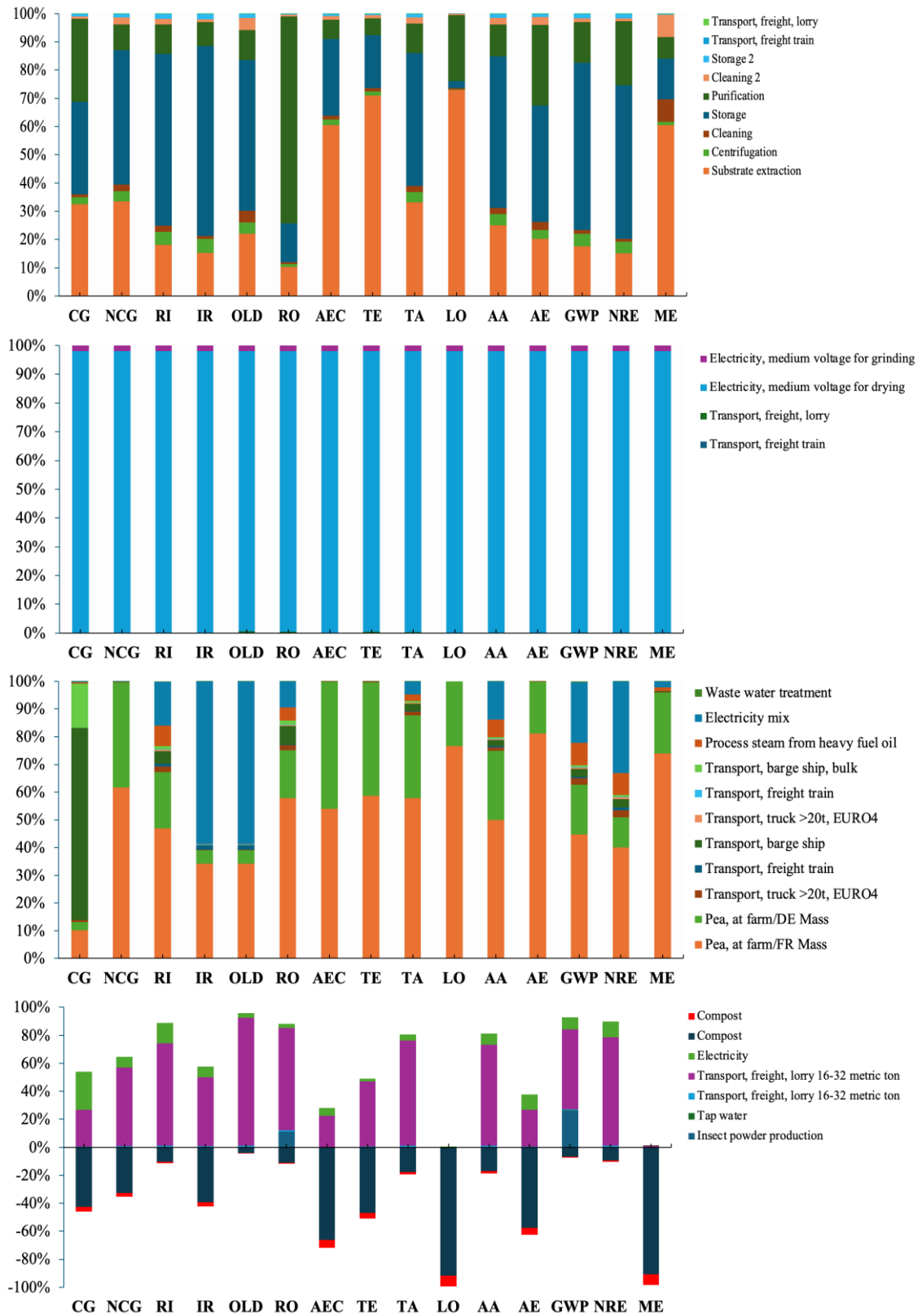

Figure 3 Environmental Impact of Functional Ingredients of (a) FOS, (b) Mangosteen Peel Extract, (c) Pea Protein Concentrate, and (d) Insect Powder

There are two scenarios for alternative protein fortification, which are being compared regarding their environmental impact. First, pea protein concentrate primarily originates from pea production at the farm, contributing to 12 out of 15 midpoint impacts. The exceptions include carcinogens in barge ship transportation, ionizing radiation, and ozone layer depletion in electricity production. In the second alternative, insect powder provides lower because it avoids biowaste treatment. In Thailand, approximately 7,500 metric tons of crickets are produced annually from 20,000 farms [17]. The environmental impact of insect powder was lower than pea protein concentrates in CG, NCG, AEC, TE, LO, AE, and ME. However, pea protein concentrates exhibit differences in RO, IR, OLD, RO, TA, AA, GWP, and NRE. Therefore, selecting alternative proteins could be considered in detail before utilization. The result corresponds to Heusala et al. [18], which shows that legume protein concentrate was lower by 50% compared to animal protein sources per kg protein.

During the process, steam and medium-voltage electricity are utilized in the chemical industry. Additionally, the process generates a substantial amount of biowaste and wastewater. The environmental impact affects human health and ecosystem quality due to production, while global warming and resource depletion primarily stem from chemical industry streams. It also generated biowaste from this product of 2.47 g and wastewater of 4.978 L. The use of FOS led to an environmental impact. Global warming increased from 0.46 to 12.78 kg CO_2 equivalent, and aquatic ecotoxicity increased from 77.72 to 3286.46 kg TEG water in scenario S1.1. The overall environmental impact results followed the same pattern across all scenarios, showing an increase of over 95%. Therefore, adding FOS in plant-based milk should not added to the formula in terms of environmental impact. For the overall life cycle assessment of each plant-based milk formula, the environmental impact of plant-based milk fortified with different functional ingredients was analyzed and shown in Figure 4. The result showed that pea milk fortified with insect power had the lowest environmental impact with the lowest environmental impact in 8 out of 15 categories. On the contrary, soybean milk fortified with insect power had the highest environmental impact with the highest environmental impact in 8 out of 15 categories.

Daily milk contributes significantly to global greenhouse gas due to methane emissions produced by approximately 2.4-3.6 kg of CO_2 equivalents per liter, water use for growing feed crops, land use for feed crops, and eutrophication from fertilizers and manure. In plant-based milk generally has a lower environmental impact (cradle to gate without electricity at retail and transportation from factory to retail) in terms of eutrophication, ecotoxicity, fossil fuel depletion, and cumulative energy demand compared to dairy milk. However, plant farming can contribute to deforestation, it still requires energy and water, particularly during processing and pasteurization [1]. In this finding, fortified plant-based milk may have slightly higher emissions than unfortified versions due to processing and ingredient sourcing. Plant-based milk is fortified with different functional ingredients to enhance the nutritional profile of plant-based milk but slightly increases its environmental impact. The production and transportation of nutrients require energy and resources, increasing the overall carbon footprint. For instance, calcium fortification has been shown to contribute approximately 10-15% more emissions to the total environmental footprint [19].

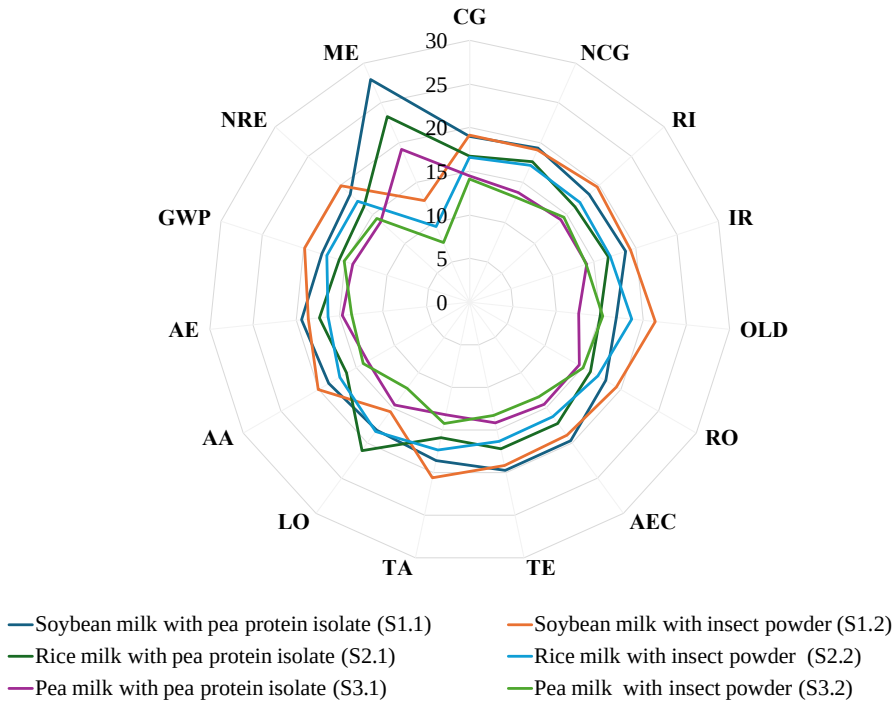

Figure 4 Environmental Impact of Plant-Based Milk

Analysis for further improvement

This work only focused on the volume of milk production as a FU. However, the comprehensive nutritional value of calories, kilogram protein, or essential amino acids should be accounted for in the allocation of environmental assessments. Extending the system boundaries to a cradle-to-grave analysis provides a more accurate and comprehensive assessment, leading to better decision-making, clearer environmental policies, and more sustainable product offerings. To mitigate environmental impact, insect powder, serving as an alternative protein, could utilize biowaste generated from plant-based production. Utilizing waste treatment to produce animal feed for insect cultivation presents a promising strategy with potential benefits. Investigating alternative processes and sources for producing prebiotics via green extraction methods could be further considered. Besides, implementing a transition to solar energy for electricity could effectively mitigate environmental impact. Further improvement could be implemented to align with sustainable practices within the food industry. To improve the reliability and relevance of LCA studies, it is crucial to consider these factors and apply sensitivity analysis to understand the robustness of the results.

Conclusions

The findings reveal that fortifying plant-based milk with functional ingredients to enhance the nutritional profile increases its environmental impact due to additional processing and sourcing of ingredients. It could be assessed in a comprehensive life cycle assessment to prevent problem shifting associated with adopting renewable sources, sustainable ingredient sourcing, and efficient production methods. Agricultural products are the primary contributors, followed by steam, water consumption, and biowaste treatment. Moreover, fortification enriches the product in terms of dietary fiber, antioxidant compounds, and protein content which is often deficient in plant-based products. The addition of pea protein concentrates and insect protein for fortification had been suggested for formulation. However, the use of FOS had not been recommended due to its significant environmental impact. In the context of sourcing and processing, apprehensions endure

concerning the adoption of novel sustainable origins and eco-friendly technologies, which could be substantially alleviated through effective waste management strategies, encompassing the retrieval of valuable ingredients from waste materials. Perspectives from life cycle assessment have been identified for improvement. The nutritional fortification with processed ingredients should be reviewed to ensure consistency and alignment with life cycle assessment principles.

Acknowledgements

This research received the funding support from Rangsit Research Institute, Rangsit University, Thailand. The authors express their gratitude to the Food Processing Pilot Plant, and the Faculty of Food Technology, the College of Agricultural Innovation and Food Technology, Rangsit University, for equipment support. The authors also thank the Center of Excellence on Hazardous Substance Management, Chulalongkorn University, for their software support.

References

[1] Grant, C.A. and Hicks, A.L. 2018. Comparative Life Cycle Assessment of Milk and Plant-Based Alternatives. Environmental Engineering Science. 35 (11): 1235-1247.

[2] Winans, K.S., Macadam-Somer, I., Kendall, A., Geyer, R. and Marvinney, E. 2020. Life Cycle Assessment of California Unsweetened Almond Milk. The International Journal of Life Cycle Assessment. 25: 577-587.

[3] Zhou, H., Zheng, B., Zhang, Z., Zhang, R., He, L. and McClements, D.J. 2021. Fortification of Plant-Based Milk with Calcium May Reduce Vitamin D Bioaccessibility: An *In Vitro* Digestion Study. Journal of Agricultural and Food Chemistry. 69(14): 4223-4233.

[4] Reyes-Jurado, F., Soto-Reyes, N., Dávila-Rodríguez, M., Lorenzo-Leal, A.C., Jiménez-Munguía, M.T., Mani-López, E., and López-Malo, A. 2023. Plant-Based Milk Alternatives: Types, Processes, Benefits, and Characteristics. Food Reviews International. 39(4): 2320-2351.

[5] Chalupa-Krebzdak, S., Long, C.J. and Bohrer, B.M. 2018. Nutrient Density and Nutritional Value of Milk and Plant-Based Milk Alternatives. International Dairy Journal. 87: 84-92.

[6] Vanga, S.K. and Raghavan, V. 2018. How Well Do Plant Based Alternatives Fare Nutritionally Compared to Cow's Milk?. Journal of Food Science and Technology. 55(1): 10-20.

[7] Rahim, M.A., Saeed, F., Khalid, W., Hussain, M. and Anjum, F.M. 2021. Functional and Nutraceutical Properties of Fructooligosaccharides Derivatives: A Review. International Journal of Food Properties. 24(1): 1588-1602.

[8] García, M.L., Carrión, M.H., Escobar, S., Rodríguez, A. and Cortina, J.R. 2021. Optimization of The Antioxidant Capacity of Mangosteen Peels (*Garcinia mangostana* L.) Extracts: Management of The Drying Extraction Processes. Food Science and Technology International. 27(5): 404-412.

[9] Rizaldy, D., Hartati, R., Nadhifa, T. and Fidrianny, I. 2022. Chemical Compounds and Pharmacological Activities of Mangosteen (*Garcinia mangostana* L.) - Updated Review. Biointerface Research in Applied Chemistry. 12(2): 2503-2516.

[10] Ge, J., Sun, C., Corke, H., Gul, K., Gan, R. and Fang Y. 2020. The Health Benefits, Functional Properties, Modifications, and Applications of Pea (*Pisum sativum* L.) Protein: Current Status, Challenges, and Perspectives. Comprehensive Reviews in Food Science and Food Safety. 19: 1835-1876.

[11] Quinteros, M.F., Martínez, J., Barrionuevo, A., Rojas, M. and Carrillo, W. 2022. Functional, Antioxidant, and Anti-Inflammatory Properties of Cricket Protein Concentrate (*Gryllus assimilis*). Biology. 11(5): 776.

[12] De Boer, I.J. 2003. Environmental Impact Assessment of Conventional and Organic Milk Production. Livestock Production Science. 80(1-2): 69-77.

[13] Riofrio, A. and Baykara, H. 2022. Techno-Environmental and Life Cycle Assessment of 'Oat-Milk'Production in Ecuador: A Cradle-to-Retail Life Cycle Assessment. International Journal of Food Science and Technology. 57(8): 4879-4886.

[14] Khanpit, V., Viswanathan, S. and Hinrichsen, O. 2024. Environmental Impact of Animal Milk Vs Plant-Based Milks: Critical Review. Journal of Cleaner Production. 449: 141703.

[15] Gerbino, E., Quentier, C. and Pénicaud, C. 2022. Dataset on The Life Cycle Assessment of Fructo-and Galacto-Oligosaccharides (FOS and GOS) Produced by Synthesis or Hydrolysis. Data in Brief. 43: 108478.

[16] Rodríguez-Meizoso, I., Castro-Puyana, M., Börjesson, P., Mendiola, J.A., Turner, C. and Ibáñez, E. 2012. Life Cycle Assessment of Green Pilot-Scale Extraction Processes to Obtain Potent Antioxidants from Rosemary Leaves. The Journal of Supercritical Fluids. 72: 205-212.

[17] Nikkhah, A., Van Haute, S., Jovanovic, V., Jung, H., Dewulf, J., Cirkovic Velickovic, T. and Ghnimi, S. 2021. Life Cycle Assessment of Edible Insects (*Protaetia brevitarsis seulensis* larvae) as A Future Protein and Fat Source. Scientific Reports. 11(1): 14030.

[18] Heusala, H., Sinkko, T., Sözer, N., Hytönen, E., Mogensen, L. and Knudsen, M.T. 2020. Carbon Footprint and Land Use of Oat and Faba Bean Protein Concentrates Using A Life Cycle Assessment Approach. Journal of Cleaner Production. 242: 118376.

[19] Heller, M.C., Keoleian, G.A. and Willett, W.C. 2013. Toward A Life Cycle-Based, Diet-Level Framework for Food Environmental Impact and Nutritional Quality Assessment: A Critical Review. Environmental Science and Technology. 47(22): 12632-12647.

Thai Environmental Engineering Journal Vol. 39 No. 1 (2025) : 13-25
www.eeat.or.th

Impact of Polyethylene Microplastic, Electrical Conductivity and *E. coli* of Composts on Seed Germination

Suchanya Wongrod[1,3], Thidarat Bunsri[2*] and Soydoa Vinitnantharat[1,3]

[1]Environmental Technology Program, School of Energy, Environment and Materials, King Mongkut's University of Technology Thonburi, Bangkok 10140, Thailand
[2]BioSmart Materials and Technology Research Group, Faculty of Science, King Mongkut's University of Technology Thonburi, Bangkok 10140, Thailand
[3]Environmental and Energy Management for Community and Circular Economy (EEC&C) Research Group, King Mongkut's University of Technology Thonburi, Bangkok 10140, Thailand
[*]E-mail : thidarat.bun@kmutt.ac.th

Article History; *Received: 13 September 2024, Accepted: 6 March 2025, Published: 30 April 2025*

Abstract

This study evaluated the influence of polyethylene (PE) microplastic, electrical conductivity (EC), and the presence of *E.coli* in different composts on the seed germination of mung bean seeds. Four types of composts were examined: T1 and T2, originating from dining food waste and kitchen waste, respectively; T3, a vermicompost produced by earthworms; and T4, a chemical organic fertiliser derived from human hair. The composts were prepared and diluted with deionised water, and PE microplastic particles were added at various concentrations. Mung bean seeds were soaked in these solutions for 8 hours, then placed on tissue paper in closed containers and kept moist by spraying with the solutions every 2 days. Germination tests were conducted over five days, and the germination index (GI), relative seed germination (RSG), and relative radicle growth (RRG) were calculated. EC and pH of the solutions were measured, and *E.coli* presence was assessed using the US EPA method 1603. PE microplastics at concentrations below 0.8% w/w stimulated seed germination, with the highest GI observed at these levels, suggesting low concentrations may not be as harmful as previously thought. High EC levels significantly inhibited seed germination, with the chemical organic fertiliser (T4) exhibiting the highest EC values and severe phytotoxicity even at high dilutions, highlighting the need to manage salt content in composts. Only the food waste compost (T1) contained *E. coli*, likely due to post-contamination, but *E.coli* did not significantly inhibit germination after dilution and filtration, indicating proper treatment can mitigate microbiological risks. The combined effects of microplastics and EC on germination were complex, underscoring the need for balanced management of both factors. These findings provide insights into the interactions between microplastics, EC, and *E.coli* in composts, informing better compost management practices and contributing to sustainable agricultural productivity.

Keywords : food waste compost; germination test; microplastics; mung bean seed; phytotoxicity

Introduction

Regarding the post-modernization era, approximately 190 million tonnes of plastic packaging was produced in Asia. Only 26% of plastic packaging was recycled, but the rest was entered either in landfills or the environment [1, 2]. Plastic wastes undergo fragmentation into particles of different sizes; microplastic (from 1 µm to < 5 mm) and nanoplastic (< 0.1 µm) [1]. Microplastics can remain in the soil for hundreds of years [3] and also have been contaminated in agro-ecosystem [4]. The accumulation of microplastics in soil has indeed reached significant levels, with studies indicating that the average accumulation in agricultural soils during long-term repeated application of compost could be up to 3.30 million particles per hectare per year [5]. This high concentration of microplastics can induce toxic effects on plants by disrupting physiological processes such as ionic homeostasis, redox regulation, and photosynthesis [6]. Additionally, microplastics can be taken up and translocated within plant tissues, potentially entering the food chain and posing risks to human health [6, 7]. Microplastics can reduce plant growth and development by altering the physiological processes, involving ionic homeostasis, redox regulation, and photosynthesis [8, 9]. During the young seedlings, microplastics can be adsorbed onto root hairs, thus retarding root growth [10].

Oxo-degradable plastic waste can be possibly entered into composting processes. The mechanical processes in composting, including crushing, granulation, drying, cooling, and sieving [11], and the biological processes, which are high temperature and microbial activities, can contribute to the fragmentation of microplastics [12]. Seed germination is highly sensitive to stress conditions [13]. Microplastics can clog the pores in the seed capsule, reducing water uptake and the imbibition process, which in turn lowers the germination rate. This blockage prevents seeds from absorbing the necessary water for germination, leading to delayed or inhibited seed growth [10, 14]. The presence of plasticisers in microplastic can induce cytotoxicity during seed germination [15]. The inhibition depends on the dose, particle size, plant species and exposure time-dependent [16]. The leachates of oxo-degradable microplastic can reduce the sorghum seed germination, and garden cress [17, 18]. Seed germination of wheat can be promoted under high concentrations of microplastic due to agglomeration and charge on microplastic particles [19, 20]. In addition, electrical conductivity (EC) and pH can interrupt the germination as they were associated with ionic strength. Oxo-degradable plastic particles mainly contain polyethylene (PE), which can affect root growth and weight [7, 8, 21]. The elliptical-shaped PE microplastic less inhibits the seed root growth and soil bacterial communities than the sharp-edged ones [22]. The mung bean is sensitive to PE microplastics with particle sizes of 57-229 µm at concentrations between 0.1-1% w/w, and the toxicity can be examined by germination index and relative root elongation [23,24]. Studies have shown that these microplastics can significantly affect the germination and growth of mung bean seeds. For instance, Lee et al. (2022) [22] found that PE microplastics within this size range and concentration can inhibit root growth and reduce the germination index of mung bean seeds. Additionally, Dey et al. (2011) [23] demonstrated that the presence of PE microplastics can alter root elongation and overall seedling development. These findings confirm that the toxicity of PE microplastics to mung bean seeds can be effectively measured using germination index and relative root elongation.

Pathogenic *Escherichia coli* (*E.coli*) is an enterohemorrhagic bacteria, which are associated with catastrophic outbreaks of food poisoning. The outbreak of Shiga toxin-producing *E.coli* (STEC) O104:H4 in 2011 occurred primarily in Germany. It resulted in approximately 4000 cases of infection and 53 registered deaths. The outbreak was associated with the consumption of raw fenugreek sprouts and affected multiple countries, including other parts of Europe and North America [cited in 24]. In 1996, an outbreak of *E.coli* O157:H7 in Sakai City, Osaka Prefecture, Japan, affected more than 6,000 primary school children who consumed radish sprouts contaminated with the bacteria. The consequences were severe, with many children developing symptoms such as

diarrhea, abdominal pain, and vomiting. A significant number of cases progressed to hemolytic uremic syndrome (HUS), a serious condition that can lead to kidney failure. The outbreak resulted in several deaths and long-term health complications for some of the affected children [25]. To ensure microbiological safety, the National Advisory Committee on Microbiological Criteria for Foods (NACMCF) recommends that treatments should reduce the pathogen population present in seeds by 100,000 times (a 5-log reduction) [26]. This research examined the seed germination and phytotoxicity of the mung bean seeds in microplastic-contaminated solutions and four composts. Additionally, statistical analysis was conducted using a two-tailed Student's t-test with a 90% confidence interval to define the correlations among factors influencing germination. A correlation matrix method was employed to identify the relationships between the variables (EC, PE concentrations, and *E.coli*) and their impact on germination.

Materials and Methods

Organic fertiliser preparation

Four fertiliser samples were introduced in this research. Two organic composts were collected from Bangkachao Farm, Samut Prakan Province, Thailand. The compost originated from food waste collected from the catering services of hotels. The hotels sorted the waste into two categories: dining room waste and kitchen waste. The kitchen waste mainly contained non-edible parts of vegetables and fruits, while the dining food waste was a mixture of cooked food. Both types of organic waste were mixed with effective microorganisms (EM) powder No.1 from the Land Development Department, which is rich in bacteria, fungi, and actinomyces. These species are non-pathogenic and can enhance the biodegradation rate of organic matter. The EM was activated according to the instructions and incubated until mature. The composts from the dining waste and the kitchen waste were labeled T1 and T2, respectively. The dining and kitchen wastes were mixed with coconut coir to absorb the residual moisture in the wastes. The composting materials were prepared with an approximate ratio (by weight) of waste: EM: coconut coir at 10:1:10 (% w/w). The mixtures were separately filled into a waste composter connected to a motor that rotated horizontally at low speed. The composting materials were mixed using stainless-steel paddles for 24 hours under aerobic conditions.

The other compost was obtained from earthworms, known as vermicompost. Due to the food waste reduction policy, the amount of dining food waste can sometimes be very low. The kitchen waste was supplied as food for earthworms, and composting took one month. This vermicompost is labeled as T3. Another sample was a chemical organic fertiliser, which served high-protein plant cultivation. The fertiliser was derived from human hair waste that was chemically extracted. This sample was labeled T4. The samples were collected quarterly and then diluted at different ratios by adding deionised (DI) water. The specific electrical conductivity (EC) of the solutions was measured after soaking for 24 hours.

Microplastic particles

Microplastic particle was supplied by Aldrich Co. Ltd., and it was a polyethylene (PE), ultra-high molecular weight, with surface-modified powder employed as a control set. The PE particle size was an average of 125 μm, which can be possibly sensitive to the germination of a microgreen plant, typically a bean sprout.

Test of phytotoxicity

To examine the effect of microplastic particles on the seed germination, mung bean was selected as the assigned size of PE particles can affect germination. Premium-grade seeds of mung bean (*Vigna radiata*) were obtained from the local market. The preliminary test was conducted, with an average germination rate greater than 95%. One hundred mung bean seeds were kept in solutions for 8 hours at room temperature and then placed onto the tissue paper, kept in closed containers, and wrapped to prevent light. A 5 mL of solution was sprayed on the tissues every 2 days, to maintain the moisture. The numbers of germinated seeds were counted,

and the lengths of roots were measured on the 5 days of incubation. Due to the non-form of the root, the thread was applied to measure the root length. Refer to the International Rules for Seed Testing Association, a seed was completely germinated when the radicle attained a length of 1 mm and the plumule had just unfolded. The tests were repeated five times. The germination viability and germination rate were examined to identify the toxicity of microplastics on the microgreen plants by Czabator (1976) calculation formula [27], as follows.

$$RSG = \left(\frac{N_t}{N_c} \right) \times 100\% \quad (1)$$

$$RRG = \left(\frac{L_t}{L_c} \right) \times 100\% \quad (2)$$

$$GI = RSG \times RRG \times 100\% \quad (3)$$

where RSG is the relative seed germination, RRG is the relative radicle growth and GI is the germination index. N_t is the number of germinated seeds in aqueous extract, N_c is the number of germinated seeds in deionized water (control), L_t is the radicle length of germinated seeds in aqueous extracts, and L_c is the radicle length germinated seeds in deionized water (control).

The microplastic particles and EC may be either stressors or stimulators for seed germination. The effect of these factors on root development is examined as follows [28].

$$TI = (RL/RL_c) \times 100 \quad (5)$$

where TI is the tolerance index calculated after 5 days of germination, RL is root length (cm) and RL_c is root length (cm) in the control, C.

The fertiliser solutions were examined to determine the specific electrical conductivity (EC) and pH, which are further calculated for the ionic strength (I) from equation.

$$EC = 6.67 \times 10^4 \times I^{0.991} \quad (6)$$

where EC is a specific electrical conductivity (mS/cm) and I is an ionic strength (mol/L).

The correlation matrix method involves calculating the Pearson correlation coefficient for pairs of variables to determine the strength and direction of their linear relationship. The formula for the Pearson correlation coefficient (r) between two variables (X) and (Y) is:

$$r_{XY} = \frac{\sum \left(X_i - \overline{X} \right) \left(Y_i - \overline{Y} \right)}{\sqrt{\sum \left(X_i - \overline{X} \right)^2 \sum \left(Y_i - \overline{Y} \right)^2}} \quad (7)$$

where, Xi and Yi are the individual sample points. $\overline{X}$ and $\overline{Y}$ are the means of the variables X and Y, respectively. $\sum$ denotes the summation over all sample points.

The correlation matrix is a table showing the correlation coefficients between many variables. Each cell in the table shows the correlation between two variables. The diagonal of the matrix is always 1, as each variable is perfectly correlated with itself. This study has three variables (X-PE concentration), (Y-EC), and (Z-*E.coli*), the correlation matrix (R) is:

$$R = \begin{pmatrix} 1 & r_{XY} & r_{XZ} \\ r_{YX} & 1 & r_{YZ} \\ r_{ZX} & r_{ZY} & 1 \end{pmatrix} \quad (8)$$

where, r_{XY} is the correlation coefficient between X and Y. r_{XZ} is the correlation coefficient between X and Z. r_{YZ} is the correlation coefficient between Y and Z.

Investigation of *E.coli* culture

The US EPA method 1603 (Modified mTEC) was used to investigate *E. coli* culture which is possibly present with enteric pathogens. The method provides a direct count of *E. coli* in sample water by developing colonies of *E. coli* which grow on the surface of the membrane filter. After filtration put the membrane on the modified mTEC agar, then incubate the agar at 35°C±0.5°C for 2 ± 0.5 hours to resuscitate injured or stressed bacteria after that, incubate at 44.5°C ± 0.2°C for 22 ± 2 hours. After incubation, the *E. coli* colonies appeared in red or magenta colonies. Statistical

analysis was done by the confidential interval of 90%, two-tailed student t-test, was applied to statistically analyse data.

Results and Discussion

Fertiliser characteristics

Table 1 presents the characteristics of the fertiliser samples. All fertiliser solutions increased the EC ionic strength. The pH of all organic composting materials ranged from slightly acidic to neutral, while the chemical organic fertiliser was relatively acidic. The C:N ratio of the T2 fertiliser exceeded the maximum of 20:1, suggesting that non-edible vegetables and fruits may contain low nitrogen levels. The macronutrient content of the T4 fertiliser was relatively high, likely due to the protein in the human hair extract. The T1 fertiliser had a slightly high sodium content, attributed to the seasoning remaining in the cooked food waste.

Effect of microplastics on germination

The control test was conducted using deionised (DI) water, which has low electrical conductivity (EC) and neutral pH, providing a baseline for the germination index of mung bean seeds. When microplastic particles were added, they did not change the EC or pH of the solution, implying low solubility of microplastic particles. This is supported by studies indicating that microplastics generally do not dissolve in water and thus do not significantly alter its EC or pH [29]. The solution containing microplastic particles may still influence the germination of mung bean seeds. Figure 1 illustrates the statistical analysis of root length in bean sprouts. The upper limit of root length increases when the PE concentration does not exceed 8,000 mg/L. However, the lower limit of root length in all treatments is lower than the control. The mean root length shows that higher PE concentrations result in shorter roots. At 10,000 mg/L, PE prohibits root elongation. A concentration of 8,000 mg/L of PE is the maximum level that may act as either a stressor or stimulator for root elongation.

Correlation between EC and pH on the dissolubility of PE Microplastics and Fertiliser

The key parameters, electrical conductivity (EC) and pH, are critical in understanding the dissolubility of polyethylene (PE) microplastics and fertilisers. EC of fertiliser solutions at varying concentrations is transformed into ionic strength (I). Higher concentrations of PE in deionised water do not significantly affect ionic strength or pH due to PE's low solubility [30]. Conversely, higher concentrations of fertiliser solutions result in increased ionic strength, as demonstrated in Table 2. This indicates that ionic strength is a reflection of fertiliser solubility, with higher concentrations leading to elevated ionic strength [31].

Table 1 Characteristics of fertilisers

Parameter	Fertiliser Samples				Standard*
	T1	T2	T3	T4	
pH (1:2)	7.45	6.44	6.64	6.40	5.5-8.52/5.5-10
Electrical Conductivity (dS/m)	9.37	5.18	2.54	83.1	<10/<15
Organic Carbon (%)	37.4	45.4	25.4	8.5	-
Organic Matter (%)	64.3	78.1	43.7	25.5	>20/>20
Total Nitrogen (%)	2.49	1.20	1.85	14.8	>1.0/>1.0
C:N ratio	15:1	38:1	14:1	0.6:1	<20:1/<20.1
Total Phosphorus (%P_2O_5)	0.78	0.62	1.69	4.2	>0.5/>2.5
Total Potassium (%K_2O)	4.14	1.84	1.22	4.9	>0.5/>1.0
Macronutrient Content (%)	7.41	3.66	4.76	23.9	>2%/> 9 % < 20%
Total Sodium (%)	1.00	0.63	0.13	0.301	<1/<1
Total Calcium (%)	32,387	23,730	19,759	12,000	-
Cation Exchange Capacity (cmol/kg)	98.0	46.7	61.0	19.7	-

Note: *Organic fertiliser standards of the Land Development Department: Compost (Grade 2)/High quality organic fertiliser.

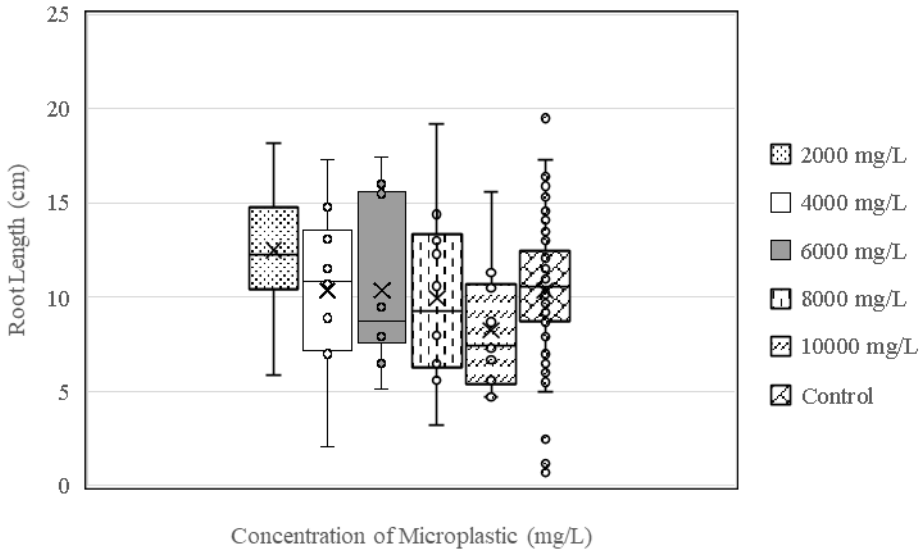

Figure 1 Box plot for root length of germinated seeds at different PE concentrations spiked into DI water

Table 2 Characteristics of microplastic, compost and fertiliser solutions

Material	Dilution by weight (mg Material: mL DI water)	EC (mS/cm)	I (mol/L)	pH
DI water (C1)	-	0.0006	0.00001	6.98
DI water with microplastic (C2)	2:1000 (0.2% *w/v*)	0.0008	0.00001	6.92
	4:1000 (0.4% *w/v*)	0.0011	0.00001	6.94
	6:1000 (0.6% *w/v*)	0.0015	0.00002	6.89
	8:1000 (0.8% *w/v*)	0.0016	0.00002	6.92
	10:1000 (1.0% *w/v*)	0.0018	0.00002	6.96
Food waste compost (T1) [Salinity 2.9 ppt*]	1:1	7.45	0.10949	7.18
	1:10	6.12	0.08979	6.95
	1:20	2.53	0.03682	6.74
Kitchen waste compost (T2) [Salinity 1.9 ppt]	1:1	6.67	0.09793	7.13
	1:10	4.12	0.06023	6.97
	1:20	1.80	0.02614	6.74
Vermicompost (T3) [Salinity 2.1 ppt]	1:1	8.60	0.12656	7.29
	1:10	2.90	0.04226	7.18
	1:20	1.42	0.02056	6.97
Chemical organic fertiliser (T4) [Salinity 2.3 ppt]	1:1	43.30	0.64663	8.76
	1:20	31.60	0.47056	8.47
	1:100	9.37	0.13800	8.04

Note: * ppt refers to parts per thousand

Influence of Electrical Conductivity (EC) and pH *on E.coli*

The presence of *E.coli* in compost was examined, as shown in Table 3. Due to the heterogeneity of composts T1 and T2, the samples were randomly selected. The numbers of *E.coli* in composts varied significantly. Only food waste compost (T1) contained *E. coli*, suggesting post-contamination or unhygienic conditions during food preparation. The kitchen waste compost (T2) was free from *E.coli*, likely because the inedible vegetables and fruits in the compost do not support *E.coli* growth. Similarly, vermicompost (T3) was free from *E.coli* since earthworms do not harbor *E.coli* in their digestive systems. The chemical organic fertiliser (T4) also had no *E.coli*, possibly due to the chemical processes involved, which can eliminate *E.coli*. This indicates that biodigestion in the composting process may not effectively eliminate *E.coli*. For food safety, organic compost may require further thermal treatment to reduce *E.coli* levels. Reducing *E. coli* contamination on seeds is crucial for public health protection [30, 31].

The EC and pH of fertiliser have less influence on *E.coli* in fertiliser compared to the dilution effect. However, EC and pH can affect the growth of *E.coli*. Studies have shown that *E.coli* can be eliminated at high pH levels, typically above 9.0, and at high EC levels, which disrupt the bacterial cell membrane [32, 33]. Heat treatment during the fermentation of T1 and T2 may also reduce *E. coli* levels.

Toxicity test of *E. coli* on germination

The presence of *E. coli* in composting may not clearly indicate germination inhibition. The compost was diluted with deionised water and then filtered, significantly reducing the amount of *E. coli*, which likely has no effect on the roots of germinated seedlings. The correlation between *E. coli* in T1 fertiliser and germination rate is undefined. Studies have shown that *E. coli* contamination does not adversely affect seed germination. For instance, research indicates that *E. coli* does not inhibit the germination of seeds, as the bacteria do not produce toxins that affect plant growth [32, 34, 35]. Therefore, the presence of *E. coli* in compost is unlikely to be toxic to seed germination.

Toxicity test of microplastic on germination

The details of Relative Seed Germination (RSG), Relative Root Growth (RRG), and Germination Index (GI) are displayed in Table 4. The data indicated that after 5 days, the final germination percentage (FGP) was obtained. A GI higher than 80% was classified as free of phytotoxicity. Adding microplastic particles, all the treatments in C2 had 100% FGP, implying that microplastic particles can stimulate the germination of mung bean seeds. The RRG and GI were highest when the microplastic concentration was lower than 8000 mg/L or 0.8% w/w. This suggests that microplastic particles can clog the root hair, reducing water absorbability [23]. The results revealed that microplastics within a lower concentration range of 0.2-0.8% can stimulate root length. None of these treatments showed phytotoxicity. The seedlings might respond to polyethylene microplastic particles similarly to amino acids, potentially altering their metabolites [36]. Further investigations are needed to fully understand plant-microplastic interactions, particularly in the long term. The radicle length of a 0.4% w/w microplastic solution seemed to follow a normal distribution. The germinated seeds exhibited uniform RSG and RRG, indicating that microplastics might stimulate root development by enhancing water absorption ability. Studies have shown that microplastics at certain concentrations can indeed stimulate root elongation. For instance, Liu et al. (2021) [37] found that polyethylene microplastics reduced shoot weight and height at high concentrations but stimulated root elongation at lower concentrations. Additionally, research on *Pisum sativum* sprouts indicated that microplastics at doses of 100 mg/L and 500 mg/L resulted in significant root length increases [38]. The uniformity in RSG and RRG suggests that the microplastic particles may enhance the water absorption ability of the roots. This enhancement could be due to the microplastics' ability to improve soil aeration and water retention, which are crucial for robust root growth. Studies have shown that microplastics can alter soil properties, such as increasing porosity and water-holding capacity, which in turn can facilitate better water uptake by plant roots [39, 40]. Additionally, microplastics can interact with root exudates, potentially enhancing nutrient availability and uptake [40].

Table 3 Numbers of *E. coli* in fertilisers

Fertiliser	Number of colonies on plates											
Dilution	Food waste compost (T1)			Kitchen waste compost (T2)			Vermicompost (T3)			Chemical organic fertiliser (T4)		
	#1	#2	#3	#1	#2	#3	#1	#2	#3	#1	#2	#3
10^{-2}	NC	NC	NC	0	NC	0	0	0	0	0	0	0
10^{-3}	NC	NC	NC	0	0	0	0	0	0	0	0	0
10^{-4}	33	0	0	0	0	0	0	0	0	0	0	0
10^{-5}	9	5	0	0	0	0	0	0	0	0	0	0
10^{-6}	2	1	2	0	0	0	0	0	0	0	0	0
10^{-7}	0	0	0	0	0	0	0	0	0	0	0	0
10^{-8}	0	0	0	0	0	0	0	0	0	0	0	0

Note: NC is non-countable when the number of single colony greater than 300 cells.

Table 4 Enhancing and inhibiting of EC and pH of fertiliser solutions upon seed germination

Treatment	Dilution by weight (mg Material: mL DI water)	PE conc. (%)	Root length (cm)			N	FGP (%)	RSG (%)	RRG (%)	GI (%)
			Min	Max	Avg.					
C1	-	-	0.7	24.0	12.0	473*	95	100	100	100
C2	-	0.2	5.9	14.7	14.7	50	100	106	122	129
	-	0.4	2.1	17.3	12.7	50	100	106	106	112
	-	0.6	5.1	17.4	12.7	50	100	106	105	111
	-	0.8	3.2	19.2	12.1	50	100	106	100	106
	-	1.0	4.7	15.6	9.8	50	100	106	82	86
T1	1:20	0.4	1.5	30.6	14.0	48	96	101	116	118
	1:20	0.6	0.9	31.5	17.3	48	96	101	144	146
T2	1:20	0.4	1.5	18.5	9.4	50	100	106	78	82
	1:20	0.6	0.8	15.0	8.0	48	96	101	66	67
T3	1:20	0.4	0.8	29.6	14.0	47	94	99	116	115
	1:20	0.6	0.8	28.0	17.3	49	98	104	144	149
T4	1:100	0.4	0.5	3.8	2.4	50	100	106	20	21
	1:100	0.6	0.5	5.3	3.3	44	88	93	28	26

Note: * Tests were conducted with 500 seeds.

Toxicity test of ionic strength on germination

By comparing data from Tables 2 and 4, it was found that the germination index (GI) of dining food waste compost (T1) was higher than that of kitchen waste compost (T2). Both types of waste underwent the same composting process. Dining food waste, which was cooked and served to clients, contained salt and other seasonings. This waste was used as raw material for composting, and the microbes might not have been able to reduce the salt content. Electrical conductivity (EC) can indicate the level of salts in fertiliser solutions [28]. All treatments showed little change in the pH of the fertiliser solution, indicating strong phytotoxicity of salinity and EC to mung bean sprouts. T1 compost required a dilution of at least 1:20, while T2 compost required at least 1:10 to enhance germination. The GI was lower than 50% at dilutions of 1:10 and 1:1 for T1 and T2 composts, respectively, indicating phytotoxicity at threshold limit concentrations.

Kitchen waste was fed to earthworms to produce vermicompost (T3). The vermicompost had slightly higher salinity and EC than T2 due to the digestion process of earthworms. The GI of T3 was slightly lower than T2, but diluting the fertiliser with deionised water at least 1:10

enhanced germination. The threshold limit concentration of T3 was the same as T2, but the GI was lower than 25%, indicating strong phytotoxicity. The chemical organic fertiliser (T4) had relatively high salinity and EC, reaching phytotoxic levels. T4 inhibited germination even at a high dilution of 1:100, presenting a GI lower than 25%, which was severely phytotoxic.

Microplastics at a concentration of 0.4% w/w resulted in the highest tolerance index. Fertilisers T1, T2, and T3 with a dilution of 1:20 had the highest tolerance index, but mung bean seeds could not tolerate T4 fertiliser at any dilution. High ionic strength in fertiliser solutions can inhibit seed germination due to osmotic stress and ion toxicity. Properly balanced ionic environments are essential for nutrient availability and microbial activity, which support germination and seedling growth. Excessive ionic strength disrupts water absorption and nutrient uptake, negatively impacting plant development [41, 42, 43].

Since Electrical Conductivity (EC) and *E.coli* have no correlation, the correlation metric cannot be determined. However, EC and ionic strength (I) are correlated. Beyond this the EC may refer the constituents in fertiliser. Organic composts might contain both essential micronutrients, such as Cu, Mg, Zn and Ni, and non-essential metalloids, such as Cd, Hg, Pb and As, all these elements can elevate the EC and I. Whenever both essential and non-essential micronutrients are in proper concentration, they can play a beneficial role in seed germination and root development [29]. The correlation between EC and TI can classify the germination into 3 categories, involving stimulation, strong inhibition, and severe inhibition, as presented in Figure 2.

Toxicity test of microplastic concentration and EC on germination

As ionic strength is a key factor in germination, the fertiliser solutions were diluted to 1:20 for T1, T2, and T3, and 1:100 for T4. These dilutions achieved the highest germination rates. Microplastic particles were mixed with fertiliser solutions at concentrations of 4 and 6 g/L to determine their inhibiting or enhancing effects on germination, as shown in Table 3. The microplastic particles and EC in food waste compost (T1) and vermicompost (T3) enhanced germination. When the concentration of microplastic particles increased, the roots and culms appeared slimmer and longer than the control. The adventitious roots and elongation of hypocotyls were stimulated, as shown in Figure 3, indicating changes in growth hormones, particularly auxins [44, 45]. Conversely, the microplastic particles and EC in kitchen waste compost (T2) and chemical organic fertiliser (T4) inhibited germination. Observations showed that the root radicles developed slowly, and the seeds absorbed little water. The microplastic particles and EC may reduce gibberellic acid, affecting the elongation growth of bean hypocotyls.

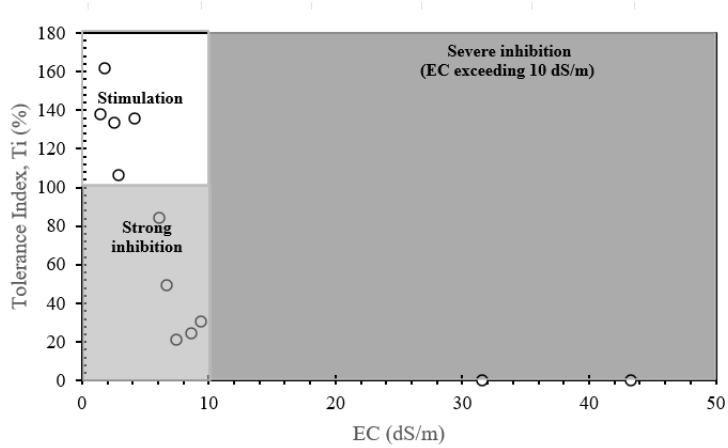

Figure 2 Classification of EC effect on germination of bean sprout

Figure 3 illustrates the physical appearance of germinating mung bean seeds under different treatments. The physical appearance of germinating seeds under different treatments shows variations in root and shoot development. Higher concentrations of microplastics in T1 and T3 resulted in slimmer and longer roots and culms compared to the control, indicating enhanced water absorption and growth hormone activity, particularly auxins. Conversely, T2 and T4 treatments showed inhibited germination, with slower root radicle development and reduced water absorption, likely due to decreased gibberellic acid levels, which are crucial for elongation growth of bean hypocotyls. Table 5 presents the plant hormones of sprouts. Polyethylene (PE) microplastics at concentrations of 0.4% and 0.6% can stimulate the production of gibberellins (GA3). T1 and T3 fertilisers can relatively stimulate GA3 hormones, as they have slightly higher electrical conductivity (EC) than T2 fertiliser. This condition may induce stress in sprouts. However, T4, with its high EC, can inhibit the synthesis of GA3.

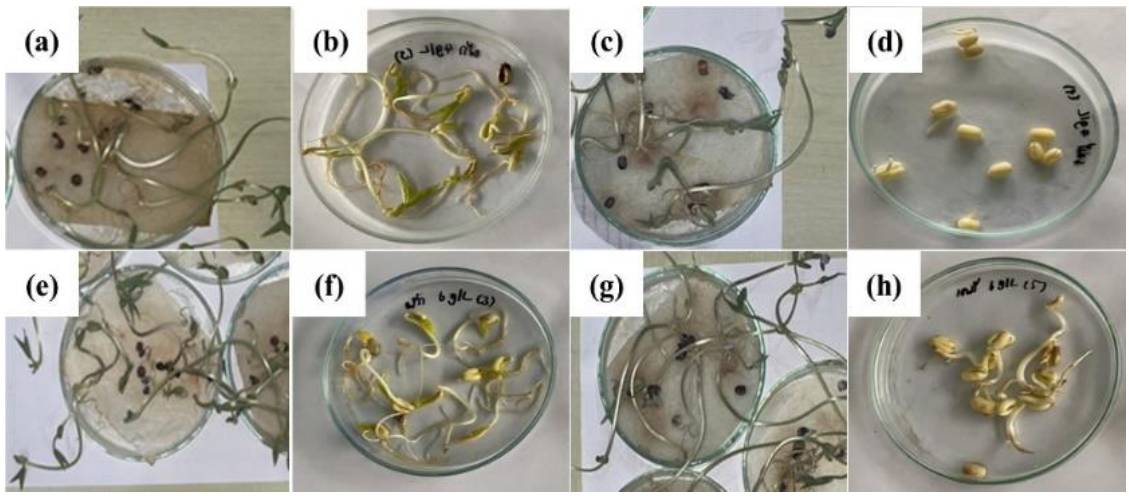

Figure 3 Physical appearance of bean sprout at 0.4% (a-d) and 0.6% (e-h) of PE particle in fertiliser solutions of T1 (a, e), T2 (b, f), T3 (c, g) and T4 (d, h) treatments

Table 5 Plant hormones of mung bean sprout

Solution	Dilution (Fertiliser: DI)	Microplastic (%)	Hormone concentration (mg/g wet weight)			
			GA3	IAA	IBA	NAA
C1	-	-	32.1	ND	ND	ND
C2	-	0.4	96.6	ND	ND	ND
	-	0.6	84.6	ND	ND	ND
T1	1:20	0.4	12.1	ND	ND	ND
T2	1:20	0.4	5.4	ND	ND	ND
T3	1:20	0.4	18.3	ND	ND	ND
T4	1:100	0.4	10.8	ND	ND	ND

Note: ND refers to non-detectable.

Conclusions

The study found that microplastic particles, particularly polyethylene (PE), can stimulate mung bean seed germination at concentrations below 0.8% w/w, challenging the perception that all microplastics are harmful to plant growth. High electrical conductivity (EC) levels in composts significantly inhibit seed germination, highlighting the need to manage salt content for beneficial plant growth. The presence of *E. coli* in food waste compost (T1) underscores the importance of hygienic conditions during compost preparation, with findings suggesting that proper treatment can mitigate microbiological risks. The combined effects of microplastics and EC on seed germination are complex; while microplastics can enhance germination in some composts, high EC levels can negate these benefits. Practical guidelines for optimising compost use include managing salt content in food waste composts (T1 and T2) and carefully diluting chemical organic fertilisers (T4) to avoid phytotoxicity. The findings support sustainable agricultural practices by highlighting the potential benefits and risks of using composts contaminated with microplastics and high EC, informing strategies to mitigate negative impacts and enhance positive effects on plant growth. The research also emphasises the importance of addressing microbiological safety in composting processes to protect public health.

Acknowledgement

This research was funded by the Thailand Science Research and Innovation (TSRI) via the Fundamental Fund 2023.

References

[1] Azeem, I., Adeel, M., Ahmad, M.A., Shakoor, N., Zain, M., Yousef, N., Yinghai, Z., Azeem, K., Zhou, P., White, J.C., Ming, X. and Rui, Y. 2022. Microplastic and Nanoplastic Interactions with Plant Species: Trends, Meta-analysis, and Perspectives. Environmental Science & Technology Letters. 9(6): 482-492.

[2] Huang, Y., Liu, Q., Jia, W., Yan, C. and Wang, J. 2020. Agricultural Plastic Mulching as a Source of Microplastics in the Terrestrial Environment. Environmental Pollution. 260: 114096.

[3] Duan, J., Bolan, N., Li, Y., Ding, S., Atugoda, T., Vithanage, M., Sarkar, B., Tsang, D.C.W. and Kirkham, M.B. 2021. Weathering of Microplastics and Interaction with Other Coexisting Constituents in Terrestrial and Aquatic Environments. Water Research. 196: 117011.

[4] Mao, X., Xu, Y., Cheng, Z., Yang, Y., Guan, Z., Jiang, L. and Tang, K. 2022. The Impact of Microplastic Pollution on Ecological Environment: A Review. Frontiers in Bioscience (Landmark Ed.). 27(2): 46.

[5] Yang, S.S., Ding, M.Q., He, L., Zhang, C.H., Li, Q.X., Xing, D.F., Cao, G.I., Zhao, L., Ding, J., Ren, N.Q. and Wu, W.M. 2021. Biodegradation of Polypropylene by Yellow Mealworms (*Tenebrio molitor*) and Superworms (*Zophobas atratus*) via Gut-microbe-dependent Depolymerization. Science of The Total Environment. 756: 144087.

[6] Corradini, F., Meza, P., Eguiluz, R., Casado, F., Huerta-Lwanga, E. and Geissen, V. 2019. Evidence of Microplastic Accumulation in Agricultural Soils from Sewage Sludge Disposal. Science of The Total Environment. 671: 411-420.

[7] Guo, M., Zhao, F., Tian, L., Ni, K., Lu, Y. and Borah, P. 2022. Effects of Polystyrene Microplastics on the Seed Germination of Herbaceous Ornamental Plants. Science of The Total Environment. 809: 151100.

[8] Li, X., Ullah, S., Chen, N., Tong, X., Yang, N., Liu, J., Guo, X., and Tang, Z. 2023. Phytotoxic Assessment of Dandelion Exposed to Microplastics Using Membership Function Value and Integrated Biological Response Index. Environmental Pollution. 333: 121933.

[9] Maity, S., Guchhait, R., Sarkar, M.B. and Pramanick, K. 2022. Occurrence and Distribution of Micro/Nanoplastics in Soils and Their Phytotoxic Effects: A Review. Plant, Cell & Environment. 45 (4): 1011-1028.

[10] Bosker, T., Bouwman, L.J., Brun, N. R., Behrens, P. and Vijver, M.G. 2019. Microplastics Accumulate on Pores in Seed Capsule and Delay Germination and Root Growth of the Terrestrial Vascular Plant *Lepidium sativum*. Chemosphere. 226: 774-781.

[11] Braun, M., Mail, M., Heyse, R. and Amelung, W. 2021. Plastic in compost: Prevalence and Potential Input into Agricultural and Horticultural Soils. Science of The Total Environment. 760: 143335.

[12] Accinelli, C., Abbas, H.K., Bruno, V., Khambhati, V.H., Little, N.S., Bellaloui, N., et al. 2022. Field Studies on the Deterioration of Microplastic Films from Ultra-thin Compostable Bags in Soil. Journal of Environmental Management. 305: 114407.

[13] Wang, J., Li, J., Liu, W., Zeb, A., Wang, Q., Zheng, Z., Shi, R., Lian, Y. and Liu, L. 2023. Three Typical Microplastics Affect the Germination and Growth of Amaranth (*Amaranthus mangostanus L.*) Seedlings. Plant Physiology and Biochemistry. 194: 589-599.

[14] Balestri, E., Menicagli, V., Ligorini, V., Fulignati, S., Galletti, A.M.R. and Lardicci, C. 2019. Phytotoxicity assessment of conventional and biodegradable plastic bags using seed germination test. Ecological Indicators 102, 569–580.

[15] Bao, Y., Pan, C., Li, D., Guo, A. and Dai, F. 2022. Stress response to oxytetracycline and microplastic-polyethylene in wheat (*Triticum aestivum L.*) during seed germination and seedling growth stages. Sci. Total Environ. 806: 150553.

[16] Sahasa, R.G.K., Dhevagi, P., Poornima, R., Ramya, A., Moorthy, P.S., Alagirisamy, B., Alagirisamy, B., Karthikeyan, S. 2023. Effect of Polyethylene Microplastics on Seed Germination of Blackgram (*Vigna mungo L.*) and Tomato (*Solanum lycopersicum L.*). Environmental Advances. 11: 100349.

[17] Schiavo, S., Oliviero, M., Chiavarini, S. and Manzo, S. 2020. Adverse Effects of Oxodegradable Plastic Leachates in Freshwater Environment. Environmental Science and Pollution Research. 27: 8586-8595.

[18] Pflugmacher, S., Sulek, A., Mader, H., Heo, J., Noh, J. H., Penttinen, O.P., Kim, Y., Kim., S. and Esterhuizen, M. 2020. The Influence of New and Artificial Aged Microplastic and Leachates on the Germination of *Lepidium sativum L.* Plants (Basel). 9(3): 339.

[19] Lian, Y., Liu, W., Shi, R., Zeb, A., Wang, Q., Li, J., Zheng, Z. and Tang, J. 2022. Effects of Polyethylene and Polylactic Acid Microplastics on Plant Growth and Bacterial Community in the Soil. Journal of Hazardous Materials. 435: 129057.

[20] Ge, J., Li, H., Liu, P., Zhang, Z., Ouyang, Z. and Guo, X. 2021. Review of the Toxic Effect of Microplastics on Terrestrial and Aquatic Plants. Science of the Total Environment. 791: 148333.

[21] Shi, R., Liu, W., Lian, Y., Wang, Q., Zeb, A. and Tang, J. 2022. Phytotoxicity of Polystyrene, Polyethylene and Polypropylene Microplastics on Tomato (*Lycopersicon esculentum L.*). Journal of Environmental Management. 317: 115441.

[22] Lian, J., Shen, M. and Liu, W. 2019. Effects of Microplastics on Wheat Seed Germination and Seedling Growth. Journal of Agro-Environment Science. 38(4): 737-745.

[23] Lee, T.Y., Kim, L., Kim, D., An, S. and An, Y.J. 2022. Microplastics from Shoe Sole Fragments Cause Oxidative Stress in a Plant (*Vigna radiata*) and Impair Soil Environment. Journal of Hazardous Materials. 429: 128306.

[24] Dey, A., Bagchi, B., Das, S., Basu, R. and Nandy, P. 2011. A Study on the Phytotoxicity of Nano Mullite and Metal-Amended Nano Mullite on Mung Bean Plants. Journal of Environmental Monitoring. 13: 1709.

[25] Uphoff, H., Hedrich, B., Strotmann, I, Arvand, M., Bettge-Weller, G. and Hauri, A. 2014. A Prolonged Investigation of an STEC-0104 Cluster in Hesse Germany, 2011 and Implications for Outbreak Management. Journal of Public Health. 22(1): 41-48.

[26] Watanebe, Y., Ozassa, K., Mermin, J.H., Griffin, P.M., Masuda, K., Imashuku, S. and Sawada, T. 1999. Factory Outbreak of *Escherichia coli* O157:H7 Infection in Japan. Emerging Infectious Diseases. 5(3): 424-428.

[27] NACMCF. 1999. Microbiological Safety Evaluations and Recommendations on Sprouted Seeds. International Journal of Food Microbiology. 52: 123-153.

[28] Parera, V., Parera, C.A. and Feresin, G.E. 2023. Germination and Early Seedling Growth of High Andean Native

Plants under Heavy Metal Stress. Diversity. 15(7): 824.
[29] Li, Y., Chen, P., Tang, Y., Yang, Y., Zhou, C., Bu, J., and Zhong, S. 2024. Microplastics in Water: A Review of Characterization and Removal Methods. Sustainability. 16(10): 4033.
[30] Seidensticker, S., Grathwohl, P., Lamprecht, J., and Zarfl, C. 2018. A Combined Experimental and Modeling Study to Evaluate pH-dependent Sorption of Polar and Non-polar Compounds to Polyethylene and Polystyrene Microplastics. Environmental Sciences Europe. 30(1): 30.
[31] Atlas Scientific. 2024. Understanding the Relationship between pH and Electrical Conductivity. https://atlas-scientific.com/blog/relationship-between-ph-and-conductivity/.
[32] Parhad, N. M., and N. U. Rao. 1984. Effect of pH on Survival of *Escherichia coli*. Journal of Water Pollution Control Federation. 56(9): 980-986.
[33] Environmental Protection Agency (EPA). 2021. *E. coli* (*Escherichia coli*). https://www.epa.gov/system/files/documents/2021-07/parameter-factsheet_e.-coli.pdf.
[34] El Kayal, W., Darwiche, L., Farhat, Y.A. Hdeib, M., AlJardaly, R., Shbaro, M. and Iskandar, C.F. 2024. Agricultural Mitigation Strategies to Reduce the Impact of Romaine Lettuce Contamination. Plants. 13(17): 2460.
[35] Robbens, J., Dardenne, F., Devriese, L., De Coen, W. and Blust, R. 2010. *Escherichia coli* as a Bioreporter in Ecotoxicology. Applied Microbiology and Biotechnology. 88: 1007-1025.
[36] Bouaicha, O., Tiziani, R., Maver, M., Lucini, L., Miras-Moreno, B., Zhang, L., Trevisan, M., Cesco, S., Borruso, L. and Mimmo, T. 2022. Plant Species-Specific Impact of Polyethylene Microspheres on Seedling Growth and the Metabolome. Science of The Total Environment. 840: 156678.
[37] Liu, L., Zhang, Y., Fu, W., Liu, X., Wang, Q., Tanveer, M. and Huang, L. 2021. Microplastic Stress in Plants: Effects on Plant Growth and Their Remediations. Frontiers in Plant Science. 14: 1226484.
[38] Zhang Y., Fu, W., Liu, X., Wang, Q., Tanveer, M. and Huang, L. 2023. The Impact of Microplastic Concentration and Particle Size on the Growth of *Pisum sativum* Sprouts. Agronomy. 14(5): 923.
[39] Panda, S. and Behera, R. 2024. Microplastic Accumulation in Agricultural Soils - Impacts on Crop Microbiomes and Soil Health. Journal of Agriculture and Livestock Farming. 1(4): 1-4.
[40] Jiang, M., Zhao, W., Liang, Q., Cai, M., Fan, X., Jiang, Y., Li, T., Wang, Y., Peng, C. and Liu, J. 2024. Advances in Physiological and Ecological Effects of Microplastic on Crop. Journal of Soil Science and Plant Nutrition. 24: 1741-1760.
[41] Dodd, G.L. and Donovan, L.A. 1999. Water Potential and Ionic Effects on Germination and Seedling Growth of Two Cold Desert Shrubs. American Journal of Botany. 86(8): 1146-1153.
[42] Ludwiczak, A., Osiak, M., Cárdenas-Pérez, S., Lubińska-Mielińska, S. and Piernik, A. 2021. Osmotic Stress or Ionic Composition: Which Affects the Early Growth of Crop Species More? Agronomy. 11(3): 435.
[43] Bartakova, I., Kummerova, M., Mandl, M. and Pospisil, M. 2001. Phytotoxicity of Iron in Relation to Its Solubility Conditions and the Effect of Ionic Strength. Plant and Soil. 235: 45-51.
[44] Li, X., Ullah, S., Chen, N., Tong, X., Yang, N., Liu, J., Guo, X. and Tang, Z. 2023. Phytotoxic Assessment of Dandelion Exposed to Microplastics Using Membership Function Value and Integrated Biological Response Index. Environmental Pollution. 333: 121933.
[45] Kollárová, K., Henselová, M. and Lišková, D. 2005. Effect of Auxin and Plant Oligosaccharides on Root Formation and Elongation Growth of Mung Bean Hypocotyls. Plant Growth Regulation. 46: 1-9.

Thai Environmental Engineering Journal Vol. 39 No. 1 (2025) : 27-37
www.eeat.or.th

Optimizing Aeration for Enhancing Biodrying Efficacy of Municipal Solid Waste in Tropical Climate Condition

Panida Payomthip[1,2], Sirintornthep Towprayoon[1,3], Chart Chiemchaisri[4] and Komsilp Wangyao[1,3*]

[1]The Joint Graduate School of Energy and Environment (JGSEE), King Mongkut's University of Technology Thonburi, Bangkok 10140, Thailand
[2]Material Cycles Division, National Institute for Environmental Studies, Tsukuba 305-8506, Japan
[3]Center of Excellence on Energy Technology and Environment (CEE), Ministry of Higher Education, Science, Research and Innovation (MHESI), Bangkok 10400, Thailand
[4]Department of Environmental Engineering, Faculty of Engineering, Kasetsart University, Bangkok 10900, Thailand
[*]E-mail : komsilp.wan@kmutt.ac.th

Article History; *Received: 17 January 2025, Accepted: 21 March 2025, Published: 30 April 2025*

Abstract

This study investigated the influence of aeration and its optimum operation for the biodrying of municipal solid waste (MSW). A series of lysimeter experiments were conducted to determine MSW's moisture content, temperature, and gas emissions during its biodrying treatment at different aeration rates over 14 days. Results indicated that low-to-moderate aeration rates of 0.3-0.5 L/min facilitated a balance between water evaporation by heat generated from biological activities and advective removal of evaporated water from the waste matrix. In contrast, higher aeration rates primarily relied on physical drying, resulting in rapid initial moisture loss but potentially inhibiting microbial activities. The optimal aeration was determined at 0.3 L/min, achieving a minimum low heating value (LHV) of 11.4 MJ/kg and reducing the moisture content to less than 30% within 7 days. These findings suggest that optimizing aeration rates can significantly enhance the efficiency of the biodrying of MSW in tropical climate condition. The data from this study could be used to promote sustainable waste management practices in regions with similar climatic and waste composition characteristics as Thailand.

Keywords : Biodrying; Mechanical Biological Treatment; Municipal Solid Waste; Waste-to-Energy; Refuse Derived Fuel

Introduction

Global climate change, attributed to anthropogenic activities, has intensified the need for sustainable waste management practices. Municipal solid waste (MSW) contributes significantly to greenhouse gas (GHG) emissions, including open burning and landfill emissions. These activities release methane, a potent greenhouse gas with a relatively short atmospheric lifetime but a high global warming potential [1]. As in many developing countries, MSW management faces challenges in Thailand due to rapid urbanization and inadequate waste management infrastructure. In 2023, the daily generation of MSW has reached approximately 73,840 tons, representing a 5% increase from the previous year [2]. The organic composition of this waste, particularly the high content of food waste (approximately 40%), poses significant challenges for traditional waste management strategies, especially in a humid tropical climate.

Improper management of food waste poses a significant threat to the environment. Food waste decomposes anaerobically, which produces methane (CH_4), a potent greenhouse gas with a global warming potential approximately 28 times greater than carbon dioxide (CO_2) [3]. While Thailand has implemented policies to promote a circular economy for plastic waste [2], challenges persist in food waste management due to the absence of a clear, dedicated policy framework in Thailand to address food waste management, waste segregation, and the efficient utilization of food waste [4]. Such food waste signifies a global challenge and highlights inefficiencies in resource allocation. Food waste contributes to approximately 8-10% of global GHG emissions with a global average generation rate of 86 kg/capita/day, among which food waste generation in Thailand (79 kg/capita/day) was comparable to those observed in neighboring countries [5]. This situation poses a significant challenge to achieving Sustainable Development Goal 12.3, which aims to halve per capita global food waste at the retail and consumer levels by 2030.

Thailand has implemented various waste management strategies to address these challenges, including mechanical biological treatment (MBT) with biodrying [6]. Biodrying is a process that involves the controlled biological degradation of organic matter within the waste and the removal of moisture through evaporation. This technology provides significant benefits, such as creating refuse-derived fuel (RDF) and reducing GHG emissions [7-9]. Moreover, MSW biodrying is generally accomplished within a short period, i.e., less than 20 days; hence, it can be considered a compact and energy-efficient process [10, 11]. According to studies by Payomthip et al. (2022) and Sutthasil et al. (2018), the biodrying process can reduce GHG emissions by 84-93.3% compared to those of landfilling [12, 13]. It also produces RDF with a higher calorific value, which cement plants can use as an alternative fuel source [9, 14, 15]. Unfortunately, only 12.6% of the RDF produced by waste management was used in cement facilities due to the potential negative impact on clinker quality from low-quality RDF input [16, 17].

Despite the potential benefits of biodrying, several challenges and knowledge gaps persist. The optimal aeration rate for biodrying depends on waste characteristics [12], climatic conditions, and waste density [18, 19]. To establish proper operating conditions for biodrying of MSW in tropical climate condition, this study investigated the effect of aeration on moisture content, temperature profiles, and gas emissions. It determined the optimum rate for maximizing moisture removal and enhancing the heating value of RDF. The study offers valuable insights into the biodrying process, which can be integrated into sustainable waste management strategies for developing countries in tropical regions.

Materials and Methods

Experimental Design and Preparation

This study investigated the biodrying of MSW in Thailand, focusing on the effect of the aeration rate. A set of lysimeter experiments was performed to examine biodrying performance under varied aeration rates of simulated mixed waste materials representing landfilled waste to gain insight into physical changes together with their associated gas emissions.

This research used an acrylic column with a diameter of 0.2 m and a height of 0.6 m covered with thermal insulation to prevent heat

losses. Each column was equipped with a perforated base connected to an aeration system to distribute air. The orifice with a 6.35 mm diameter was installed at the center of the lysimeter for inner gas sampling. Meanwhile, the exhaust gas was collected from the top of the lysimeter for emitting gas evaluation. The temperature and moisture content inside the waste material were measured in the middle of the lysimeter, as described in Figure 1. The range of airflow rates to each column was adjusted using this system with a compressor and flow regulators.

Experiments were designed using a simulated waste mixture representing the typical composition of MSW in Thailand, in which food waste was the predominant component at 45%, follows by paper, plastic, yard waste, textile and other at 12%, 6%, 5% and 7%, respectively [2]. The size of the simulated waste was reduced to about 10 cm and mixed manually. After the preparation, 2.9 kg of simulated waste was loaded into each lysimeter, and its compaction density was 340 kg/m^3.

While porosity and size distribution are recognized as factors in biodrying, these parameters were not measured in this study. This decision was primarily due to the focus of this research on the impact of aeration rates on biodrying performance. We acknowledge that the absence of these measurements may limit a comprehensive understanding of the physical changes within the waste matrix. Furthermore, output waste composition was not measured as the primary objective of this study was to evaluate the effect of aeration rates on MSW biodrying. However, the initial composition was controlled to replicate the MSW composition found in Thailand.

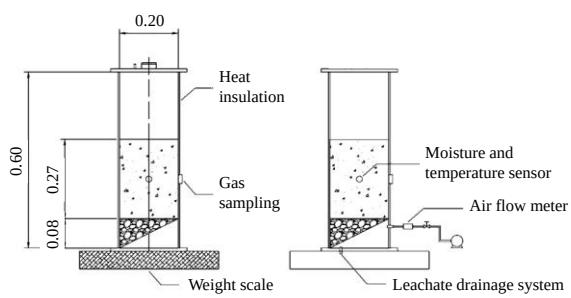

Figure 1 Configuration and cross-sections of simulated lysimeters

Aeration Rate Selection

Six different aeration rates were studied, ranging from 0.1 to 2.0 L/min, as described in Table 1. These rates were selected based on a review of prior research on the biodrying process. It was intended to be used as the theoretical underpinning for the study and literature on optimal conditions for maximal moisture removal and microbial activity. An air pump was installed to provide different aeration rates into each lysimeter, with silicon tubing of 6.35 mm diameter connecting the pump to the perforated base of each column. The inlet air supplied by the air pump had an average temperature of 30°C with approximately 60% moisture content, representing the ambient room temperature of the laboratory, under an atmospheric pressure of 1 atm. The aeration was applied continuously for 14 days, maintaining a constant flow rate from the bottom to the top of the waste material. A control lysimeter was included to simulate passive aeration (natural ventilation), and by allowing ambient air to enter and exit freely without forced airflow, to provide a baseline for comparison with the lysimeters subjected to forced aeration.

Table 1 The aeration provided for the lysimeter

Code	A	B	C	D	E	F	G
Aeration rate (L/min)	0.1	0.3	0.5	0.7	1.0	2.0	-

Measurement and Analysis

The measurements comprised temperature, moisture content, inner gas, and gas emissions as follows:

Temperature Measurement:

Each lysimeter contained a port through which testers could insert temperature sensors at the center, which were recorded using a data logger to get a temperature profile. The temperature measurements monitored the thermal profile of waste periodically because this parameter is critical to characterize the microbial activity and effectiveness of the biodrying process. The data collected made it possible to analyze and explain how, by different aeration rates, the temperature distribution profiles inside the lysimeter lead to moisture evaporation and microbial activity.

Moisture Content and Low Heating Value Measurement:

The initial and final waste materials were analyzed for water content and LHV using air-dried at 105°C for 24 h. (ISO-5068-1 standard) and Bomb Calorimeter (ASTM D 5865-11a standard), respectively. The moisture content of waste material during the experiment was tracked using moisture sensors (EN 61326-1:2013, EN 50581:2012 standard) and recorded by a data logger. This method is frequently employed in studies on waste processing to control drying technologies and calculate moisture retention after the treatment of wastes [12, 14, 17].

Gas Sample Analyses:

Gas samples at the mid-depth of waste layer and emitting gas at the top of the lysimeters were collected along the experimental period and analyzed for CO_2, CH_4, and nitrous oxide (N_2O) concentrations using gas chromatography (GC) equipped with flame ionization detector (FID) and electron capture detector (ECD). These gases were used to indicate biological activities occurring in the waste layer: CO_2 corresponds to aerobic respiration, CH_4 indicates anaerobic conditions and N_2O points to incomplete denitrification processes. Monitoring these gases was essential to evaluate the environmental impact of the biodrying process.

Process Efficiency Evaluation:

The primary objective of biodrying is to reduce moisture content while minimizing organic matter loss. Various researchers have used the biodrying index to evaluate the efficiency of the biodrying process [12, 17, 20]. In this study, the biodrying index was calculated as the ratio of carbon loss (measured by CO_2 and CH_4 emissions) to water loss. This index measures the extent to which the process relies on biological degradation versus physical drying. A higher biodrying index indicates a more significant contribution of biological processes to moisture reduction.

Data Analysis

The information gathered from measuring temperature and moisture levels underwent statistical examination to pinpoint variations across aeration levels. A regression analysis was used to show the link between aeration rate and moisture reduction, and an analysis of variance was used to establish the significance of the differences among the rates. A normalized approach was employed to assess the overall efficiency of the biodrying process through moisture removal, increasing LHV, and weight reduction. All data analysis was carried out using data analysis through Excel for Windows.

Results and Discussion

The experiment was conducted to examine the effects of aeration on waste materials through the biodrying process by investigating basic phenomena; hence, optimal aeration on tropical MSW was achieved.

Effect of Aeration on Waste Characteristics

Temperature, Moisture Content Profiles and Their Implications

As a vital factor in the biodrying process, temperature directly influences the microbial activities responsible for the biodegradation of organic matter, which subsequently releases heat for evaporating moisture. Throughout the 14 days of this experiment, the temperature and moisture content profiles within the lysimeters changed considerably depending on airflow conditions. Figure 2 shows the temperatures and moisture observed at different aeration rates.

The temperature inside waste materials varied between 36 and 44°C in all lysimeters. The statistical analysis reveals an insignificant difference between the temperature profile over the entire biodrying period in the lysimeters operated under different aeration rates ($p > 0.05$). However, significant differences were observed in the moisture content of waste between the lysimeters, thus suggesting the impact of the aeration rate on moisture removal from waste.

Regarding the temperature profile, higher initial temperatures were observed in low-to-moderate aeration rates (0.1 to 0.5 L/min), likely due to intense microbial activities. Subsequently, a decline in temperature was noted, followed by a secondary rise, possibly attributed to the degradation of more recalcitrant organic matter by thermophilic microorganisms. Interestingly, the lysimeter

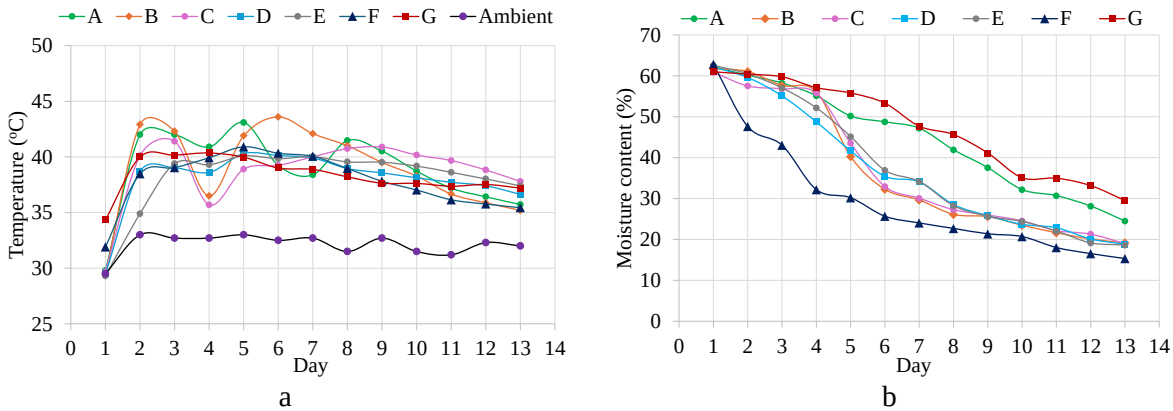

Figure 2 The profiles of temperature (a) and moisture content (b) during biodrying process

with upper moderate-to-high aeration rates (0.7 to 2.0 L/min) shows similar trends in temperature profiles as the control lysimeter. This could be attributed to excessively high aeration, leading to rapid moisture loss and hindering microbial activity. Nevertheless, high aeration rates did not accelerate the process to the thermophilic phase due to increased convective heat loss, which counteracted the heat generated by microbial activities [21, 22], leading to a lower temperature.

While upper moderate-to-high aeration rates show similar trends in temperature profiles, the trends in daily moisture content were observed in different directions. In the highest aeration rates (F – 2.0 L/min), the moisture content decreased rapidly in the initial stages, primarily due to physical drying, as the high airflow rate facilitated moisture evaporation. The moisture level in this lysimeter can reach 30% within 5 days, while over 40% was observed in other lysimeters. In contrast, other aeration rates (0.3 to 2.0 L/min) exhibited a slower moisture reduction rate, indicating a balance between biological and physical drying processes. The lowest aeration lysimeter (A – 0.1 L/min) shows a similar trend as the control lysimeter. The moisture content gradually decreased starting on day 5 of the experiment. In low-aeration conditions, moisture transport within the waste material may be limited, hindering evaporation, whereas moderate aeration can improve moisture transport. However, the evaporation rate may be limited if the airflow is insufficient to overcome the resistance to moisture diffusion within the waste material. In fact, temperature can influence moisture evaporation. Notwithstanding, the relatively similar temperature profiles across different aeration rates suggest that temperature may not be the primary driver of moisture loss in this case.

While the moisture content profiles varied significantly across different aeration rates, the temperature profiles exhibited a more complex and non-linear relationship with aeration. As depicted in Figure 3, the maximum temperature was observed in lysimeter B (0.3 L/min) on day 2, whereas the minimum temperature was recorded in lysimeter E (1.0 L/min) on the same day. On day 4, the lowest temperatures were attained in lysimeters B and C (0.3 L/min and 0.5 L/min). This non-linear behavior suggests that increasing the aeration rate does not always result in a commensurate increase in temperature. In some instances, excessive aeration can even suppress microbial activities, leading to decreased heat generation. This can occur when the airflow is too strong, leading to excessive drying of the waste material and hindering the growth of microorganisms. As a result, the biodegradation process is slowed down, and the temperature within the waste material decreases.

When comparing the relationship between temperature and decreasing moisture content (Figure 4), it is observed that the highest aeration rate exhibited a rapid initial decrease in moisture content, reaching 40% on day 1, followed by a gradual decline. Concurrently, the

temperature increased to a maximum on day 5 and then gradually decreased. This suggests that in the initial stages, biodrying processes were dominant, with microbial activities contributing to heat generation and moisture reduction. However, as the moisture content decreased significantly, advective removal of moisture, driven by airflow, became more prominent. The excessive aeration rate is likely to reduce microbial activities under low moisture content conditions, leading to a decline in biological activities; thus, removing water through evaporation from releasing heat would be imited.

For low-to-moderate aeration (lysimeter B to D – 0.3, 0.5, and 0.7 L/min), a similar trend was observed, which suggests that the initial temperature rise was likely due to the degradation of readily biodegradable materials, while the subsequent decrease may be attributed to the degradation of more recalcitrant substances. However, three aeration rates of B, C, and D achieved the targeted moisture content of produced RDF set by end users at 30% within 7 days, as illustrated in Figure 5. However, selecting an appropriate aeration rate for the biodrying process in practical operation would also depend on other factors such as energy and equipment costs. In this context, the lysimeter B could be considered the most appropriate condition as it could achieve the desired end-user product while creating lower environmental impacts. However, further analysis and optimization studies may be necessary to definitively conclude the optimal aeration rate for specific waste types and operational conditions. Notwithstanding, even though the moisture content in lysimeter F reached 30% on day 5, it could be dried only through advective removal from the waste matrix without a significant contribution from biodrying phenomena.

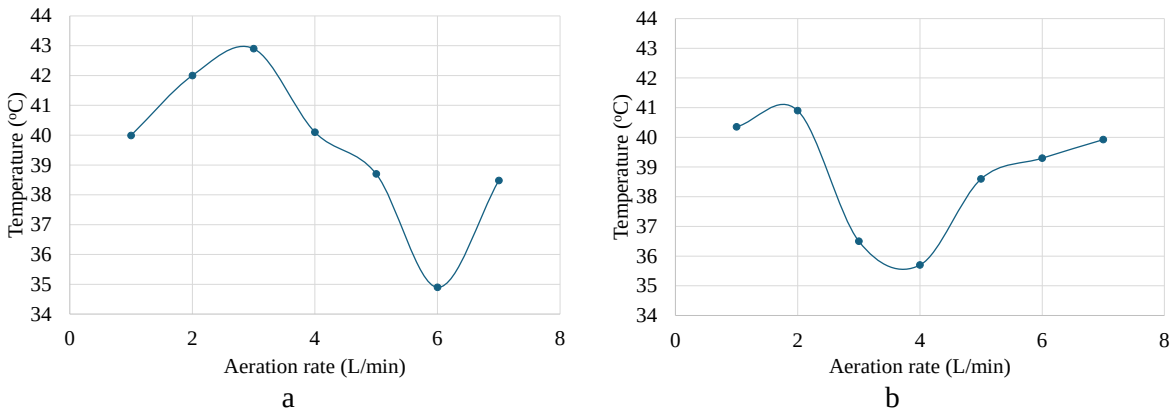

Figure 3 The relationship between the temperature change period and aeration rate on day 2 (a) and day 4 (b)

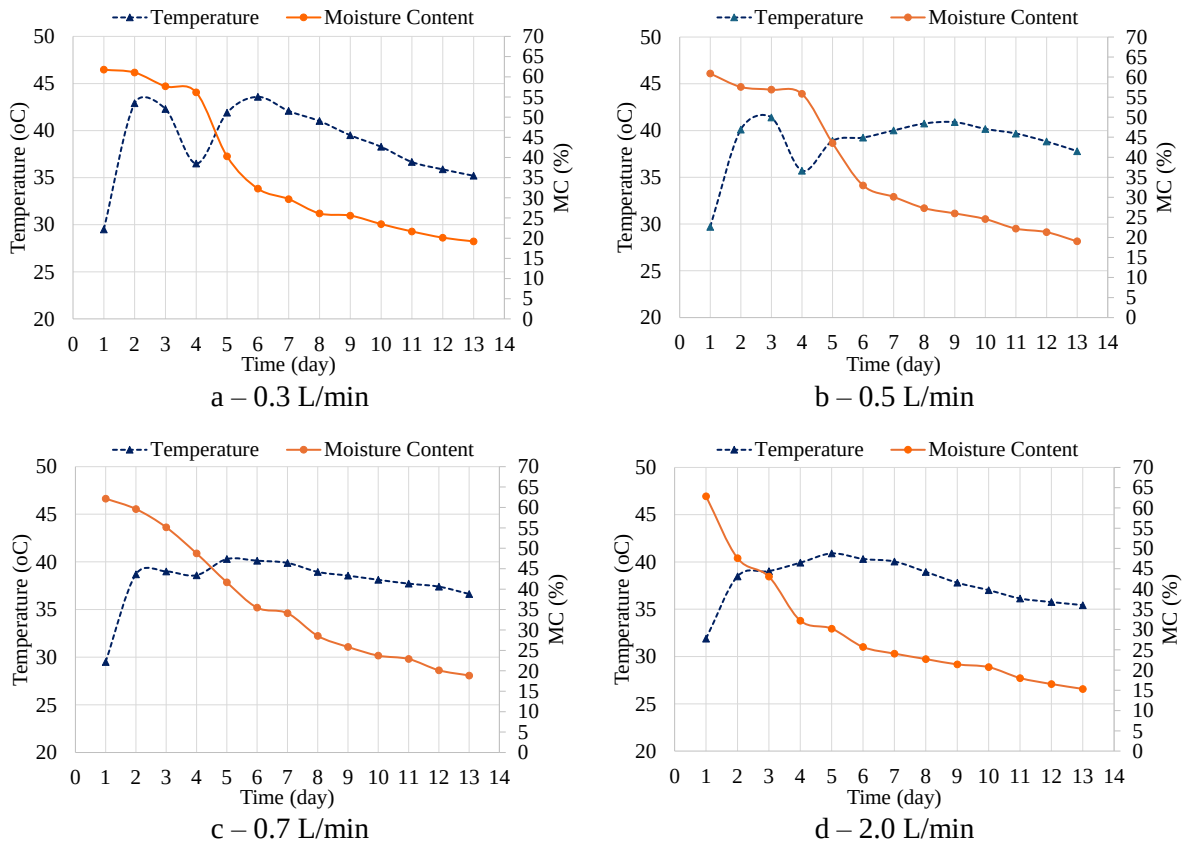

Figure 4 The variation of moisture content and the temperature in lysimeter with 0.3 (a), 0.5 (b), 0.7 (c), and 2.0 L/min (d) aeration supplied

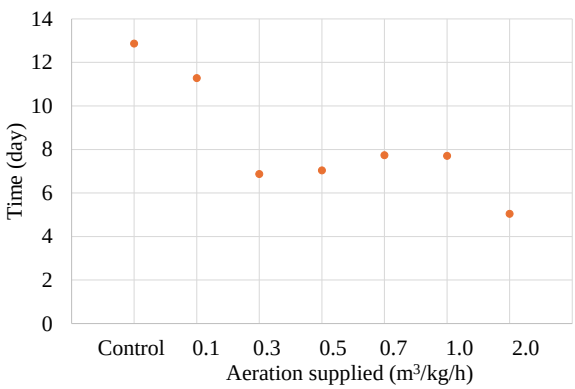

Figure 5 The correlation between the time to achieve target RDF qualities set by end-users and the aeration rate

Gas Concentration Inside Waste Material

The production of greenhouse gases, including CO_2, CH_4, and N_2O, was closely linked to the biodrying process. CO_2 emissions were highest in the initial stages, reflecting active microbial activity. Subsequently, CO_2 levels decreased as organic matter was consumed and microbial activity decreased. Figure 6 illustrates the variation of gas inside the waste materials among lysimeters B, C (low-to-moderate aeration), and F (highest aeration). The highest CO_2 levels were observed in lysimeter C, particularly on the 3rd day. This peak indicates a period of intense microbial activity that the moderate aeration rate could drive. However, it is essential to note that this peak is a transient phenomenon, and as readily biodegradable organic matter is consumed, the rate of CO2 production decreases.

In contrast, lysimeter F exhibited the lowest CO_2 levels, indicating excessive aeration can accelerate moisture evaporation, potentially limiting the growth of certain microorganisms' growth and reducing CO_2 production. Moreover, lysimeter B showed intermediate CO_2 levels, suggesting a balance between the evaporation of water by heat generated from biological activities and the

advective removal of evaporated water from the waste matrix. However, it should be noted that the relationship between aeration rate and CO_2 production is complex and can be influenced by various factors, including waste composition, initial moisture content, and environmental conditions. Further research is required to clarify the mechanisms inside waste material for effective biodrying.

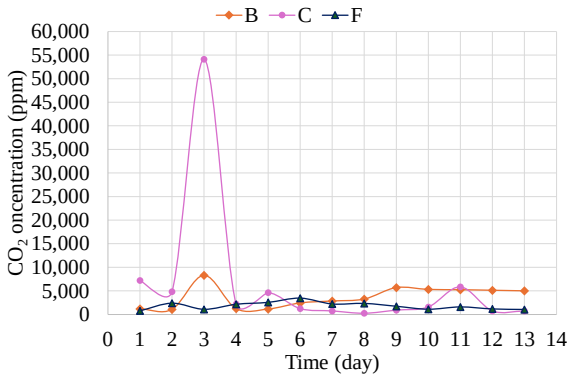

a

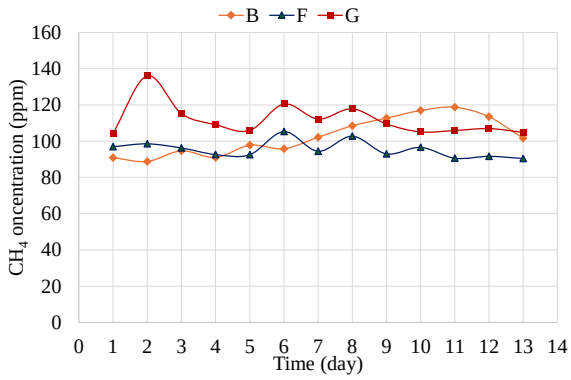

b

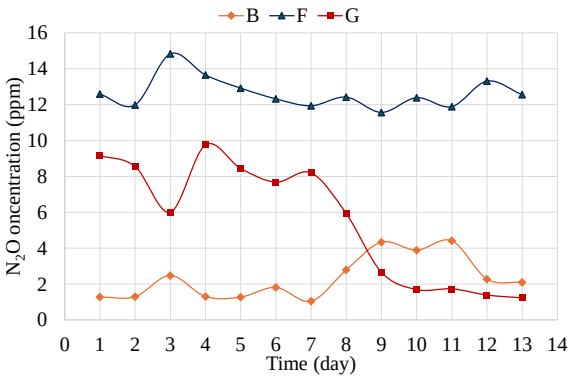

c

Figure 6 The variation of CO_2 (a), CH_4 (b), and N_2O (c) gas inside the waste materials

The comparison of CH_4 gas production among lysimeters B, F, and G shows that the CH_4 concentration profiles varied across different aeration rates. However, statistical analysis showed non-significant differences among the lysimeter operation conditions ($p > 0.05$). It should be noted that even though the statistical analysis did not reveal significant differences in CH_4 concentrations, it is crucial to consider the underlying biological and environmental factors that may influence CH_4 production. Further research is needed to fully understand these factors' complex interactions and optimize biodrying processes for efficient waste management and reduced greenhouse gas emissions.

Regarding N_2O inside the lysimeter, the statistics show a significant difference among the lysimeters ($p < 0.05$). Lysimeter F shows a higher and more stable N_2O concentration, indicating that a high aeration rate promotes nitrification. In contrast, a decreasing trend over time was observed in lysimeter G, which could result from the limited oxygen availability, inhibiting nitrification and favoring denitrification. Lysimeter B exhibits a relatively stable N_2O concentration with some fluctuations. This suggests a balance between nitrification and denitrification processes.

Weight Loss and Heating Value

The weight loss of the waste was directly correlated with moisture reduction. The heating value of the biodried waste increased significantly, making it a potential feedstock for energy recovery. Normalization was used to compare the effects of different aeration rates on the moisture content, low heating value, and weight loss. Each triangle represents a different treatment, with the vertices representing the percentage reduction in moisture, the increase in low heating value, and the percentage weight loss, as illustrated in Figure 7. No leachate was observed throughout the experimental period, which aligns with the findings of previous studies [23]. Please note that the highest aeration rate was not included in the calculation because the loss in moisture content was mainly due to the advective removal of moisture under high airflow

conditions rather than the evaporation of water from heat generated by biological activities.

The figure shows that moisture content decreases and LHV increases with increasing aeration rates. This suggests that increased aeration can promote microbial activity, leading to higher energy content in organic matter. However, more aeration can decrease LHV, as observed in certain lysimeters. This might be affected by the inhibition or nutrient loss associated with increased oxygen. Low-to-moderate aeration rates (0.3 and 0.5 L/min) showed greater normalized efficiency scores, suggesting a more balanced combination of biological and physical drying processes. The highest LHV achieved was 11.4 MJ/kg and 13.3 MJ/kg after 7 days and 14 days in the lysimeter with 0.3 L/min aeration, meeting the end-user standard of at least 10.5 MJ/kg LHV for RDF utilization in power plant [16].

These rates resulted in significant moisture reduction with minimal organic matter loss and yielded optimum biodrying conditions.

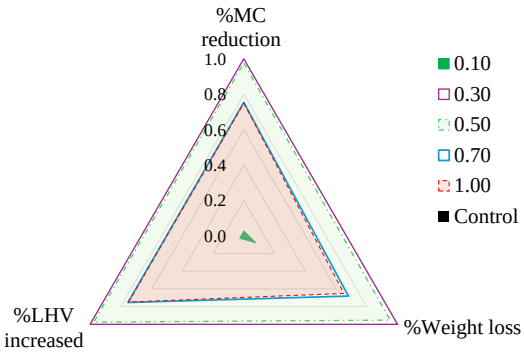

Figure 7 A comparison of process efficiency among different aeration rates on day 7

Optimal Aeration Rate for Biodrying and its Index

From Figure 8, the lowest aeration rate (0.1 L/min) resulted in minimal water loss due to limited airflow and reduced microbial activities. However, this condition also led to a higher carbon loss, suggesting inefficient biodegradation and potentially anaerobic processes. In contrast, the high aeration rates of 1.0 and 2.0 L/min led to increased CO_2 emissions, implying that physical drying dominated biological processes. While these higher aeration rates showed higher carbon loss, they resulted in similar levels of water loss as the low-to-moderate aeration rates of 0.3 and 0.5 L/min.

These low-to-moderate aeration rates demonstrated a better balance between biological and physical drying processes. These rates resulted in higher water loss with lower carbon loss through CO_2 and CH_4 emissions, indicating more efficient biodegradation and reduced organic matter loss. The optimal biodrying index was observed at 0.3 L/min, suggesting a balance between microbial activity and moisture removal.

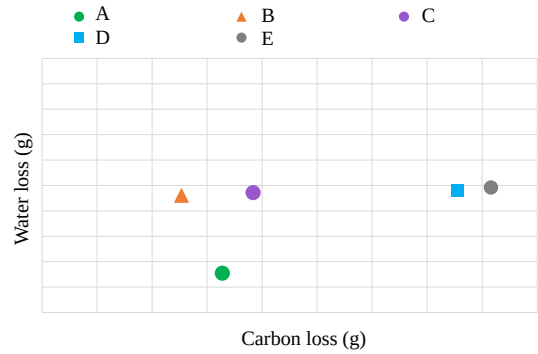

Figure 8 The correlation between C loss in terms of CO_2 emission loss and water loss

Conclusions

This study examined the effects of aeration rate on the biodrying of MSW in Thailand, a representative of tropical developing countries. The findings of this research contribute to the advancement of waste-to-energy technologies, explicitly highlighting the potential of biodrying as a suitable treatment option for regions with climatic conditions and similar waste management challenges to Thailand. The results demonstrated that aeration significantly influenced the lysimeters' moisture reduction, temperature profile, and gas emissions. It was found that low-to-moderate aeration (0.3 and 0.5 L/min) promoted a biodrying process, combining biological and physical drying phenomena. Under high aeration condition (2.0 L/min), rapid initial moisture loss resulted from the dominance of active moisture removal. In contrast, the

evaporative removals due to heat released from microbial activities were limited. The study recommends maintaining an aeration rate of 0.3 L/min as optimal for the biodrying process in this study. This rate balanced moisture removal, microbial activity, and gas emissions, producing efficient biodrying and high-quality biodried products. Further research is needed to assess how these findings can be implemented and explore the potential for scaling up the technology, including the effects of different waste compositions and seasonal variations on biodrying performance. Moreover, developing monitoring and control systems to optimize aeration rates and environmental conditions can significantly enhance the effectiveness of biodrying processes.

References

[1] Afifa., Arshad, K., Hussain, N., Ashraf, M. H. and Saleem, M. Z. 2024. Air pollution and climate change as grand challenges to sustainability. Sci Tot Environ. 928: 172370.

[2] Pollution Control Department. 2023. Thailand State of Pollution Report 2023, Pollution Control Department, Ministry of Natural Resources and Environment, Thailand. Retrieved from https://www.pcd.go.th/ebook/book18/PCD%202024.html. Access: October 20, 2024.

[3] Myhre, G., D. Shindell, F.-M. Bréon., *et. al*. 2013. Anthropogenic and Natural Radiative Forcing. In: Climate Change 2013: The Physical Science Basis. Contribution of Working Group I to the Fifth Assessment Report of the Intergovernmental Panel on Climate Change [Stocker, T.F., D. Qin, G.-K. Plattner., *et al* (eds.)]. Cambridge University Press, Cambridge, United Kingdom and New York, NY, USA.

[4] Pollution Control Department. 2024. Food Waste Management Roadmap (2023-2030) and Food Waste Management Action Plan (2023-2027), Pollution Control Department, Ministry of Natural Resources and Environment, Thailand. Retrieved from https://www.pcd.go.th/garbage/. Access: October 15, 2024.

[5] United Nations Environment Programme. 2024. Food Waste Index Report 2024 Think Eat Save: Tracking Progress to Halve Global Food Waste. Retrieved from https://wedocs.unep.org/20.500.11822/45230. Access: November 10, 2024.

[6] Office of Natural Resources and Environmental Policy and Planning. 2022. Thailand's Long-Term Low Greenhouse Gas Emission Development Strategy (Revise Version), Climate Change Management and Coordination Division, Ministry of Natural Resources and Environment, Thailand. Retrieved from https://unfccc.int/sites/default/files/resource/Thailand%20LT-LEDS%20%28Revised%20Version%29_08Nov2022.pdf. Access: November 5, 2024.

[7] Wang, K., Wang, Y.Y., Chen, T.B., Zheng, G.D., Cao, M.K. and Cai, L. 2020a. Adding a recyclable amendment to facilitate sewage sludge biodrying and reduce costs. Chemosphere. 256: 127009.

[8] Cao, M. K., Guo, H. T., Zheng, G. D., Chen, T. B. and Cai, L. 2021. Microbial succession and degradation during kitchen waste biodrying, highlighting the thermophilic phase. Bioresour. Technol. 326: 124762.

[9] Payomthip, P., Towprayoon, S., Chiemchaisri, C., Patumsawad, S. and Wangyao, K. 2020. Effect of Intermittent Negative Ventilation in Biodrying Process for Treating Pre-Shredded Waste. In: IOP Conference Series: Earth and Environmental Science. 581(1).

[10] Lu, J. and Xu, S. 2021. Post-treatment of food waste digestate towards land application: a review. J. Clean. Prod. 303: 127033.

[11] Yuan, J., Li, Y., Zhang, H., *et. al*. 2018. Effects of adding bulking agents on the biodrying of kitchen waste and the odor emissions produced. J. Environ. Sci. 67: 344-355.

[12] Payomthip, P., Towprayoon, S., Chiemchaisri, C., Patumsawad, S. and Wangyao, K. 2022. Optimization of Aeration for Accelerating Municipal Solid Waste Biodrying. Int J Renew Energy Dev. 11: 878-888.

[13] Sutthasil, N., Ishigaki, T., Ochiai, S., Chiemchaisri, C. and Yamada, M. Greenhouse Gas Emissions Reduction from Biodrying MBT in Tropical Climate. At The 29th Annual Conference of Japan Society of Material Cycles and Waste Management on September 12-14, 2018.

[14] Bhatsada, A., Patumsawad, S., Itsarathorn, T., *et. al*. 2023. Improvement of energy recovery potential of wet-refuse-derived fuel through bio-drying process. J Mater Cycles Waste Manag. 25: 637-649.

[15] Bhatsada, A., Patumsawad, S., Towprayoon, S., Chiemchaisri, C., Phongphiphat, A. and Wangyao, K. 2023. Modification of the Aeration-Supplied Configuration in the Biodrying Process for Refuse-Derived Fuel (RDF) Production. Energies (Basel). 16(7): 3235.

[16] Itsarathorn, T., Towprayoon, S., Chiemchaisri, C., Patumsawad, S., Wangyao, K. and Phongphipat, A. The Situation of RDF Utilization in the Cement Industry in Thailand. At The International Conference and Utility Exhibition 2022 (ICUE2022) on Energy, Environment and Climate Change, Thailand on October 26-28, 2022.

[17] Ngamket, K., Wangyao, K., Patumsawad, S., Chaiwiwatworakul, P. and Towprayoon, S. 2021. Quality improvement of mixed MSW drying using a pilot-scale solar greenhouse biodrying system. J Mater Cycles Waste Manag. 23: 436-448.

[18] Itsarathorn, T., Towprayoon, S., Chiemchaisri, C., *et al*. 2023. The effect of aeration rate and feedstock density on biodrying performance for wet refuse-derived fuel quality improvement. Int J Renew Energy Dev. 12: 1091-1103.

[19] Wahyanti, E., Bhatsada, A., Towprayoon, S., Sutthasil, N., Patumsawad, S. and Wangyao, K. 2024. Impact of Feedstock Density on Biodrying for Enhancing Heat Retention and Moisture Reduction. Thai Environ Eng J. 38(2): 35-46.

[20] Sutthasil, N., Ishigaki, T., Ochiai, S., Yamada, M. and Chiemchaisri C. 2023. Carbon conversion during biodrying of municipal solid waste generated under tropical Asian conditions. Biomass Convers Biorefin. 13: 16791-16805.

[21] Lai, JC., Then, YL., Hwang, SS. and Lee, CS. 2024. Optimal aeration management strategy for a small-scale food waste composting. Carbon Resour Convers: 7(1). 100190.

[22] Zhang, D., Xu, Z., Wang, G., Huda, N., Li, G. and Luo, W. 2020. Insights into characteristics of organic matter during co-biodrying of sewage sludge and kitchen waste under different aeration intensities. Environ Technol Inno. 20: 101117.

[23] Feltrim, F., Izzo, R. L. S., Rose, J. L., Machado, A. B. and Oro, S. R. 2021. Evaluation of the bio-drying process of municipal solid waste using rotating drums bio-drying rotary drum. Ana Acad Bras Cienc, 93(4).

Thai Environmental Engineering Journal Vol. 39 No. 1 (2025) : 39-50
www.eeat.or.th

Steel Furnace Temperature Optimization for Wasted of Scale Reduction During Reheating Process by Experimental Design

Gan Yimyam[1], Ailada Treerattrakoon[2] and Peerakarn Banjerdkij[1*]

[1]Department of Environmental Engineering, Faculty of Engineering,
Kasetsart University, Bangkok 10900, Thailand
[2]Department of Industrial Engineering, Faculty of Engineering,
Kasetsart University, Bangkok 10900, Thailand
[*]E-mail : fengpkba@ku.ac.th

Article History; *Received: 22 December 2024, Accepted: 2 April 2025, Published: 30 April 2025*

Abstract

In the hot rolling steel mill industry, substantial energy resources are consumed, and significant amounts of waste are produced. One notable waste product is scale formation, or iron oxide, on the surfaces of billets. Minimizing and properly treating this scale is crucial, as its disposal in landfills can lead to leachate contamination of groundwater and soil. The rate of scale growth increases with higher furnace temperatures. This study employs experimental design to investigate the impact of different furnace zone temperatures on scale formation. Scale thickness was measured and analysed using analysis of variance (ANOVA). The results indicated that the temperatures in the heating and soaking zones significantly affect the scale growth rate, while the preheating zone temperature does not, within a 95% confidence interval. Optimizing the temperatures reduced the scale thickness from 0.764 mm to 0.467 mm, with a 95% confidence interval. Overall, the waste from scale was reduced from 2.29% to 1.22%.

Keywords : Reheating furnace; Scale Formation; Experimental Design

Introduction

Scale formation is one of the significant wastes in the steel manufacturing process. It forms on steel surfaces through oxidation, with the growth rate increasing as surface temperature and oxygen content rise. When disposed of in landfills, scale can release toxins that contaminate groundwater and soil [1]. Therefore, minimizing and properly treating scale is crucial. Besides its environmental impact, scale causes substantial production yield losses, especially at the high temperatures used during the reheating process. Imperfections on the steel surface can occur, affecting production quality if scale enters the rolling mill process. To prevent this, scale must be removed using high-pressure descaling units before the rolling mill process. Numerous investigations have described the characteristics of scale and predicted its growth rate. This study focuses on optimizing process parameters to minimize scale formation in a factory setting.

Steel is oxidized during the billets are heated up to rolling temperature as 1300 Celsius degrees [2]. The scale is formed on the steel as high as furnace temperature. Ferrous (Fe) and O (excess oxygen) are the main compositional elements of scale. Scale is growth by three layers including outer layer of hematite (Fe_2O_3), an intermediate of magnetite (Fe_3O_4), and a thicken inner of wustite (FeO) [1]. In this study, the thickness of scale formation on steel billets (grade SS400) was examined during the reheating process. SS400 billets were the most selected for utilization, accounting for more than 60% of total production, minimizing variations caused by different steel grades in the

process [2]. The experimental methodology employed a factorial design to evaluate the correlation between processing variables and the resulting scale formation. Three process variables, each tested at two levels, were analyzed to identify significant factors influencing the reheating process [3]. A Taguchi experimental design was used to determine the key variables affecting scale formation. To examine the impact of zone temperature on scale formation thickness (mm) during reheating, a 3^k full factorial design approach was implemented, where 3 represents the number of levels, and k denotes the number of input parameters [3]. This approach allowed for a comprehensive assessment of the influence of temperature variations across different zones on oxidation behavior.

The main objective, to determine the furnace temperatures optimization in each combustion zones that significantly effect to the growth rate of scale. The effects of zone temperatures on responses of interest in the reheating process are generated by general full factorial design method of experimental design approach, where the number of levels and the number of input variable factor are used [4]. Three of significant factors that affected to the scale formation are surface temperature of steel holding time in furnace and the percentage of oxygen in furnace atmosphere but furnace temperature is the most important factor which is strongly influences the oxidation of steel [5].

Methodology

In this experiment is applied at one of Thailand's walking beam reheating furnace where is designed by SMS Group (Germany) and combustion system is automated by Prometheus Level II 2013 series system [2]. There are 63 billets containing in furnace for 2 hours 37 minutes of heating time with heating pattern as Figure 1. The methodology is design of experiment for scale thickness minimization by furnace temperature analysis. The result was analyses by analysis of variance (ANOVA) and retest of experiment was implemented in order to compare the differential between before and after the improvement by 2 sample t test.

The oxidation rate of steel in the reheating furnace is influenced by three main factors: free oxygen level, furnace temperature, and steel duration time [5]. Among these, furnace temperature is the most critical factor affecting oxidation and is also the most controllable, as it can be directly adjusted via the furnace control panel. The growth rate of the scale increases as the temperature of the furnace increases and the temperature of the steel with scale is lower 10 Celsius degrees than without scale at the exit of the reheating furnace [6]. This study focuses on the effect of furnace temperature, while the oxygen level and steel duration time are treated as fixed parameters. The oxygen level, a key factor in scale formation, originates from two sources [7-9]: excess oxygen from the air-to-fuel combustion ratio, which is set at 1.10 for all experiments, and furnace pressure, which influences air infiltration. The furnace pressure is maintained at 10 Pascal, as per the manufacturer's default settings. Similarly, the billet charging temperature is fixed at room temperature, following a cold charging process. The steel duration time in the furnace is set at 2 hours and 30 minutes, with a continuous pacing of 2 minutes and 30 seconds, without considering heat conduction to the steel core. The experiments are conducted using a randomized approach, consisting of 16 trials, each producing 16 sample pieces across 16 production batches, all operated by the same personnel.

Furnace temperature analysis for scale thickness minimization by design of experiment

This study investigates the effects of temperature variations in three combustion zones (preheating, heating, and soaking) on scale formation thickness during the reheating process. The response variable of interest, scale formation thickness, is examined at two levels (maximum and minimum temperatures) for each combustion zone, based on normal operational adjustments in billet reheating furnaces.

A full factorial design was used to systematically plan and analyze all experimental combinations. The study follows a 2^k full factorial design approach, where each

factor has two levels. In this case, the experimental design considers three factors (k=3), corresponding to the three combustion zones (preheating, heating, and soaking), with each factor varied at two levels (high and low), based on the minimum and maximum set points of the furnace recipe. To optimize scale minimization, the experiment follows a 2^3 full factorial design with two replicates. The results are analyzed using analysis of variance (ANOVA), including main effect plots and interaction plots to assess the influence of each factor on the response variable. Additionally, the relationship between input factors and scale thickness is modeled using a regression equation, as shown in Figure 2.

There are 16 runs number of experiments with three input variable factors with 2 levels following as minimum and maximum set point recipes of preheating temperature (X_1) with level of 990 and 1090 Celsius degrees, heating temperature (X_2) with level of 1210 and 1260 Celsius degrees and soaking temperature (X_3) with level of 1250 and 1290 Celsius degrees [2] as per Table 1. The level of each factor is referenced from the minimum and maximum setup criteria, as defined by the equipment limitations established by the main machine designer and manufacturer [2] as per Figure 3.

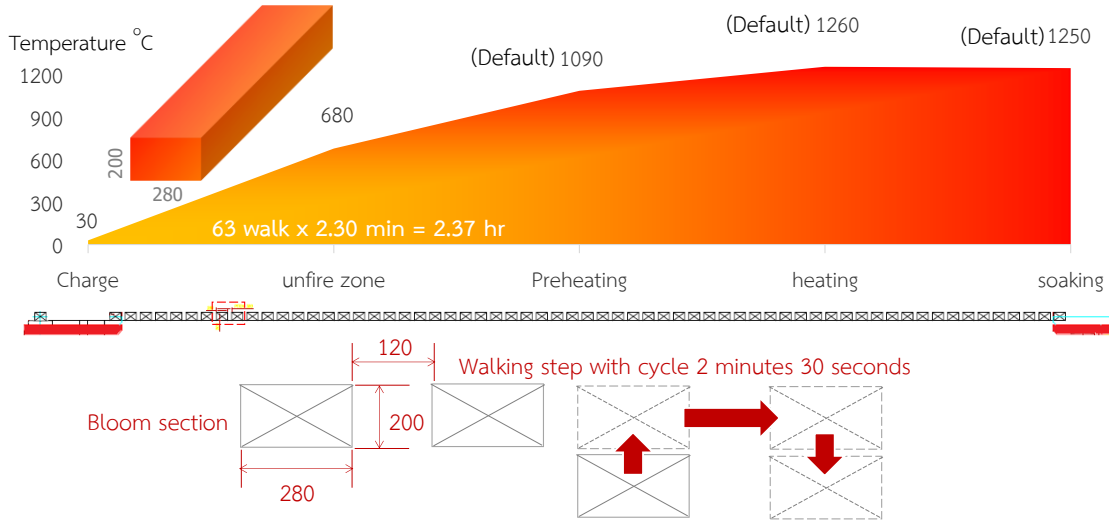

Figure 1 Default of furnace heating pattern and handling controlled

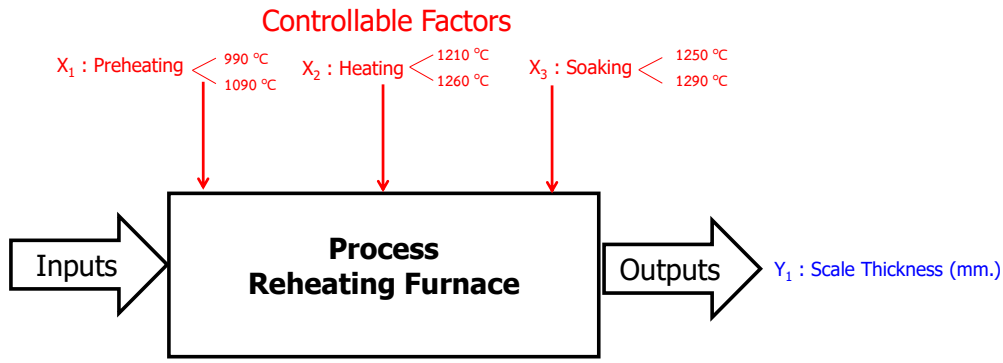

Figure 2 Input variable factor with experimental level

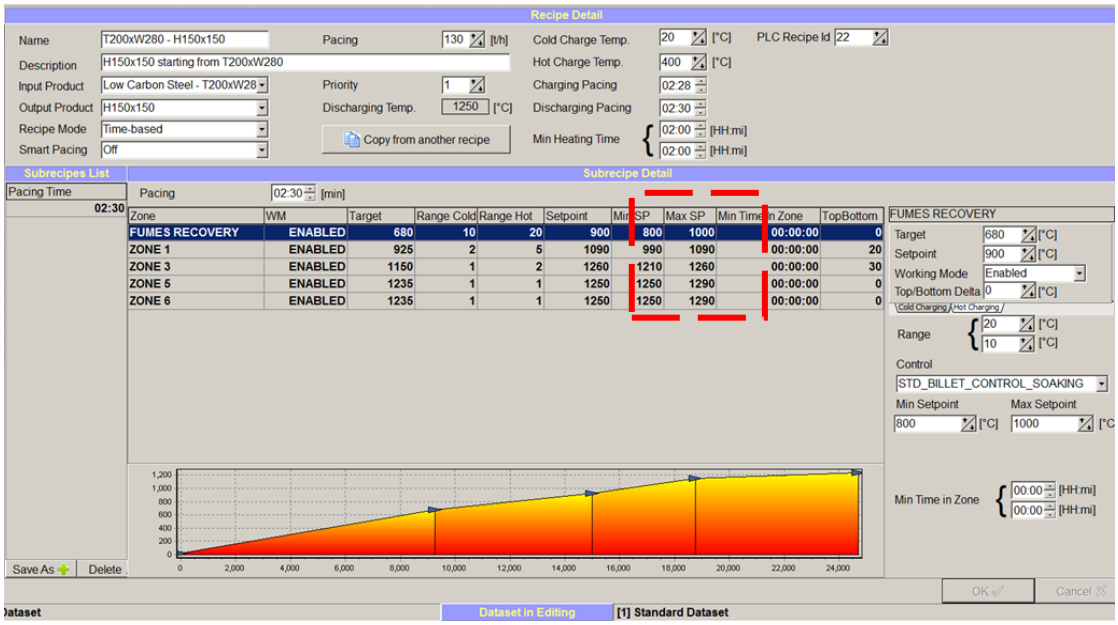

Figure 3 The temperature control criteria for each combustion zone in the setup recipe

Table 1 Input variable factors and level of factor

Input Variable Factors	*Level of factor : K*	
Controllable Factors	*Low (-1)*	*High (+1)*
X_1 : Preheating Temperature ^oC	990	1090
X_2 : Heating Temperature ^oC	1210	1260
X_3 : Soaking Temperature ^oC	1250	1290

The billets are charged into the furnace using a charging machine. During the process of reaching a steady state under different conditions, as per the experimental design, only 1 out of 63 billets in each of the 16 batches (a total of 16 billets) was rejected by the discharging machine. The response variable (Y1), which represents the scale thickness, is measured using a certified and calibrated micrometer (Mitutoyo IP65).

The scale thickness measurement follows the same standardized procedure used for measuring the thickness of test specimens in the laboratory. The laboratory is accredited under ISO 17025 by the Thai Industrial Standards Institute (TISI). Measurements are taken at three specific locations on the billets—head, middle, and tail—as illustrated in Figure 4. Each measurement point is measured twice, and the average value is used. The measuring instruments are calibrated according to internal standards and comply with the requirements of ISO 17025.

Results and Discussion

Results of temperature determining for scale minimization by experimental design

In this experiment, general full factorial analysis was implemented to evaluate, there are 16 totals run based on condition of 3 input factors and 2 levels of factor with 2 replicated of tests. The result of statistic power and samples size is 0.936743 with 0.05 significant level in 95% confidential level as shown in Figure 5.

The response of scale thickness (Y_1) are measured and averaged at three position of head middle and tail by instrument of micrometer following as run order of experiment tested with three input variable factors and two levels of preheating zone temperature (X_1), heating zone temperature (X_2) and soaking zone temperature (X_3). There are 16 results of 16 experiments from 2^3 general full factorial with 2 replicates. The average of scale thickness are varied from 0.396 mm. to 1.117 mm. The responses of data was recorded following as Table 2.

According to Figure 6, the residual plots for the response variable were analyzed to evaluate the adequacy of the statistical model. The residual analysis was conducted using a 4-in-1 residual plot, which includes the Normal Probability Plot, Versus Fits Plot, Histogram, and Versus Order Plot to assess model assumptions and reliability.

The Normal Probability Plot indicates that the residuals are approximately normally distributed, as most data points align well with the reference line, suggesting no significant deviation from normality. The Versus Fits Plot shows a random scatter of residuals without any discernible pattern, confirming that the residuals do not exhibit systematic trends related to the predicted values. The Histogram of residuals displays a roughly symmetric shape, further supporting the assumption of normality, although minor deviations are observed. Lastly, the Versus Order Plot demonstrates that the residuals are randomly distributed over time, indicating no autocorrelation or systematic bias. The Overall, the residual plots confirm that the assumptions of normality, independence, and homoscedasticity are reasonably met.

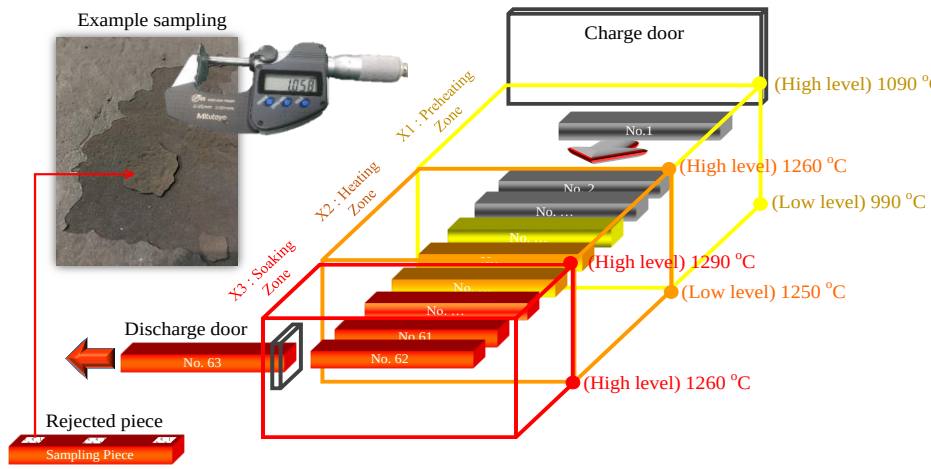

Figure 4 Scale thickness measured

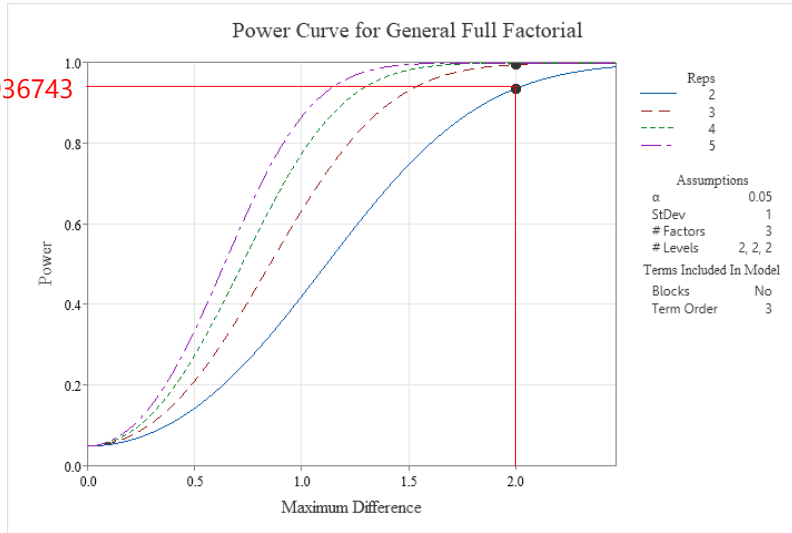

Figure 5 Power and errors of sample size for general full factorial in experimental design

Table 2 Result of response as standard run of experimental design

Standard run	Temperature Factor ^{o}C			Y_1 : Scale Thickness (mm.)			
	X_1	X_2	X_3	Head	Middle	Tail	Average
1	990	1210	1250	0.447	0.428	0.433	0.436
2	990	1210	1290	0.712	0.709	0.715	0.712
3	990	1260	1250	0.849	0.823	0.842	0.838
4	990	1260	1290	1.056	1.012	1.094	1.054
5	1090	1210	1250	0.431	0.411	0.421	0.421
6	1090	1210	1290	0.694	0.676	0.688	0.686
7	1090	1260	1250	0.839	0.746	0.809	0.798
8	1090	1260	1290	0.988	0.976	0.991	0.985
9	990	1210	1250	0.407	0.375	0.406	0.396
10	990	1210	1290	0.716	0.675	0.706	0.699
11	990	1260	1250	0.861	0.896	0.898	0.885
12	990	1260	1290	1.141	1.098	1.112	1.117
13	1090	1210	1250	0.425	0.398	0.416	0.413
14	1090	1210	1290	0.737	0.721	0.756	0.738
15	1090	1260	1250	0.915	0.856	0.911	0.894
16	1090	1260	1290	1.054	1.021	1.042	1.039

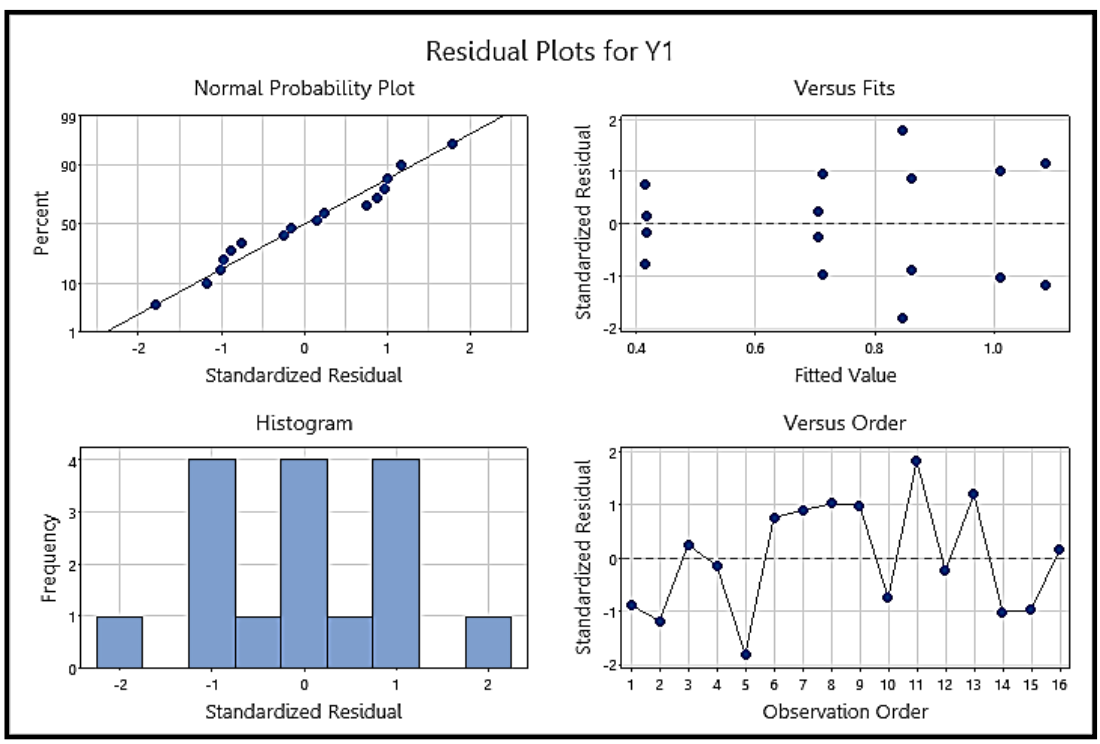

Figure 6 Residual plots on response

Table 3 Analysis of Variance for Average

Source	DF	SS	MS	F-Value	P-Value
Model	7	0.856673	0.122382	85.71	0.000
Linear	3	0.843191	0.281064	196.83	0.000
X_1	1	0.001661	0.001661	1.16	0.312
X_2	1	0.604118	0.604118	423.07	0.000
X_3	1	0.237413	0.237413	166.26	0.000
2-Way Interactions	3	0.012475	0.004158	2.91	0.101
X_1*X_2	1	0.002328	0.002328	1.63	0.237
X_1*X_3	1	0.000689	0.000689	0.48	0.507
X_2*X_3	1	0.009458	0.009458	6.62	0.033
3-Way Interactions	1	0.001008	0.001008	0.71	0.425
$X_1*X_2*X_3$	1	0.001008	0.001008	0.71	0.425
Error	8	0.011424	0.001428		
Total	15	0.868097			

According Table 3 demonstrate the results from the Analysis of Variance (ANOVA) indicate that the overall model is statistically significant, with an F-Value of 85.71 and a P-Value of 0.000, suggesting that at least one of the examined factors has a significant effect on the response. When analyzing the main effects, it was found that X_2 (P-Value = 0.000) and X_3 (P-Value = 0.000) significantly influence the response, whereas X_1 (P-Value = 0.312) does not exhibit a significant effect. This implies that variations in X_2 and X_3 contribute significantly to changes in the response, while X_1 does not play a critical role in determining the outcome.

In terms of interaction effects, the two-way interaction between $X_2$and X_3 (P-Value = 0.033) was found to be statistically significant, indicating that the combined influence of these two factors has a notable impact on the response. However, other interaction terms, including X_1X_2 (P-Value = 0.237), X_1X_3 (P-Value = 0.507), and the three-way interaction $X_1X_2X_3$ (P-Value = 0.425), did not show statistical significance, suggesting that their combined effects do not meaningfully alter the response.

Table 4 Coefficients for Average

Term	Coef	SE Coef	T-Value	P-Value	VIF
Constant	0.75694	0.00945	80.12	0.000	
X_1					
990	0.01019	0.00945	1.08	0.312	1.00
X_2					
1210	-0.19431	0.00945	-20.57	0.000	1.00
X_3					
1250	-0.12181	0.00945	-12.89	0.000	1.00
X_1*X_2					
990 1210	-0.01206	0.00945	-1.28	0.237	1.00
X_1*X_3					
990 1250	-0.00656	0.00945	-0.69	0.507	1.00
X_2*X_3					
1210 1250	-0.02431	0.00945	-2.57	0.033	1.00
$X_1*X_2*X_3$					
990 1210 1250	0.00794	0.00945	0.84	0.425	1.00

Further analysis of the coefficients as per Table 4 provides additional insights into the magnitude and direction of the effects. X_2 has a coefficient of -0.19431, and X_3 has a coefficient of -0.12181, both with P-Values of 0.000, confirming that increases in X_2 and X_3 result in a decrease in the response variable. In contrast, X_1 has a coefficient of 0.01019 with a P-Value of 0.312, reaffirming that its effect is not statistically significant. The interaction between X_2 and X_3 has a coefficient of -0.02431 with a P-Value of 0.033, indicating that the joint effect of these two factors leads to a further reduction in the response. The other interaction terms exhibit higher P-Values, confirming that they do not contribute significantly to the variation in the response variable.

Based on these findings, it can be concluded that X_2 and X_3 are the primary factors influencing the response, both individually and in combination with each other, while X_1 does not play a significant role in determining the outcome. This highlights the importance of considering X_2 and X_3 when optimizing the response variable, as well as acknowledging the interaction effect between them. Future studies may further investigate the underlying mechanisms driving these relationships and explore potential modifications to improve predictive accuracy.

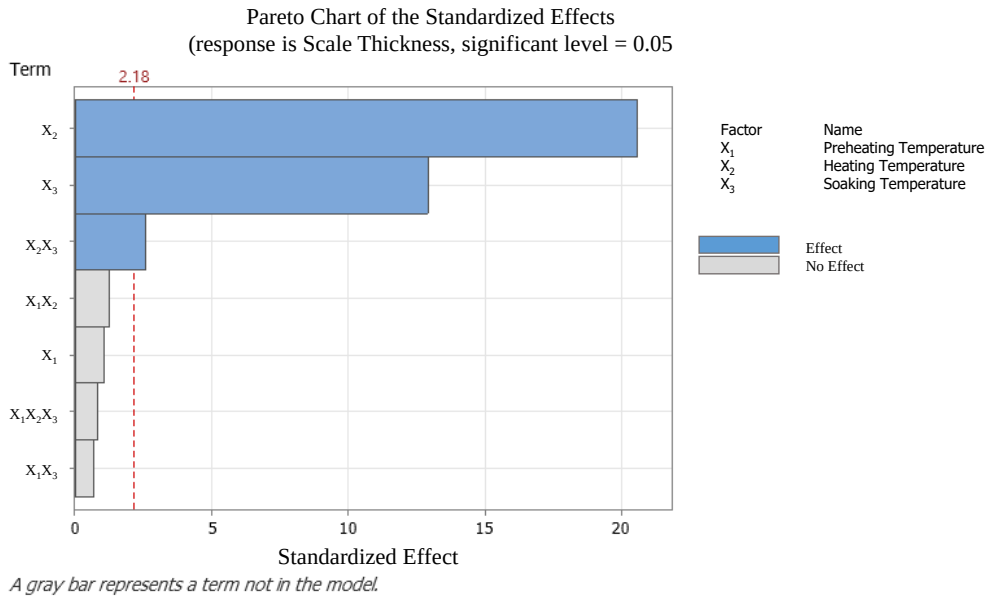

Figure 7 The statistically significant factors affecting the response by Pareto chart

Figure 7 shows the results analysis of standardized effect by pereto chart. There are only 2 out of 3 main input variable factor of heating zone temperature (X_2) and soaking zone temperature (X_3) are affected to the differentiate of scale thickness in the reheating furnace whereby the heating zone temperature (X_2) has the significantly greatest effect and soaking zone temperature (X_3) has the lower than heating zone temperature (X_2) effect meanwhile, both of main effect factors are also interaction between factor of heating and soaking temperature but the preheating zone temperature of X_1 has on effect to the changed of scale thickness.

The result of general full factorial analysis were analyzed to evaluate the correlation of input variable factors with the mean values of the scale thickness by analysis of variance (ANOVA). The details of effect are analyzed by main and interaction effect plot. The results of factorial analysis are demonstrated in Figure 8 for main effect and for interaction between factor effects.

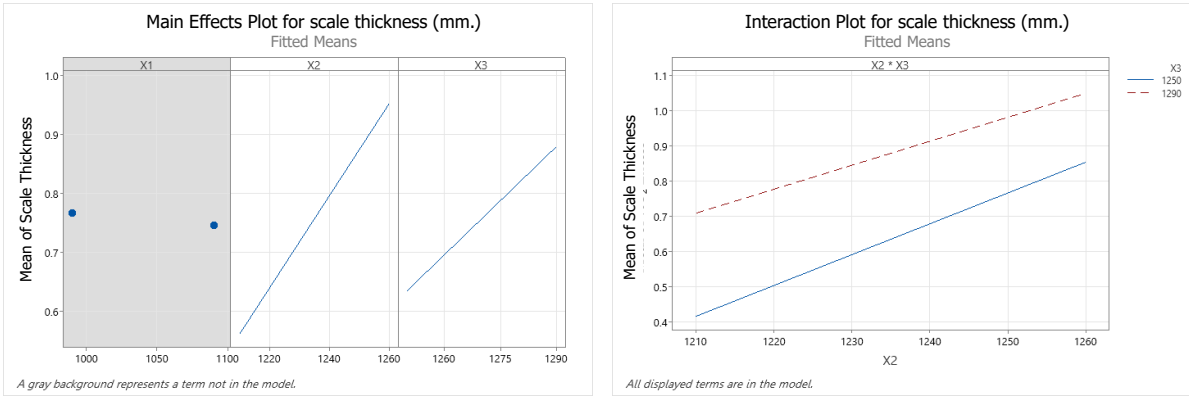

Figure 8 Main effect plot and interaction plot of each input variable factors for scale thickness

Figure 8 shows the factors affecting the change of scale thickness during reheating process. The variable input factors of preheating zone temperature (X_1) has no effect to the response and would not in term of model. In meanwhile heating zone temperature (X_2) and soaking zone temperature (X_3) are significantly affected to growth of scale thickness. The largest inclination of (X_2) heating zone temperature has the highest effect, the runner up inclination is (X_3) soaking zone temperature. The result only main effect and interaction effect of input variable factors, the lowest of scale thickness are result from low level of X_2 at 1210 Celsius degrees and while low level of X_3 at 1250 Celsius degrees.

The results of scale thickness value is optimized by response optimizer in Figure 9. The optimal of scale thickness minimization are analysed and predicted through regression. The optimization are demonstrated that value of input variable factors that affected the lowest of scale thickness at 0.4165 mm. There are set temperature of heating zone (X_2) at low level of 1210 Celsius degrees, also of soaking zone (X_3) at low level of 1250 Celsius degrees with result desirability 0.9716. The growth of scale thickness is predicted by regression equation (1)

$$Y_1 = -92.8 + 0.0695\ X2 + 0.0661\ X_3 - 0.000049\ X_2{*}X_3 \quad (1)$$

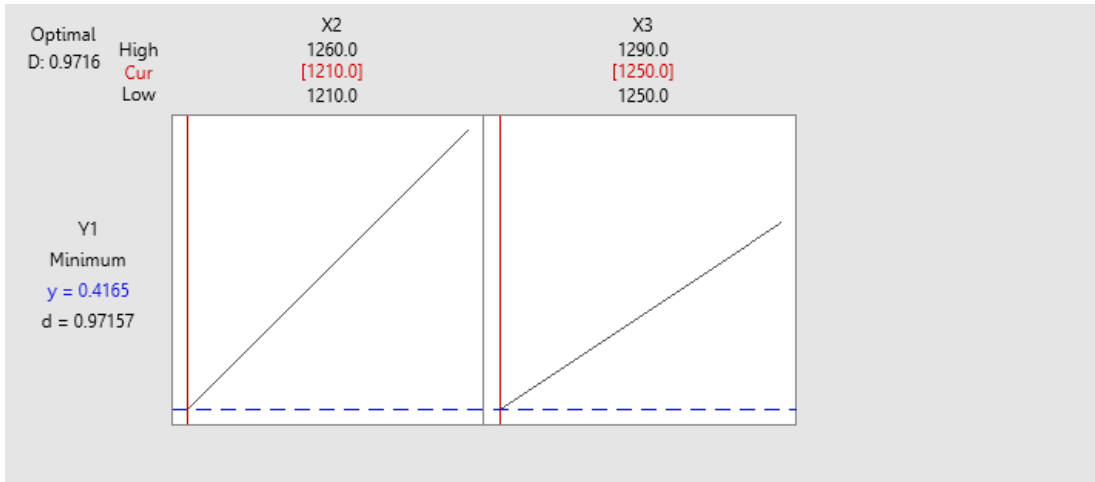

Figure 9 Response of scale thickness optimization

Process implemented and compared the differential between exist set point and optimize set point the improvement by 2 sample t test

The process implementation is retested by comparison between before and after experimental design. The beginning test is set all of parameter as a default factory data and after is set all of parameter as an optimizing data from experimental design. The result between before and after is compared by hypothesis 2 sample t-test with 0.05 significant level. The result of hypothesis test is significant difference by P-Value of 0.000.

Regarding As a results of scale thickness value is optimized in Figure 8. The process implementation are set following as optimizer of (X_2) heating temperature at low level of 1210 Celsius degrees, also of soaking zone (X_3) at low level of 1250 Celsius degrees. Fiure11 shows the bow plot of scale thickness reduction rate is compared between before and after improvement. Result indicates that the growth of scale thickness is significantly reduced. The average growth of experiment are reduced from 0.7644 mm. to 0.4670 mm. as Figure 10. Due to temperature optimization, the decrease in scale thickness contributed to a reduction in total annual factory waste loss from scale oxide, lowering it from 2.29% to 1.22%, as reference reported in the 2023 case study factory report.

According discussed to empirical equation of E. M. Kotliarevsky [5], the actual result of scale thickness is lower than empirical equation of E. M. Kotliarevsky [5] and kinetic parameter [6] at 2.525 mm. and 1.025 respectively. After using set point of optimization, the existing set point is reduced from 0.764 mm. to 0.467 mm. as Figure 11.

In this paper is only experimental designed for temperature optimized to minimized growth of scale formation in walking beam reheating furnace but the significant effect of oxygen excess and heating time are not evaluated. Three significant factor of temperature, oxygen level and heating time including to evaluate of side effect and engineering economic [10].

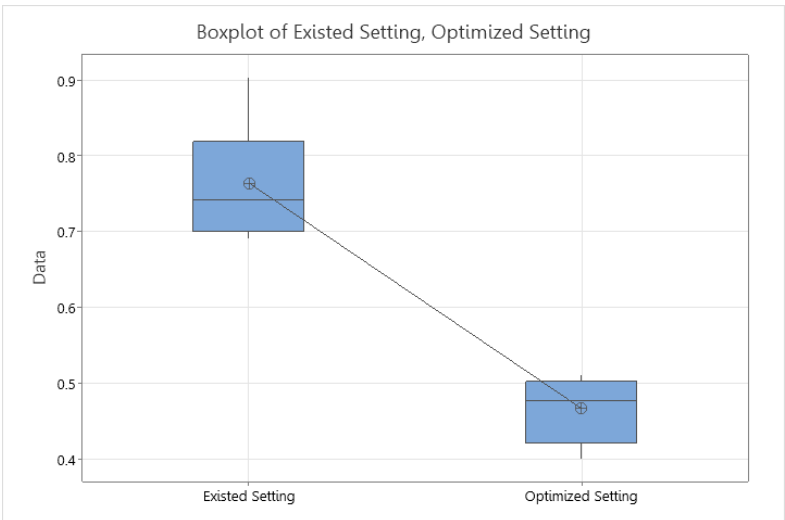

Figure 10 Boxplot of exist setting and optimized setting

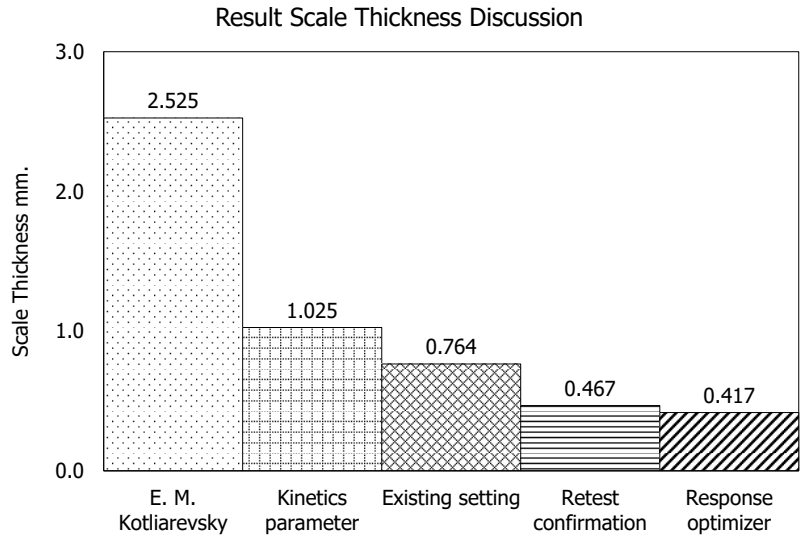

Figure 11 Result discussion and comparison

Conclusions

The reheating furnace is always highly oxidizing and the billet are heated up and rate of scaling will increase as the surface temperature. The one of several wasted in steel manufacturing is scale formation. The effect of highly temperature of furnace are cause of iron oxide or scale formation. In this research is involved the method of temperature determining to maintain a low scale formation that the thickness of scale are collected and measured by instrument of micrometre and the method of design of experiment are defined by 16 experimental of 2^3 general full factorial design of 2 levels with 3 input variable factors multiply by 2 replicates with statistic power of 0.9367 and analyses by analysis of variance (ANOVA) and the minimum of scale thickness are analysed. There are only 2 main input variable factors of heating zone (X_2) and soaking zone (X_3) effect to response. The result demonstrated that the optimization value that made the lowest of scale thickness at 0.4165 mm. at 95% confidential interval (0.3754, 0.4576) where was set temperature of heating zone (X_2) at low level of 1210 Celsius degrees and while temperature of soaking zone (X_3) was set at low level 1250 Celsius degrees but results of heating zone (X_2) and soaking zone (X_3) are related by interaction between factors. There is a reason of result indicates that the difference of scale thickness between exist and optimum set point is significantly differed. The scale thickness of experiment are reduced from 0.7644 to 0.4670 with standard deviation of 0.0748 and 0.0411 respectively. For future research, addressing the limitations of this study is essential. It is crucial to comprehensively consider other key factors, including (1) oxygen levels, (2) steel residence time duration, (3) air pollution factors such as nitrogen oxides and carbon monoxide, and (4) thermal efficiency. Additionally, both the engineering and economic implications of scale minimization should be evaluated. Incorporating these factors into future studies will provide a more comprehensive understanding of the overall benefits of scale oxide formation in industrial processes.

References

[1] Kargin, J. 2022. Characterization of iron oxide waste scales obtained by rolling mill steel industry. Hyperfine Interactions. 243: 14.

[2] SMS Group. 2009. 2131E783 Furnace control system maintenance and user manual. In Control system for walking beams furnace human mahcine interface. SMS – MEER Manual Instruction. 1(3): 1-59.

[3] Soek, B. H., Soon, H. H., Seok, C. S., Deuk, J. Y. and Won, J. S. 2010. Optimization of process parameters for

recycling of mill scale using Taguchi experimenal design. Journal of Mechanical Science and Technology. 24 (10): 2127-2134.

[4] Dubey, S. K. 2014. Steel billet reheat simulation with growth of oxide layer and investigation on zone temperature sensitivity. Journal of Mechanical Science and Technology. 28(3): 1113-1124.

[5] Shri, T. P., Shri, P. K., Bahl, V. and Shri, D. S. 2015. A review on efficient energy optimization in reheating furnaces. International Journal of Mechanical And Production Engineering. 3(2): 2320-2092.

[6] Jung, J. H., Dong, L. E. and Man, K. Y. 2010. Investigation of the slab heating characteristics in a reheating furnace with the formation and growth of scale on the slab surface. International Journal of Heat and Mass Transfer. 53: 4326-4332.

[7] Heng-Hsing, C., Yuan-Liang, H. and Chao-Hua, W. 2011. Control Method for Low Oxygen Concentration in Reheating Furnace. China Steel Corporation, Iron and Steel Research & Development Department. China Steel Technical Report. 24: 20-27.

[8] Sung, Y. 2021. Nitric Oxide Emission Reduction in Reheating Furnaces through Burner and Furnace Air-Staged Combustions. Energies. 14: 1599.

[9] Schwotzer, C. 2018. Low scale reheating of semi-finished metal products in furnaces with recuperative burners. Applied Thermal Engineering. 128: 586-594.

[10] Koushik, C. and Sunil, K. 2020. Increase in energy efficiency of a steel billet reheating furnace by heat balance study and process improvement. Energy Reports. 6: 343-349.

Thai Environmental Engineering Journal Vol. 39 No. 1 (2025) : 51-58
www.eeat.or.th

Antibiotic Contamination in Wastewater of Phranangklao Hospital

Jaruwan Manui[1], Nuttaporn Pimpha[2], Chainarong Sakulthaew[3], Chanat Chokejaroenrat[4] and Peerakarn Banjerdkij[1*]

[1*]Department of Environmental Engineering, Faculty of Engineering, Kasetsart University, Bangkok 10900, Thailand
[2]National Nanotechnology Center, National Science and Technology Development Agency, Thailand Science Park, Pathum Thani 12120, Thailand
[3]Department of Veterinary Nursing, Faculty of Veterinary Technology, Kasetsart University, Bangkok 10900, Thailand
[4]Department of Environmental Technology and Management, Faculty of Environmental Science, Kasetsart University, Bangkok 10900, Thailand
[*]E-mail : fengpkba@ku.ac.th

Article History; *Received: 18 December 2024, Accepted: 10 April 2025, Published: 30 April 2025*

Abstract

The issue of residual antibiotics in wastewater from hospital treatment systems has become a major factor driving the emergence of antimicrobial resistance globally. This study investigates the sources and evaluates the extent of antibiotic contamination in hospital wastewater, with a case study of Phranangklao Hospital in Nonthaburi Province. Wastewater samples were collected from three representative buildings: Jindamanee Building (Outpatient Department Building; OPD Building), the 18-story Medical Center Building (Inpatient Department Building; IPD Building) and Ngeun Tung Daeng Building (Hemodialysis Building) in April 2024. Samples were also taken from the hospital's centralized wastewater treatment system, including influent, the flow measurements tank, effluent from the sedimentation tanks using both grab sampling and composite sampling methods, and the effluent discharge points in December 2023, during the dry season to minimize contamination from rainwater. Sampling was conducted between 10:00 a.m. and 12:00 p.m., during peak hospital water usage periods. The results showed that the IPD Building had the highest contamination levels, followed by the OPD Building and the Hemodialysis Building. Sulfamethoxazole (SMX) was the most frequently detected antibiotic across all operational units, indicating its environmental persistence. The hospital's centralized wastewater treatment system was able to reduce certain antibiotic residues, such as ciprofloxacin (CIP), by more than 90%, but SMX was still found in the treated effluent. The study highlights the need for improvements in hospital wastewater treatment systems to reduce antibiotic residues in effluent, as well as to minimize contamination at the source, such as from various medical activities. The findings can serve as a foundation for developing effective wastewater treatment measures and contamination control strategies to prevent long-term environmental and health impacts.

Keywords : Antibiotics; Hospital wastewater treatment system; Activated sludge treatment system

Introduction

Currently, the contamination of antibiotics in hospital wastewater has been increasingly detected in various areas of Thailand. This issue has garnered significant attention as the wastewater treatment systems in many hospitals are inefficient in removing antibiotics and their derivatives. This leads to residual antibiotics in the environment, particularly in natural water bodies that receive untreated or inadequately treated hospital wastewater [1-2]. This problem has become a critical concern that is being studied and addressed globally. Residual antibiotics in the environment can spread widely, with contamination levels in natural environments ranging from nanograms to micrograms per liter [3-4]. These antibiotics are persistent and resistant to natural degradation, resulting in environmental accumulation. This poses a risk of antimicrobial resistance (AMR) that can spread through food chains and impact humans, particularly in cases where bacterial infections fail to respond to treatment, potentially leading to fatalities [5-7]. Antibiotics found in hospital wastewater and natural environments are from various groups, such as beta-lactams, tetracyclines, and sulfonamides. Thus, reducing the contamination of antibiotics in hospital wastewater before it enters natural environments, especially water bodies, is the best preventive approach. [8] One key strategy is improving centralized wastewater treatment systems in hospitals to enhance treatment efficiency. Additionally, efforts should focus on reducing antibiotic contamination at the source, originating from various hospital activities. An assessment of relevant legal tools in Thailand reveals that hospital wastewater is regulated under the "Standards for Controlling Wastewater Discharge from Certain Types and Sizes of Buildings." [9] In this regulation, hospital wastewater must undergo additional bacterial control before discharge, limiting Total Coliform Bacteria to no more than 5,000 MPN/100 ml, Fecal Coliform Bacteria to no more than 1,000 MPN/100 ml, and Residual Chlorine to a range of 0.2-1.0 mg/l as Cl_2, in compliance with the Hospital Accreditation (HA) standards set by the Institute of Hospital Quality Improvement and Accreditation under the Ministry of Public Health [10]. However, there are currently no established thresholds for antibiotics discharged into the environment. Preventing and controlling antibiotic contamination requires process improvements related to the removal of antibiotics from hospital wastewater sources. This study aims to identify and quantify antibiotic residues in wastewater from Phranangklao Hospital. It evaluates the effectiveness of current treatment processes in removing these contaminants. Seasonal variations in antibiotic levels will also be analyzed. The research assesses potential environmental and health risks, particularly in relation to antimicrobial resistance. Finally, it proposes strategies to improve hospital wastewater management and reduce antibiotic pollution.

Equipment and Methods

Survey on the usage and dispensing of target antibiotics in 8 groups or at least 5 groups of Phranangklao Hospital under the guidance of the Department of Health and surveying sources of pollution to find the origins of antibiotics. Collecting wastewater samples was done by grab sampling aligned with the sampling requirements for wastewater characteristics following the wastewater standard [10]. Before collecting samples, all containers were cleaned and sterilized to prevent contamination. Samples were immediately placed in sterile, amber glass bottles to minimize photodegradation of antibiotic compounds. Transportation to the laboratory was conducted in cooled containers (4°C), and analysis was carried out within 24 hours to ensure sample integrity. To study the origins of hospital antibiotics, wastewater samples were collected from representative buildings: Jindamanee Building (Outpatient Department Building; OPD Building), 18-story Medical Center Building (Inpatient Department Building; IPD Building), and Ngeun Tung Daeng Building (Hemodialysis Building), as shown in Figure 1. Collection of water samples from the Completely Mix Activated Sludge (CAS) was made as follows: grab sampling for influent (S1), flow measurements tank (S2), sedimentation tank (S3), composite sampling for sedimentation tank (S4), and effluent (S5), as shown in Figure 2. Sampling was conducted from 10:00 to 12:00 a.m., during the peak hospital water usage periods (it is thought that there was a high use of

antibiotics during that time period). The highest wastewater flow rates were recorded between 8:00 a.m. and 3:00 p.m. [11]. The confirmation of the type and amount of antibiotic residues in the wastewater sources and the Completely Mixed Activated Sludge (CAS) wastewater treatment system of Phranangklao Hospital was conducted. The type and amount of antibiotics detected in the wastewater were analyzed by preparing wastewater samples for antibiotic quantification following EPA Method 1694 (2007) [12] and analyzing them using LC/MS/MS and LC/MS/MS-QTOF techniques.

Experimental Results and Discussion

Antibiotic Contamination in Wastewater from Phranangklao Hospital

From the survey of wastewater from buildings on March 8, 2024, along with interviews with responsible officials, it was found that most antibiotic contamination in hospital wastewater comes from the excretion of waste of the patients, which is a major source of antibiotic contamination in the hospitals. The source of antibiotic contamination from service buildings is the OPD Building, IPD Building, and Hemodialysis Building. Collecting wastewater samples from the service buildings was performed during the dry season (April 2024) to reduce the chance of contamination from rainwater, as shown in Figure 1: For the OPD Building, wastewater samples were selected from the 3 toilets of outpatient users only to avoid collection of wastewater from the toilets of hospital staff. The wastewater sampling location in the building is an equalization tank (EQ). For the IPD Building, wastewater samples are taken from the overnight patient water usage activities only, such as toilets, showers, and sinks. The wastewater sampling point is outside the building, which is the collection point of the buildings before entering Completely Mix Activated Sludge (CAS). The hemodialysis building is used for dialysis only but has 3 main water usage activities including (1) dialysis water for patients during treatment (2) water for washing vessels and dialysis cones, and (3) RO wastewater. Due to the nature of water usage in the Hemodialysis Building, it is necessary to install specific water sampling equipment for each activity to enable detailed analysis of residual antibiotics, as the combination of wastewater from different activities may affect the analysis of antibiotic contamination resulting from the treatment of hemodialysis patients.

Antibiotic content in wastewater from the representative buildings

The study results revealed that the IPD Building had the highest amount of antibiotic contamination, followed by the OPD Building and Hemodialysis Building, respectively, as shown in Table 1, which is consistent with the data of Panadda, 2562 [13], Chiemchaisri W., *et al*. (2022) [14], Hamjinda *et al*. (2018) [15], Muhammad T.K *et al*. (2021) [16], Rozman U., *et al*. (2020) [17], which reported higher antibiotic loads in wastewater from inpatient activities due to greater water use. Sulfamethoxazole (SMX) was the most frequently detected antibiotic, present in all collected samples, reflecting its persistence in the environment. Previous studies corroborate SMX's widespread presence in river water, wastewater, and imported fish, highlighting its environmental resilience. According to Si LY.L. *et al*. (2022) [8], a study on antibiotics in rivers worldwide across 76 countries, encompassing over 600 research articles from 1999 to 2021 and collecting more than 90,000 data points, revealed the presence of 169 types of antibiotics in river water and sediments. Sulfamethoxazole (SMX) and trimethoprim (TMP) were found to be the most persistent, with average concentrations in river water at 4,320 ng/L and 1,200 ng/L, respectively. The data also indicated that the continents with the highest levels of antibiotic contamination in rivers were Africa, followed by Asia. These findings suggest that SMX and TMP can serve as effective indicators of environmental antibiotic contamination. The persistence of SMX and other antibiotics in hospital wastewater poses a significant risk for the development and spread of antimicrobial resistance (AMR). Their continued presence in effluents discharged into municipal wastewater systems or natural water bodies could contribute to the proliferation of resistant bacteria, which has global public health implications. Therefore, monitoring and managing antibiotic residues in hospital wastewater is essential for reducing the risk of AMR spread.

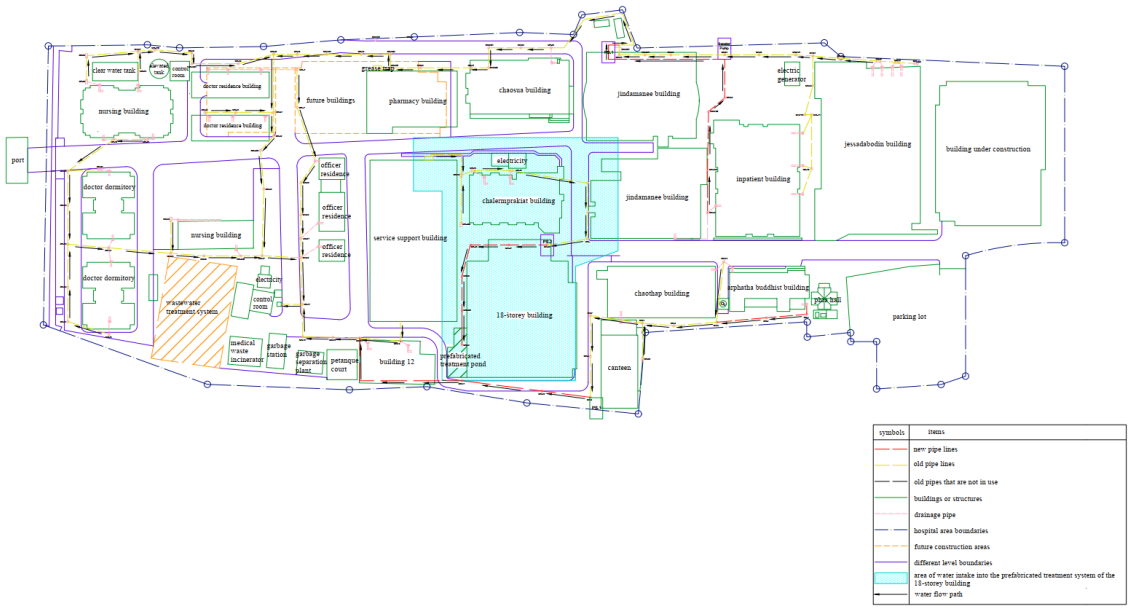

Figure 1 Diagram of wastewater collection system of Phranangklao Hospital

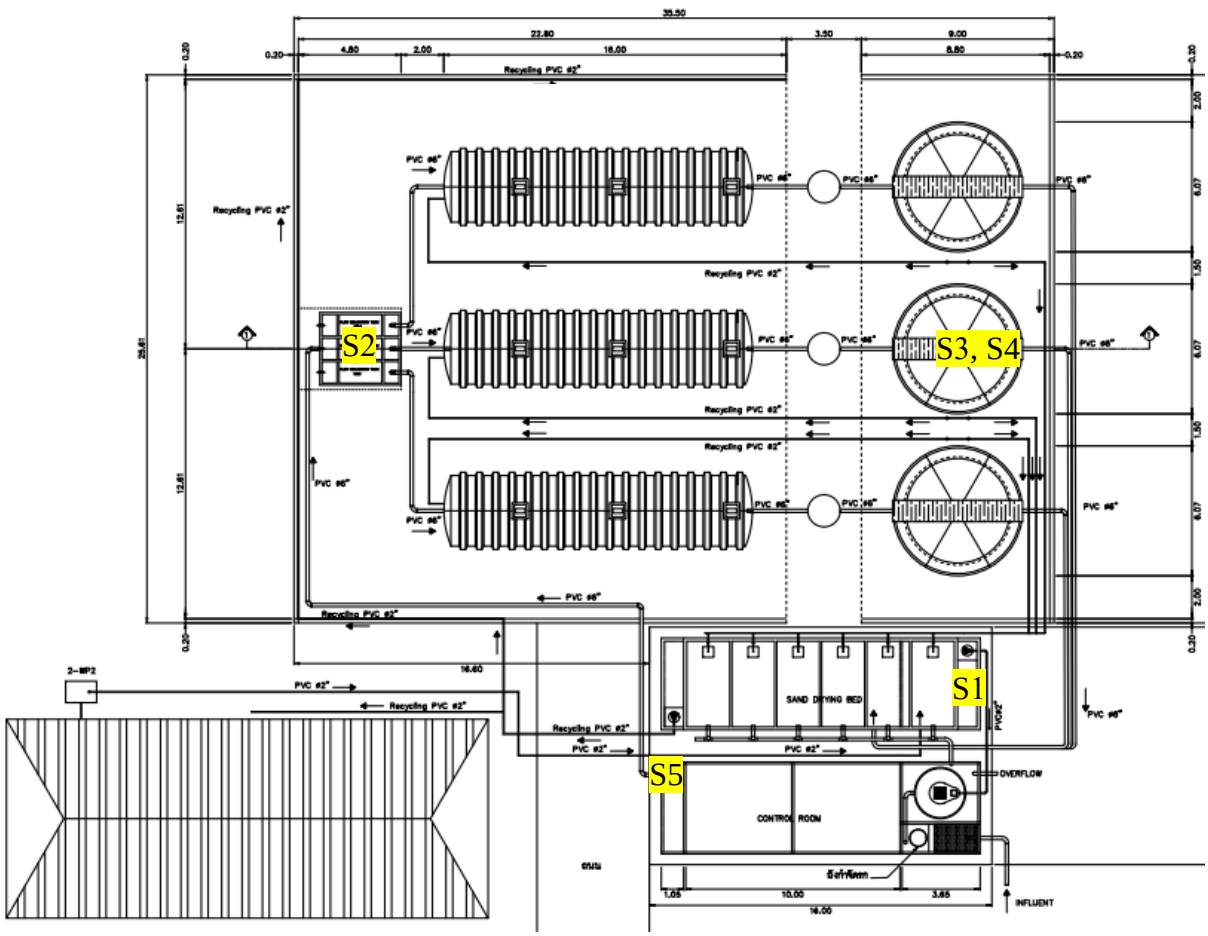

Figure 2 Wastewater sampling point of the Completely Mix Activated Sludge (CAS) wastewater treatment system

Table 1 Amount of antibiotics detected in wastewater of representative buildings

Group	Antibiotic group	Antibiotic name	Antibiotic Concentration (µg/L)[1]		
			OPD building	IPD building	Hemodialysis building
1	Beta-Lactam	Ampicillin	0.061-1.134	0.709-3.645	0.412-2.219
3	Cephalosporin	Ceftriaxone	NF-0.238	NF-0.184	NF-3.619
4	Macrolide	Erythromycin	NF-10.129	NF	NF
5	Tetracycline	Oxytetracycline	NF-0.504	NF-0.647	NF-0.176
		Doxycycline	NF	NF	NF
6	Quinolones	Ofloxacin	NF-1.131	0.275-2.511	NF
		Levofloxacin	NF-1.152	0.264-2.377	NF
		Norfloxacin	0.137-0.626	0.148-1.926	NF-0.059
7	Sulfonamide	Sulfadiazine	NF	NF	NF-0.674
		Sulfamethoxazole	NF-0.924	0.369-40.620	NF
		Trimethoprim	NF-0.051	NF-4.097	NF

Note: [1/] Wastewater samples were collected from buildings before entering the hospital's centralized wastewater treatment system during the dry season (April 2024).
NF = Not Found

Amount of antibiotics detected in the centralized wastewater treatment system of Phranangklao Hospital

Confirmation of the type and amount of antibiotic residue in the Completely Mix Activated Sludge (CAS) wastewater treatment system of Phranangklao Hospital was made. Therefore, the research team chose to collect wastewater samples in December 2023 (dry season) at the water sampling points, including grab sampling for influent (S1), flow measurements tank (S2), sedimentation tank (S3), composite sampling for sedimentation tank (S4), and effluent (S5), as shown in Figure 2. Table 2 shows the study results of the amount of antibiotics detected in wastewater of the Completely Mix Activated Sludge (CAS) wastewater treatment system in December 2023. It was found that the wastewater entering the system had the highest amount of contamination of ciprofloxacin (2.091-6.456 µg/l), followed by ampicillin (0.474-4.747 µg/l) and ceftriaxone (NF-2.726 µg/l), respectively. The difference in the amount of antibiotics detected by the method of collecting water samples from the sedimentation tank using grab sampling (S3) or composite sampling (S4) showed no difference. However, composite sampling is recommended due to the operational nature of the hospital's wastewater treatment system, which functions intermittently, especially during peak hours (10:00–12:00 a.m.). When considering the half-life of antibiotics in water, it was found to be less significant compared to the solubility of each antibiotic. For instance, amoxicillin (AMX), with a half-life of 20 days [18], was not detected in any of the sampled water at positions S1–S5. Conversely, sulfamethoxazole (SMX), which has a shorter half-life of only 4.9 days [19], was detected in all samples. The degradation ratio of SMX varied across different treatment stages, from influent wastewater (S1) through primary treatment (S2) and secondary treatment (S3, S4). While SMX showed partial degradation during

Table 2 Amount of antibiotics detected in the Conventional Activated Sludge (CAS) system of Phranangklao Hospital

Group	Antibiotic group	Antibiotic name	Antibiotic Concentration (µg/L) [1/]					Half-life in water [2/]
			S1	S2	S3	S4	S5	
1	Beta-Lactam	Amoxicillin	NF	NF	NF	NF	NF	20 days
		Ampicillin	0.474-4.747	0.792-2.481	0.094-0.420	0.174-0.468	0.111-0.577	27 days
3	Cephalosporines	Ceftriaxone	NF-2.726	NF-2.530	NF	NF	NF	4.1 days
4	Macrolide	Clarithromycin	0.011-0.292	0.016-0.372	0.003-0.046	0.005-0.050	0.005-0.045	2 hr.
5	Tetracyclines	Oxytetracycline	0.377-0.400	0.295-0.450	0.340-0.498	0.320-0.403	0.365-0.400	66 hr.
		Doxycycline	0.450-0.665	0.402-0.618	0.251-0.301	0.278-0.307	0.241-0.281	107 hr.
6	Quinolone	Ofloxacin	0.435-1.301	0.773-2.542	0.388-0.662	0.274-0.692	0.391-0.488	10.6 days
		Levofloxacin	0.388-1.310	0.817-2.493	0.398-0.626	0.254-0.695	0.406-0.477	6.3 days
		Norfloxacin	1.062-1.663	0.648-1.178	0.083-0.155	0.091-0.129	0.122-0.133	77 days
		Ciprofloxacin	2.091-6.456	1.304-3.189	0.086-0.224	0.098-0.203	0.165-0.197	< 46 hr.
7	Sulfonamide	Sulfadiazine	1.469-2.161	1.237-1.409	0.603-0.803	0.635-0.814	0.615-0.843	13.2 hr.
		Sulfathiazole	0.063-0.090	0.049-0.061	0.037-0.041	0.034-0.044	0.033-0.044	13 days
		Sulfamethoxazole	1.753-1.961	1.291-2.995	0.089-0.189	0.124-0.289	0.332-0.610	4.9 days
-	Diaminopyrimidines	Trimethoprim	0.266-0.447	0.190-0.412	0.009-0.014	0.010-0.014	0.010-0.014	< 11.8 days
-	Lincosamide	Lincomycin	0.021-0.038	0.030-0.049	0.007-0.009	0.007-0.009	0.006-0.009	12 days

Note: [1/] Wastewater samples were collected from the Conventional Activated Sludge (CAS) system during the dry season (December 2023)
[2/] limit of detection (LOD) = 0.003 µg/L or 3 ng/L
NF = Not Found

secondary treatment, it still persisted in the treated effluent (S5). This finding suggests that the solubility of antibiotics plays a more critical role in their detectability in wastewater than their half-life alone. Some antibiotics, despite having a relatively long half-life, such as amoxicillin (AMX), with 20 days, may not be detected in the water samples if they are poorly soluble in water, readily degraded under environmental conditions (e.g., light, temperature), or strongly adsorbed onto sludge particles during the treatment process. In contrast, antibiotics with high water solubility and low affinity for adsorption, such as sulfamethoxazole (SMX), may remain present throughout the treatment stages and persist in the final effluent, even though their half-life in water is shorter. SMX is one of the most commonly found and environmentally persistent antibiotics, particularly in water bodies, as confirmed by Si LY.L., *et al.* (2022) [8]. Although ciprofloxacin (CIP) showed higher concentrations at S1 compared to other antibiotics, it was reduced by over 90% during the wastewater treatment process. Consistent with the report by Chiemchaisri *et al.* (2022) [14], it was found that certain groups of antibiotics were removed by more than 80% in the aeration tank and were adsorbed onto sludge. Therefore, many antibiotic resistant infections can be effectively treated using the CAS system. Consequently, it is highly likely that certain types or groups of antibiotics may not be detected in the treated effluent from hospital wastewater treatment systems.

These findings affirm that the CAS system used at Phranangklao Hospital is moderately effective at removing certain antibiotics, particularly those that adsorb onto sludge or degrade readily. However, the persistence of SMX and similar compounds in the effluent highlights the limitations of conventional treatment technologies. To address this, hospitals could consider Implementing advanced treatment technologies such as membrane filtration, ozonation, or advanced oxidation processes (AOPs) to improve removal efficiency. Segregating pharmaceutical wastewater streams at the source (e.g., from pharmacy or ICU departments) for specialized treatment. Conducting routine surveillance of antibiotic residues in effluent and sludge to track long-term trends and ensure compliance with environmental safety standards.

Conclusions

The study of residual antibiotic concentrations in wastewater from buildings and the Conventional Activated Sludge (CAS) system of Phranangklao Hospital in Nonthaburi Province has provided insights into the levels of antibiotic contamination in hospital wastewater. These findings can inform the development and improvement of effective strategies for addressing antibiotic contamination. The survey revealed that Phranangklao Hospital utilizes and dispenses antibiotics across 8 target groups. Most antibiotics are treated with more than 50% efficiency at each stage of the Conventional Activated Sludge (CAS) system. However, an analysis of the types and concentrations of residual antibiotics found that ampicillin, clarithromycin, ciprofloxacin, sulfathiazole, and lincomycin were not detected in wastewater from the representative buildings. Some residual antibiotics were observed to increase in concentration within the centralized treatment system, possibly due to wastewater inflow from other service buildings. On the other hand, the concentrations of certain residual antibiotics in wastewater from representative buildings decreased upon entering the hospital's centralized wastewater treatment system, as they were biodegraded during the process. For example, amoxicillin was completely degraded within the treatment system. These findings highlight both the effectiveness and limitations of the current CAS system in treating antibiotic residues. The presence of certain antibiotics at increased concentrations after centralized treatment suggests the need for more comprehensive sampling and monitoring across all sources within the hospital. Additionally, the results emphasize the importance of optimizing existing wastewater treatment protocols and considering advanced treatment technologies to ensure the effective removal of residual antibiotics. This is crucial not only for environmental protection but also for mitigating the risk of promoting antimicrobial resistance in aquatic ecosystems.

Acknowledgments

The research project titled "Antibiotic Contamination in Wastewater of Phranangklao Hospital" was successfully completed with funding support from the National Research Council of Thailand (NRCT) for the fiscal year 2023, conducted under " Removal of antibiotic from hospital wastewater using the combination processes of ozonation and surface modification of activated carbon". The project also received invaluable cooperation from personnel and partner organizations, including the National Nanotechnology Center (NANOTEC), the National Science and Technology Development Agency (NSTDA), the Faculty of Public Health at Mahidol University, the Faculty of Veterinary Technology at the College of Integrated Science, and the Faculty of Engineering at Kasetsart University.

References

[1] Chaturvedi, P., Shukla, P., Giri, B. S., Chowdhary, P., Chandra, R., Gupta, P. and Pandey, A. 2021. Prevalence and hazardous impact of pharmaceutical and personal care products and antibiotics in environment: A review on emerging contaminants. Environmental Research. 194: 1-17.

[2] Chaturvedi, P., Chaurasia, D., Pandey, A. and Gupta, P. 2020. Co-occurrence of multidrug resistance, β-lactamase, and plasmid-mediated AmpC genes in

bacteria isolated from river Ganga, northern India. Environmental Pollution. 267: 1-12.

[3] Wang, J., Zhuan, R. and Chu, L. 2019. The occurrence, distribution, and degradation of antibiotics by ionizing radiation: An overview. Science of The Total Environment. 646: 1385-1397.

[4] Huang, Y. H., Liu, Y., Du, P. P., Zeng, L. J., Mo, C. H., Li, Y. W. and Cai, Q. Y. 2019. Occurrence and distribution of antibiotics and antibiotic-resistant genes in water and sediments of urban rivers with black-odor water in Guangzhou, South China. Science of The Total Environment. 670: 170-180.

[5] Kümmerer, K., Al-Ahmad, A. and Mersch-Sundermann, V. 2000. Biodegradability of some antibiotics, elimination of the genotoxicity, and affection of wastewater bacteria in a simple test. Chemosphere. 40(7): 701-710.

[6] Prado, N., Ochoa, J. and Amrane, A. 2009. Biodegradation and biosorption of tetracycline and tylosin antibiotics in activated sludge system. Process Biochemistry. 44(11): 1302-1306.

[7] Wang, J. and Wang, S. 2018. Activation of persulfate (PS) and peroxymonosulfate (PMS) and application for the degradation of emerging contaminants. Chemical Engineering Journal. 334: 1502-1517.

[8] Si, L. Y. L., Yang, W., Jingrun, H., Yiqing, Z., Qian, S., Weiling, S., Jiagen, G., Xiaoying, L., Dantong, J., Xiuqi, Y., Dianqing, Q., Moran, T., Yitao, L., Fanguang, K., Leilei, C., Yufan, A., Yichu, W. and Jinren, N. 2022. Antibiotics in global rivers. Earth and Environmental Sciences. 1(2): 1-21.

[9] Institute of Hospital Quality Improvement & Accreditation (IHQIA). 2005. Standards for Hospital Accreditation (HA). Ministry of Public Health, Thailand.

[10] Ministry of Natural Resources and Environment. 2005. Notification on standards for controlling wastewater discharge from certain types and sizes of buildings. Royal Gazette, Volume 122, Section 125 ง, December 29, 2005.

[11] Department of Health Administration, Ministry of Public Health. 2022. Situation analysis on wastewater treatment systems in hospitals under the Office of the Permanent Secretary, Ministry of Public Health, fiscal year 2022. Printed by Born to Be Publishing Co., Ltd. ISBN 978-616-11-4876-8.

[12] U.S. Environmental Protection Agency (EPA). 2007. Pharmaceuticals and personal care products in water, soil, sediment, and biosolids by HPLC/MS/MS. Method 1694. EPA, Washington, DC.

[13] Panatda, K. 2019. Study of antibiotic residues in hospital effluents. Master's Thesis in Public Health Sciences, Thammasat University.

[14] Chiemchaisri, W., Chiemchaisri, C., Hamjinda, N. S., Jeensalute, C., Buranapakdee, P. and Thamlikitkul, V. 2022. Field investigation of antibiotic removal efficiencies in different hospital wastewater treatments in Thailand. Engineering Contaminants. 8: 321-339.

[15] Hamjinda, N. S., Chiemchaisri, W., Watanabe, T., Honda, R. and Chiemchaisri, C. 2018. Toxicological assessment of hospital wastewater in different treatment processes. Environmental Science and Pollution Research. 25: 7271-7279.

[16] Muhammad, T. K., Izaz, A. S., Ihsanullah, I., Mu, N., Sharafat, A., Syed, H. A. S. and Abdul, W. M. 2021. Hospital wastewater as a source of environmental contamination: An overview of management practices, environmental risks, and treatment processes. Journal of Water Process Engineering. 41: 1-17.

[17] Rozman, U., Duh, D., Cimerman, M. and Sostar, S. T. 2020. Hospital wastewater effluent: Hotspot for antibiotic-resistant bacteria. Journal of Water, Sanitation, and Hygiene for Development.10(2): 171-178.

[18] Gozlan, I., Rotstein, A. and Avisar, D. 2013. Amoxicillin degradation products formed under controlled environmental conditions: Identification and determination in the aquatic environment. Chemosphere. 91(7): 985-992.

[19] Straub, J. O. 2016. Aquatic environmental risk assessment for human use of the old antibiotic sulfamethoxazole in Europe. Environmental Toxicology and Chemistry. 35(4): 767-779.

Thai Environmental Engineering Journal Vol. 39 No. 1 (2025) : 59-68
www.eeat.or.th

Study on Biogas Production from Broiler Manure by GAC-dosed Anaerobic Biological Treatment System for Renewable Energy

Thidarat Jitjanesuwan[1] and Peerakarn Banjerdkij[1*]

[1]Department of Environmental Engineering, Faculty of Engineering,
Kasetsart University, Bangkok 10900, Thailand
[*]E-mail : fengpkba@ku.ac.th

Article History; *Received: 18 December 2024, Accepted: 10 April 2025, Published: 30 April 2025*

Abstract

The rising consumption of chicken has led to an expansion in poultry farming, resulting in increased accumulation of Broiler Chicken Manure. If not properly managed, this can lead to pollution and the spread of diseases. While Broiler Chicken Manure is often used as organic fertilizer, it emits nitrogen gases, contributing to odor problems. However, anaerobic digestion of Broiler Chicken Manure can produce biogas, offering an effective alternative energy source that helps reduce pollution and greenhouse gas emissions. This study investigates the biogas production potential of two types of Broiler Chicken Manure: Broiler chicken manure and Broiler Chicken Breed, Breeding period 45 and 440 days, respectively, with rice husk used as bedding material. The study focuses on two main aspects: 1) comparing the efficiency of biogas production from Broiler chicken manure and Broiler Chicken Breed, manure collection time, and the effect of mixing with rice husk, and 2) examining the impact of different mixing ratios of additive 4 type including Iron particles-A (Fe-A) with a size of <75µm, Iron particles-B (Fe-B) with a size of 75-180µm, Activated carbon powder-A (GAC-A) with a size of <75µm, Activated carbon powder -B (GAC-B) with a size of 75-180µm (Fe-A, Fe-B, GAC-A, GAC-B) at concentrations of 5, 10, and 20 mg/l. The results showed that Broiler Chicken Manure, with a 1:4 water-to-manure ratio and mixed with rice husk, had a methane production potential of up to 55 m³/ton. The highest biogas production was achieved with GAC-B at 5 mg/l, showing a 59.98% increase in biogas potential.

Keywords : Broiler chicken manure; Rice husk; Ferric Oxide; Anaerobic treatment; Biogas; Renewable energy

Introduction

Broiler chicken manure has gained increasing attention due to the rising demand for chicken meat, which has increased by 50% in recent years [1]. Broiler chicken is an essential protein source suitable for all age groups, and this increased demand has led to the growth of poultry farming. However, improper management of the resulting manure can lead to the spread of diseases, air pollution, and environmental degradation. While chicken manure is often used to produce organic fertilizers, these fertilizers release a significant amount of nitrogen (N), which leads to odor issues [2].

Numerous studies have highlighted that broiler chicken manure, when subjected to anaerobic digestion (AD), is highly efficient in producing biogas and can be converted into renewable energy. This biogas can serve as a direct fuel substitute for fossil fuels, contributing to circular economy models for energy and utilities, while being environmentally friendly by reducing pollution, greenhouse gas emissions, and environmental impacts. The optimal

chemical oxygen demand (COD) for biogas production from chicken manure is around 54,000 mg/L [3], producing between 50-100 m^3 of biogas per ton of manure. In Thailand, rice husk is often used as bedding material for chickens, resulting in mixed manure that includes rice husk. Rice husk, a lignocellulosic material, contains cellulose, lignin, and hemicellulose, making it suitable for biofuel production. Lignocellulosic materials have a high carbon content and are not easily biodegradable through anaerobic digestion, due to the slow degradation rate and low methane production. Although pretreatment can improve biogas production, such processes may not be economically viable due to the limitations of cellulose hydrolysis. However, rice husk can act as a co-substrate, improving the C/N ratio of nitrogen-rich materials like chicken manure and helping to prevent rapid acidification during anaerobic digestion [4].

Studies have also shown that biogas production and methane yields from chicken manure fermentation decrease when ammonia nitrogen (TAN) concentration reaches 6,000 mg/L, necessitating the use of large amounts of water for dilution to restore the process, which is costly. Co-fermentation of chicken manure with materials like corn stover or rice straw can adjust the C/N ratio to mitigate ammonia toxicity. Chicken manure has high ammonia nitrogen and sulfur content, which can disrupt biogas production. To prevent ammonia from exceeding toxic levels (1.1 g/L), water must be added to dilute it [5].

Anaerobic digestion (AD) is one of the most effective techniques for converting organic waste into renewable energy, primarily in the form of biogas or methane [4-5]. This biological treatment process occurs in the absence of oxygen, utilizing bacteria capable of producing biogas, a clean fuel primarily composed of methane (CH_4) and carbon dioxide (CO_2) (Reynolds, J., & Richards, A. (1996). Factors affecting anaerobic digestion include organic matter concentration, pH, temperature, alkalinity, volatile fatty acids, and nutrients. Rice husk, which is commonly used in poultry farming in Thailand, degrades slowly under anaerobic conditions due to its high lignin content and carbon sources, making it unsuitable for efficient anaerobic digestion when present in concentrations higher than 30% [4]. Ferric oxide particles have been employed to enhance the anaerobic digestion process and accelerate the breakdown of organic matter, resulting in higher biogas production [6].

In anaerobic digestion, trace elements are crucial for the growth and metabolism of microorganisms, particularly in the methane production (methanogenesis) stage. Iron (Fe) is the most abundant trace element in the system and plays an essential role in electron transport and the acceleration of chemical reactions involved in methane production. A lack of iron can limit the efficiency of the digestion process and reduce methane production. Supplementing iron and other trace elements in AD processes has been shown to significantly increase biogas production rates and improve process stability. Iron supplementation stimulates the growth of methane-producing bacteria and enhances the efficiency of anaerobic digestion systems [7]. The optimal ratio for adding ferric oxide is 20 mL per liter, which can increase natural gas production by up to 1.6 times [8].

This study focuses on assessing the potential for biogas production from broiler chicken manure through anaerobic digestion, with the addition of trace elements such as ferric oxide to improve the biogas yield. The economic and environmental viability of this process, in terms of reducing greenhouse gas emissions and providing a sustainable alternative to fossil fuels, will be evaluated. Biogas can be used directly as fuel, replacing fossil fuels, and it can also be converted into electricity, reducing energy costs for organizations and countries. Furthermore, this process helps mitigate organic waste accumulation and is environmentally friendly. Future research may explore the conversion of natural gas into biomethane or hydrogen to increase its value further.

Materials and Methods

1. Preparation of Chicken Manure Samples. The chicken manure samples were divided into two types: (1.1) Broiler Chicken Manure and (1.2) Broiler Chicken Breed Manure The Different periods of these animals

differ significantly, resulting in variations in the properties of their manure. These differences can influence characteristics such as moisture content and ammonia levels.

2. The manure was extracted as a manure solution. The manure-to-water ratios used for extraction were 1:2, 1:4, and 1:6 using a mixer with a speed range of 300-450 RPM for 5 minutes. The condition mentioned is a process to completely separate the manure and rice husk, based on an experiment conducted in a laboratory.

3. BMP Testing Under Experimental Conditions (2.1) A study on the biogas production efficiency of broiler chicken manure was conducted by comparing broiler chicken manure with broiler chicken breed manure, considering the time of manure collection and the differences between mixing and not mixing rice husk. (2.2) The study also examined the biogas production efficiency of broiler chicken manure with different mixing ratios of four types: Fe-A (<75µm), Fe-B (75-180µm), GAC-A(<75µm), and GAC-B (75-180µm) at concentrations of 5, 10, and 20 mg/l using the BMP equation. The addition of iron at the nanoparticle level (10 ppm) helps improve the efficiency of biogas and methane production. The research hypothesis was based on testing at the nm level, which is smaller in size and has a larger surface area. Additionally, if carbon particles are included as a component, it can help reduce the required concentration of iron [8].

$$\text{BMP (ml/gCOD}_{\text{removal}}) = \frac{\text{(ml Methane)}}{\text{gCOD removal}} = \frac{\text{Biogas(l)} \times \text{Methane(\%)}}{\text{(COD influence-COD effluence)}(\frac{\text{mg}}{\text{L}})} \quad (1)$$

$$\text{BMP (ml/gVS}_{\text{removal}}) = \frac{\text{(ml Methane)}}{\text{gVS removal}} = \frac{\text{Biogas(l)} \times \text{Methane(\%)}}{\text{(VS influence-VS effluence)}(\frac{\text{mg}}{\text{L}})} \quad (2)$$

4. Analysis of Experimental Parameters. The parameters of the experimental samples, as shown in Table 1, were analyzed both before and after the BMP test, including pH, VFA, Alkalinity, BOD, COD, TKN, Ammonia, TS, VS, SS, TP, and Iron, using the methods outlined in the *Standard Methods for the Examination of Water and Wastewater* (24th edition, 2023).

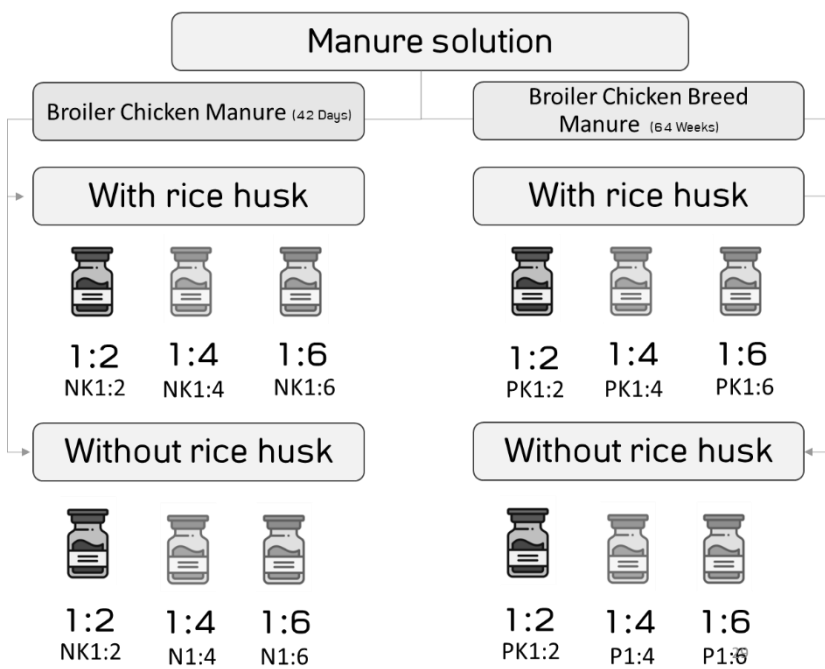

Figure 1 The manure solution were divided into two types: (1.1) Broiler Chicken Manure and (1.2) Broiler Chicken Breed Manure

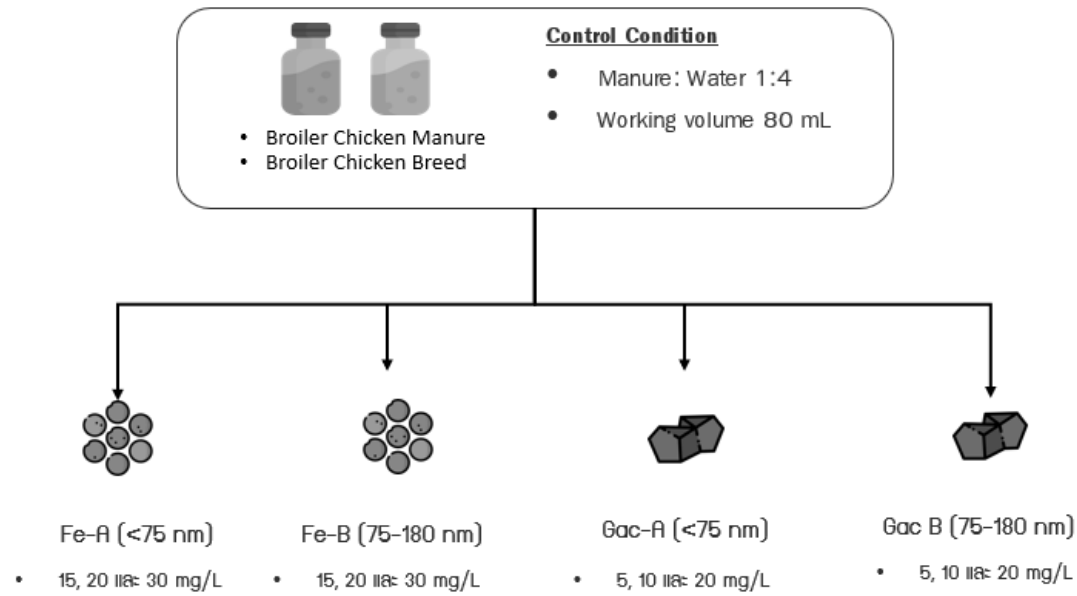

Figure 2 Shows the proportions of additive materials at different ratios

Results and Discussion

1. Study on the Biogas Production Efficiency of Broiler Chicken Manure. The comparison of biogas production efficiency between Broiler Chicken Manure and Broiler Chicken Breed Manure, considering different manure collection periods and the differences between mixing and not mixing rice husk.

Table 1 Properties of Extracted Broiler Chicken Manure and Broiler Chicken Breed Manure

Parameter	Average value of this research		Ref Data	Ref
	Broiler Chicken Manure	Broiler Chicken Breed Manure		
pH	7.40	7.53	6.94-7.29	[2],[3]
COD (mg/L)	116,133	104,133	53,500 -	[3]
Alkaline (mg/L as CaCo3)	25,969	45,689	-	
VFA (mg/L as CH3COOH)	4,444	6,111	-	
TKN (mg/L as N)	20,300	15,400	-	
Ammonia (mg/L as NH3)	1,400	840	≤5,000	[10]
TS (%V/V)	65%	70%	70 – 75%	[2],[3]
VS (%V/V as Dried)	75%	71%	60 – 80%	[7]

Table 1 presents the properties of Broiler Chicken manure and Broiler Chicken Breed manure, compared to poultry manure from other research studies. Broiler Chicken Breed manure, which is stored for a longer period, shows a higher pH value of 7.53, due to the increased release of ammonia. In contrast, Broiler Chicken manure and poultry manure from other research studies had pH values ranging from 6.94 to 7.29. This higher pH is a result of the ammonia produced during the extended storage of the manure, as ammonia is a basic compound that increases the pH.

Regarding Chemical Oxygen Demand (COD), Broiler Chicken manure had a COD value of 116,133 mg/l, and Broiler Chicken Breed manure had 104,133 mg/l. These values are approximately twice as high as those reported in other studies. This difference is mainly due to the bedding material used in the farms. In Thailand, rice husk, which contains lignin, is commonly used as bedding material. Lignin is a complex compound that is resistant to decomposition which some chemical for test COD, and when mixed with manure, it increases the COD value. In contrast, other studies abroad often use rice straw or sawdust, which have lower lignin content and therefore lower COD values.

The higher COD values indicate that both types of manure have significant potential for biogas production, as a higher COD correlates with more organic matter available for microbial digestion in anaerobic conditions. According to previous research, a gas yield of 1,270 mg/l per gCOD was observed, suggesting that Broiler Chicken and Broiler Chicken Breed manure can effectively produce biogas. However, while rice husk increases the COD, its lignin content can also slow down the degradation process in anaerobic digestion, which may slightly affect the overall gas yield. This phenomenon is supported by studies on lignin-rich materials, which often show slower biogas production rates due to the resistance of lignin to microbial degradation [4].

After analyzing the properties of both types of manure, it was found that both Broiler Chicken manure and Broiler Chicken Breed manure have high dryness due to the presence of rice husk as a component, and the manure is not regularly removed from the poultry houses. This results in the need to improve the moisture content to an appropriate level by adding water. The next step was to determine the suitable water mixing ratio.

From the experimental results in Table 2, it was found that the water mixing ratios of 1:2, 1:4, and 1:6, both with and without separating the rice husk, affected the COD values and the potential toxicity in the anaerobic digestion system of the manure. The COD values decreased as the water content increased in the higher ratios, which corresponds to the reduction of organic and inorganic substances in the manure extract. Separating the rice husk from the manure also significantly reduced the COD values. Additionally, this reduction in COD resulted in better decomposition during the subsequent anaerobic digestion process [8, 9].

Table 2 Average composition of different water mixing ratios

Substrates (Manure mixture ratio by weight)	Broiler Chicken manure					Broiler Chicken Breed manure				
	With Rice husk			Without Rice husk		With Rice husk			Without Rice husk	
	1:2 (NK1:2)	1:4 (NK1:4)	1:6 (NK1:6)	1:4 (N1:4)	1:6 (N1:6)	1:2 (PK1:2)	1:4 (PK1:4)	1:6 (PK1:6)	1:4 (P1:4)	1:6 (P1:6)
pH	7.4	8.65	8.64	6.55	6.47	7.53	6.29	6.68	7.25	7.23
COD (mg/L)	116,133	24,080	18,440	23,800	16,000	104,133	49,587	30,680	15,600	13,100
Alkaline (mg/L as CaCo3)	6,589	5,730	3,220	4,268	4987	4,876	3,425	2,120	2,864	3,879
VFA (mg/L as CH3COOH)	4,444	6,334	4,083	2,927	2,511	6,111	8,000	5,330	1,025	1,239
TKN (mg/L as N)	20,300	2,600	2,500	1,500	1,197	15,400	2,200	1,064	712	663
Ammonia (mg/L as NH3)	1,400	705	465	272	119	1,167	633	362	182	85
TS (mg/L)	259,000	148,280	65,360	36,987	34,330	220,000	173,420	67,380	33,000	27,320
VS (mg/L)	195,000	106,260	44,660	27,674	15,000	156,000	147,720	55,760	24,420	20,020
C/N Ratio	5.7	9.3	7.4	15.9	13.4	6.8	22.5	28.8	21.9	19.8
Ammonia (g/L) as NH3)	1.4	0.7	0.46	0.27	0.19	1.1	0.63	0.36	0.18	0.085
VFA/Alkaline	0.7	1.1	1.3	0.7	0.5	1.3	2.3	2.5	0.4	0.3

The high initial COD values of both types of manure make them suitable for use in anaerobic digestion processes because COD values greater than 2,000 mg/l are ideal for biogas production without the need for additional energy to heat the reactor to stimulate decomposition [8]. The gas production rate per COD value in this study was 1,270 mg/l per gCOD for Broiler Chicken Breed manure mixed with water at a 1:4 ratio (PK1:4). This value indicates good biogas production efficiency from the manure and helps dilute the toxicity within the system [10].

It was also found that mixing ratios greater than 1:4 result in ammonia concentrations that do not reach toxic levels in the system. According to research, ammonia levels in anaerobic digestion systems should not exceed 1.1 g/L to avoid toxicity [5]. This adjustment allows for a 30% reduction in water use costs compared to the 1:6 ratio. Additionally, the rice husk mixture eliminates the need for a pre-treatment system, reducing construction costs by at least 30% and increasing COD values while maintaining an appropriate C/N ratio.

This research is based on farms in Thailand, where rice husk is commonly used as bedding material due to its abundance, availability, and low cost. However, rice husk contains lignin, which reacts with the chemicals used to measure COD, resulting in higher values. This leads to higher potential for biogas production from manure that contains rice husk as a component.

An appropriate C/N ratio can reduce the impact of ammonia and increase methane production efficiency. Research has shown that increasing the C/N ratio helps reduce ammonia impacts. For C/N ratios between 20 and 32, which align with the study by, the ideal C/N ratio for anaerobic digestion of chicken manure is between 23 and 25, as it promotes effective decomposition and reduces ammonia nitrogen concentrations. An excessively high C/N ratio may lead to lower methane production because microbial growth tends to focus on protein use instead of carbon degradation in nutrients [11].

Samples with VFA/Alkaline values exceeding 0.3 [14] indicate instability in the system and are often associated with acid accumulation due to organic overload or insufficient buffering capacity. The optimal value should not exceed 0.3 to ensure efficient biogas production. It is necessary to adjust the organic loading rate, modify the C/N ratio, or add buffering agents to maintain system balance. Particular attention should be given to the C/N ratio, as it plays a crucial role in microbial activity and the overall stability of the anaerobic digestion process.

The findings from this research indicate that Broiler Chicken Breed manure has a C/N ratio ranging from 19.8 to 22.5, which is within the optimal range. The longer rearing period results in greater ammonia release than Broiler Chicken manure, making Broiler Chicken Breed manure more likely to produce higher methane quantities. This is expected to be most pronounced in the PK1:4 sample. The experimental sample PK1:4 (Broiler Chicken Breed manure mixed with water at a 1:4 ratio and containing rice husk) demonstrated strong potential for biogas production when considering both the COD, C/N ratio, and the volume of biogas produced, which reached 55 m^3/ton. This finding is consistent with previous research [1], where poultry manure typically produces biogas volumes ranging from 50 to 100 m^3/ton, as shown in Figure 3.

Figure 4 illustrates that the methane production efficiency of the PK1:4 sample is only 15%, which is approximately twice as low as the P1:6 sample, which has the highest methane production at 34%. The key factor behind this discrepancy is the presence of rice husk in the PK1:6 sample. Rice husk is composed of lignin and cellulose, which are more challenging to break down biologically compared to other organic materials [4] As a result, the degradation process in the PK1:6 sample takes longer, leading to reduced methane production within the same time frame. This extended degradation time also results in a slower accumulation of biogas compared to samples with easier-to-degrade materials.

Furthermore, the lower water mixing ratio in PK1:4 results in higher ammonia concentrations in the system. Ammonia, particularly in high concentrations, can be toxic to the microbial communities responsible for anaerobic digestion. Studies have shown that

elevated ammonia levels can inhibit the activity of methanogenic bacteria, thereby slowing down the biogas production rate. In this study, the higher ammonia concentration in the PK1:4 sample likely contributed to the observed decrease in methane production efficiency. Additionally, the higher ammonia levels can disrupt the microbial metabolic processes, resulting in slower anaerobic digestion reactions and lower overall methane yield. These findings underscore the importance of balancing water mixing ratios and feedstock composition in optimizing methane production in anaerobic digestion systems [5].

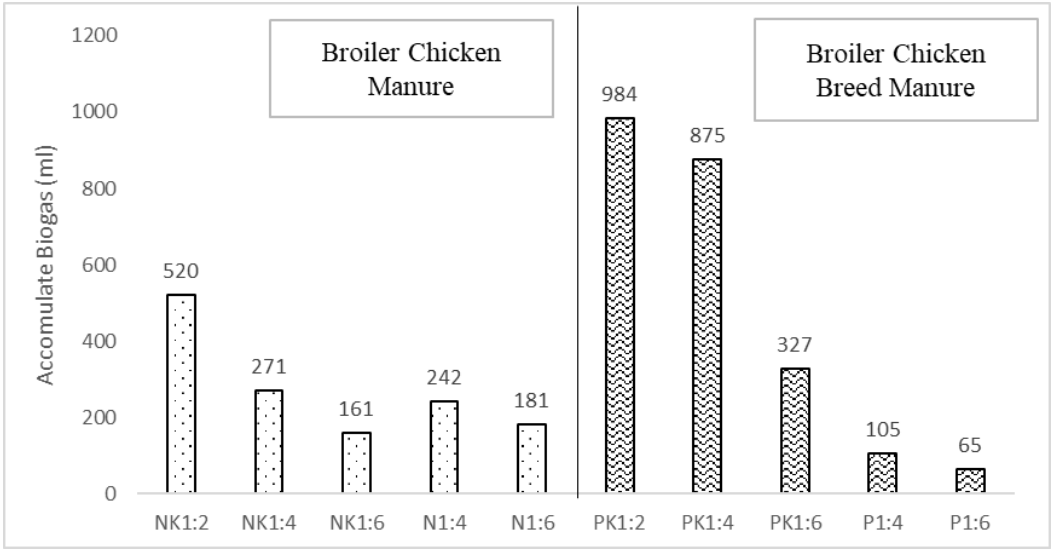

Figure 3 Biogas production from experimental with different water mixing ratios, with and without rice husk as a component

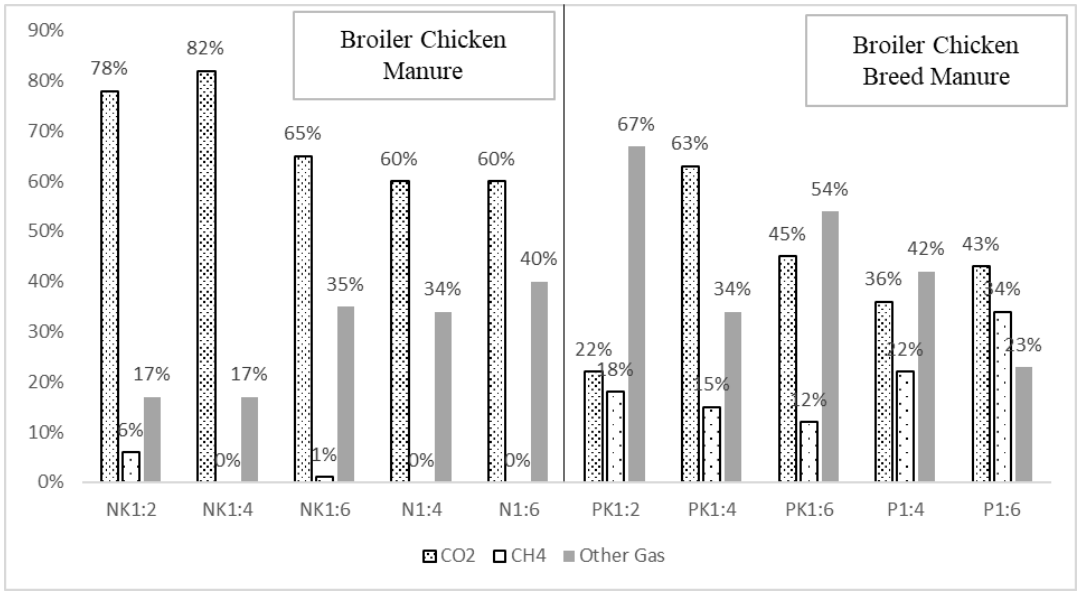

Figure 4 Study of the methane production efficiency of two types of broiler chicken manure at different mixing ratios

The experiment in section 1 led to the subsequent experiment aimed at enhancing methane production efficiency in the PK1:4 sample.

2. The biogas production from Broiler Chicken Breed manure with different mixing ratios of 4 types: Fe-A, Fe-B at 15, 20, 30 mg/l and GAC-A, GAC-B at 5, 10, 20 mg/l.

The biogas production potential from 45-day-old Broiler Chicken Breed manure at a manure-to-water ratio of 1:4, combined with iron scales Fe-A, Fe-B, GAC-A, and GAC-B at the difference specified concentrations, was tested. It was found that biogas production began within 24 hours and increased until day 37, where gas production stabilized as shown in the figure. In the Broiler Chicken Breed GAC-B experimental group at 5 mg/l, the accumulated biogas volume reached a maximum of 1,727 milliliters, with a maximum methane content of 60%, which is approximately 30% higher than the control group. When comparing the composition of biogas produced from different substrates, as shown in Table 3, the results indicate that The biogas volume in each experiment did not increase significantly. However, what made the experiment interesting was that the addition of only 5 mg/l of GAC-B resulted in a rapid increase in methane production, reaching up to 60%. This led to a more than 50% reduction in the digestion time, to just 17 days compared to the control group. This effect is due to the carbon content of GAC, which helps absorb ammonia and reduce toxicity. Additionally, the presence of Fe contributes to enhancing bacterial activity and helps absorb H_2S The shape and size of the iron particles have an impact on biogas production in this system by optimal biogas production occurred when 5 mg/l of GAC-B was added [12, 13].

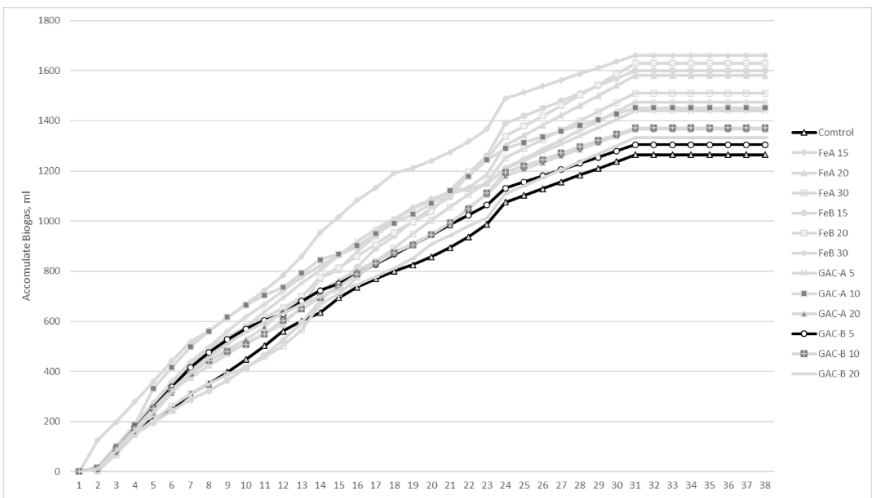

Figure 5 shows the cumulative biogas production (a) and cumulative methane production (b) after the addition of iron particles (Fe-A, Fe-B) at concentrations of 15, 20, and 30 mg/l, and GAC-A, GAC-B at concentrations of 5, 10, and 15 mg/l

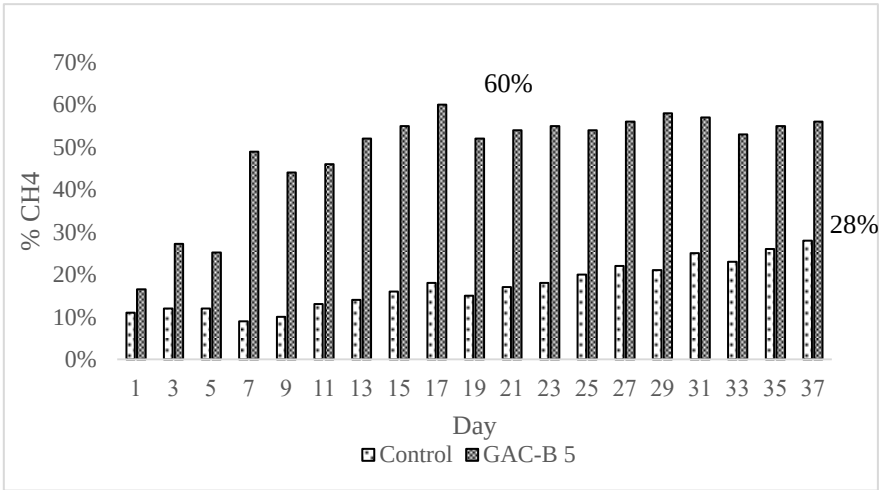

Figure 6 shows the duration of methane production (% CH_4) between the control group and the experimental group with the addition of GAC-B at 5 mg/l

Conclusions

The potential for biogas production from broiler chicken manure and broiler chicken breed manure was tested by adding activated carbon mixed with iron scale. The results indicated that iron scale of the type GAC-B, at a concentration of 5 mg/l, was the most effective in enhancing biogas production, particularly for broiler chicken breed manure. This concentration was found to be optimal due to the role of sulfate levels, which influence the selection of iron scale concentration in the system. The iron scale helps prevent sulfate formation in the system, reducing toxicity. Additionally, the addition of iron scale was found to outperform the addition of granular activated carbon in increasing biogas production capacity. It also accelerated the production of methane, increasing its production rate by up to two times, leading to a reduction in the required size of the reactor and cutting investment costs by up to 30%.

Acknowledgments

The research project titled “Study on Biogas production from broiler manure by GAC-dosedAnaerobic Biological Treatment System for Renewable Energy” was supported by the National Nanotechnology Center (NANOTEC), National Science and Technology Development Agency (NSTDA), for the synthesis of the additive (iron scale).

References

[1] AVEC. 2016. Annual report 2016. Association of Poultry Processors and Poultry Trade in the EU countries.

[2] Fuchs, W., Wang, X., Gabauer, W., Ortner, M., & Li, Z. 2018. Tackling ammonia inhibition for efficient biogas production from chicken manure: Status and technical trends in Europe and China. Renewable and Sustainable Energy Reviews. 86: 186-199.

[3] Miles, D. M., Logan, J. W., Arora, S., & Jenkins, J. N. 2016. On-farm resources and renewable energy in broiler chicken production: Brinson farms case study. International Journal of Poultry Science. 15(2): 41-47.

[4] Haider, M. R., Zeshan, Yousaf, S., Malik, R. N., & Visvanathan, C. 2015. Effect of mixing ratio of food waste and rice husk co-digestion and substrate to inoculum ratio on biogas production. Bioresource Technology. 190: 451-457.

[5] Xu, Y. and Li, Y. 2015. Ammonia inhibition on anaerobic digestion: Effects and mitigation strategies. Bioresource Technology. 179: 191-197.

[6] Abdelsalam, E., Samer, M., Attia, Y. A., Abdel-Hadi, M. A., Hassan, H. E., & Badr, Y. 2017. Influence of zero valent iron nanoparticles and magnetic iron oxide nanoparticles on biogas and methane production from anaerobic digestion of manure. Energy. 120: 842-853.

[7] Baek, G., Kim, J., & Lee, C. 2019. A review of the effects of iron compounds on methanogenesis in anaerobic environments. Renewable and Sustainable Energy Reviews. 113: 1-14.

[8] Feng, Y., Zhang, Y., Quan, X., & Chen, S. 2014. Enhanced anaerobic digestion of waste activated sludge by the addition of zero valent iron. Water Research. 52: 242-250.

[9] Holm-Nielsen, J. B., Al Seadi, T., & Oleskowicz-Popiel, P. 2009. The future of anaerobic digestion and biogas utilization. Bioresource Technology. 100(22): 5478-5484.

[10] Wang, L., Aziz, T. N., & de los Reyes, F. L. III. 2013. Determining the limits of anaerobic co-digestion of thickened waste activated sludge with grease interceptor waste. Water Research. 47(11): 3835-3844.

[11] Wang, X., Lu, X., Li, F., & Yang, G. 2014. Effects of temperature and carbon-nitrogen (C/N) ratio on the performance of anaerobic co-digestion of dairy manure, chicken manure, and rice straw: Focusing on ammonia inhibition. PLOS ONE. 9(5): e97265.

[12] Ortner, M., Rameder, M., Rachbauer, L., Bochmann, G., & Fuchs, W. 2015. Bioavailability of essential trace elements and their impact on anaerobic digestion of slaughterhouse waste. Biochemical Engineering Journal. 99: 107-113.

[13] Al Mamun, M. R., & Torii, S. 2015. Removal of hydrogen sulfide (H_2S) from biogas using zero-valent iron. Journal of Clean Energy Technologies. 3(6): 428-435.

[14] Chen, Y., Cheng, J. J. and Creamer, K. S. 2008. Inhibition of anaerobic digestion process: A review. Bioresource Technology. 99(10): 4044-4064.

Thai Environmental Engineering Journal Vol. 39 No. 1 (2025) : 69-79
www.eeat.or.th

Analysis of Spatial Distribution Patterns of Non-Communicable Diseases (NCDs) and Risk Factors with GIS in Central Regions of Thailand

May Myat Myat Aung[1], Kritsanat Surakit[2], Nawatch Surinkul[3] and Romanee Thongdara[3*]

[1,2,3]Department of Civil and Environmental Engineering, Faculty of Engineering,
Mahidol University, Nakorn Pathom 73170, Thailand
[*]E-mail : romanee.tho@mahidol.ac.th

Article History; *Received: 31 March 2025, Accepted: 18 April 2025, Published: 30 April 2025*

Abstract

Non-communicable diseases (NCDs) are leading causes of mortality in Thailand, representing 74% of all deaths. Behavioral, social and environmental issues are the primary drivers contributing to the increasing incidence of NCDs across Thailand. This study aimed to examine the spatial distribution trends of hypertension, diabetes, and coronary heart diseases in Thailand using Geographic Information System (GIS) techniques, including Inverse Distance Weighting (IDW), clustered analysis with local Moran's I and bivariate correlation analysis, to identify associations with urbanization, demographic aging, and environmental exposure. The consolidation of national health statistics, demographic and environmental datasets, applied spatial interpolation (IDW) and correlation analysis examined the relationship between the prevalence of NCDs and risk factors. As a result, the highest concentration of NCDs was observed in Bangkok Metropolitan Regions (BMR)and industrial corridors, while coastal areas showed decelerated rates of increase based on the result of spatial distribution pattern and clustered analysis. And the most severe air pollution occurred in winter season therefore the government should focus on the tackle of air pollution affected on the community in this season, especially in the Mueang Samut Songkhram, Mueang Ratchaburi, Mueang Phetchaburi, Mueang Supanburi, Mueang Samut Sakhon Districts and Saraburi Province. From correlation results, hypertension and diabetes prevalence showed a strong positive correlation with urbanization and aging population density, while no significant correlation was found with $PM_{2.5}$ exposure and income. Therefore, this study can support the recommendations of prioritization provinces and districts in the cases of NCDs control and prevention. By combining GIS and spatial statistical analysis on health data, it would be helpful to expose the relationship of NCDs risk factors and beneficial to policy makers in decision making of prevention and surveillance NCDs.

Keywords : NCDs; risk factors; spatial statistical analysis; Local Moran's I; GIS

Introduction

Non-communicable diseases (NCDs) are a kind of chronic disease that derives from genetic, physiological, environmental and behavioral factors. According to the statistical data of WHO, 41 million people died every year due to NCDs [1]. NCDs such as cardiovascular diseases, chronic obstructive pulmonary diseases, diabetes, and cancers are leading causes of mortality in Thailand, which is 400,000 deaths each year, referring 74% of all deaths nationally. The risk factors – tobacco use, harmful alcohol consumption, unhealthy diets, physical inactivity and environmental pollution are the primary drivers contributing to the increasing incidence of non-communicable diseases (NCDs) across Thailand [2]. The Thai Health Report 2023 indicated that Samut Sakhon, located in the Central Region of Thailand, is among the provinces with the lowest percentage of adequate physical activity, with only 25.4%. Air pollution is the most significant factor, causing 6.7 million deaths worldwide, with around 5.7 million of these due to NCDs [3]. Besides air pollution, solid and hazardous industrial wastes continue to be a challenge across Thailand. The highest levels of hazardous industrial waste were found in provinces with significant industrial activity, such as Rayong, Chonburi, and Samut Prakan [3]. Addressing NCDs issues as urgency, 2030 Agenda for Sustainable Development identified NCDs as a significant obstacle to sustainable development. By 2030, one third of premature mortality from non-communicable diseases will be reduced through prevention and treatment and promote mental health and well-being [4]. As a literature review, Nawamawat et al. (2020) examined the prevalence and behavioral risk factors of NCDs in a semi-urban Thai community, identifying significant associations with demographic and lifestyle variables. However, the limited geographical scope and small sample size underscored the need for broader spatial analyses to inform targeted public health strategies [5]. Laohasiriwong et al. (2018) utilized Night-Time Light (NTL) data and spatial association techniques to understand hypertension hotspots across Thailand's 76 provinces, revealing strong spatial clustering in urban areas such as Bangkok. But the study did not explore underlying environmental determinants and integration with other diseases, indicating a gap for more comprehensive spatial analyses, especially air pollution [6]. Based on the existing gaps in the literature, Regional Health Zones 4, 5, and 6 among 13 Regional Health Zones divided by the Ministry of Public Health were selected for this study based on their geographical positions, socio-environmental characteristics, and the availability of health, social, and environmental datasets across all provinces. Each zone contains 8 provinces, therefore sufficient data in 24 provinces including 201 districts for 3 zones were captured to explore spatial patterns in NCD prevalence. This study aimed to analyze spatial distribution patterns of NCDs including coronary heart diseases, hypertension and diabetes across 24 provinces (201 districts). And risk factors such as air quality, landuse and demographics associated with prevalence of NCDs at district level were assessed and correlation and clustered analysis between NCDs and related factors were applied to detect and explore the relationships of diseases and factors. Surveillance, in the healthcare industry, of the diseases and conditions that are significant public health threats is necessary for the development of healthy communities. GIS can track patient demographics and where the source of diseases began and spread. It can also help state and local governments understand the condition of a public health emergency, predict its movement to inform resource deployment and monitor processes and outcomes [7]. GIS can provide a conceptual framework for understanding the geographic variability of diseases and health. To effectively control NCDs transmission, it's crucial to prioritize regions with the high incidence of NCDs by applying GIS tools. Based on this analysis, policymakers and health authorities could strategically execute the control plan of NCDs and devote resources to strengthen NCDs prevention and control activities from the perspective of environmental and health science.

Methodology

The yearly incident data of NCDs - Coronary Heart Diseases, Hypertension and Diabetes which occurred in the Regional Health Zone 4, 5 and 6 as shown in Figure 1 were collected from the Ministry of Public Health for 5 years spanning 2019 to 2023 [8]. These data were compiled and verified national

health data reports, ensuring the reliability and representativeness of the health outcomes used in this study. The social data including total population, age group and number of hospitals were also downloaded from the Ministry of Public Health for the year 2023. And income data was collected from the Community Development Department (CDD). For environmental factors, the updated landuse data for each district between 2019, 2021 and 2023 was downloaded from Land Development Department (LDD), which updated its datasets based on survey of the provinces [9]. As the changes of landuse occur slowly, the updated frequency was deemed appropriate for the scope of this analysis. As well as the daily $PM_{2.5}$ data in 2023 from fixed ground-based monitoring stations were collected from the Pollution Control Department (PCD). As initial state, the social data – total population, age, number of hospitals and income were manipulated to be useful and applicable in ArcGIS by data cleaning, sorting, filtering and joining. For $PM_{2.5}$ analysis, the locations of $PM_{2.5}$ monitoring stations and the daily $PM_{2.5}$ value across stations were obtained from Air4Thai for year of 2023 [10]. There are 34 monitoring stations in Regional Health Zone 4,5 and 6. Data for each station was gathered on a daily basis, although there were gaps in some data points. The $PM_{2.5}$ concentrations for 31 days in January were added up and the result was divided by 31 to determine monthly average $PM_{2.5}$ for January. And similar method was used to convert into monthly data in the following months. Of the two monthly data stations, 21T station in Samut Prakan Province has no January data while 84T station in Supanburi Province was also missing data for February. For that, the IDW calculation method was applied to more accurately calculate missing value. The 2023 annual data was calculated by totaling the 12-month data from each monitoring station and dividing that total by 12 after obtaining monthly data for all stations. Once the process of data preparation was completed, the monthly and annual point value of $PM_{2.5}$ were converted into polygon value with IDW interpolation and zonal statistics in ArcGIS, enabling an estimated pollution value for each district. The reason for choosing IDW interpolation method was due to its computational simplicity, suitability for datasets, evenly distributed monitoring points and calculation of concentrations at unsampled locations based on the weighted average of nearby monitoring points. Unlike Kring and Spline methods, IDW focuses on the influence of closer observations which allow for continuous surface that reflects localized variations in air pollution levels. Furthermore, the landuse was classified into 5 classes – Agriculture, Forest, Urban, Water and Miscellaneous to identify the influenced land area in the study area. After getting all data at the district level, the spatial distribution pattern of diseases and related factors was evaluated in order to understand the distribution pattern across districts. And then, the correlation analysis was conducted to find the relationship between them by using SPSS. If the data were statistically correlated with each other, the clustered analysis with Local Moran's I was carried out to investigate the specific districts of high and low prevalence rate of diseases and other factors.

Results and Discussion

The rates of non-communicable diseases (NCDs) between 2019 and 2023, as shown in Figure 2, have shown a simultaneous increase in the cases of diabetes and hypertension and minimal gradual increase in coronary heart disease. Cases of hypertension increased from 13,000 in 100,000 population in 2019 to 15,000 in 2023. Likewise, diabetes was set to increase from around 6000 to 7500 per 100,000 population. While 3 diseases revealed a steady upward growth in the prevalence of NCDs for 5 years, the most widespread disease was in hypertension cases and coronary heart diseases remained the lowest occurrence. These trends could potentially be caused by several factors such as more sedentary lifestyles, diet, lack of physical exercise associated with urbanization, and an aging population. Understanding these drivers helps the public health system to take relevant action. The data for all factors in this study was done through 2023 due to lack of multi-year environmental and social information. Trend analysis was only used for prevalence of NCDs from 2019 to 2023. As the temporal changes on environmental and social risk determinants could not be fully captured, this

limitation may impact on the findings. Certain urban districts - particularly Mueang Samut Prakan, Mueang Nonthaburi and Mueang Nakhon Pathom – should be focused on further study as these districts contributed to the rise of hypertension and diabetes cases throughout five-year period. These regions both included high baseline prevalence and showed a steady yearly rise, suggesting a growing burden of NCDs.

The rates of non-communicable diseases (NCDs) between 2019 and 2023, as shown in Figure 2, have shown a simultaneous increase in the cases of diabetes and hypertension and minimal gradual increase in coronary heart disease. Cases of hypertension increased from 13,000 in 100,000 population in 2019 to 15,000 in 2023. Likewise, diabetes was set to increase from around 6000 to 7500 per 100,000 population. While 3 diseases revealed a steady upward growth in the prevalence of NCDs for 5 years, the most widespread disease was in hypertension cases and coronary heart diseases remained the lowest occurrence. These trends could potentially be caused by several factors such as more sedentary lifestyles, diet, lack of physical exercise associated with urbanization, and an aging population. Understanding these drivers helps the public health system to take relevant action. The data for all factors in this study was done through 2023 due to lack of multi-year environmental and social information. Trend analysis was only used for prevalence of NCDs from 2019 to 2023. As the temporal changes on environmental and social risk determinants could not be fully captured, this limitation may impact on the findings. Certain urban districts - particularly Mueang Samut Prakan, Mueang Nonthaburi and Mueang Nakhon Pathom – should be focused on further study as these districts contributed to the rise of hypertension and diabetes cases throughout five-year period. These regions both included high baseline prevalence and showed a steady yearly rise, suggesting a growing burden of NCDs.

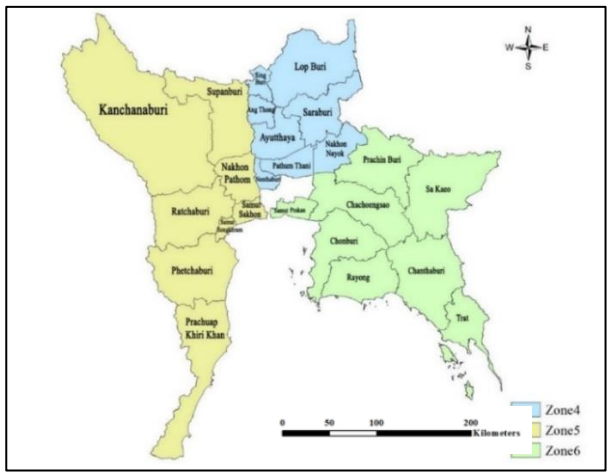

Figure 1 Locations of Regional Health Zone 4, 5 and 6

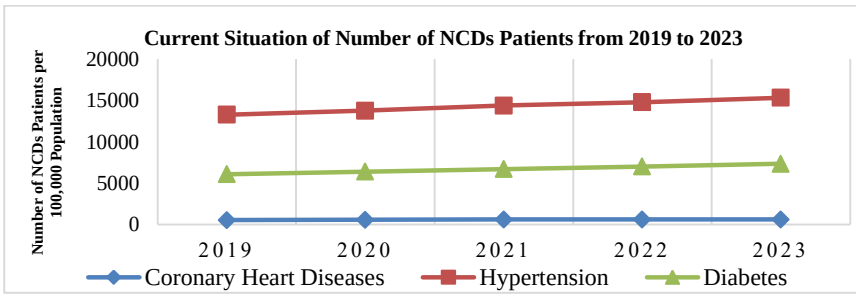

Figure 2 Current Situation of NCDs Prevalence from 2019 to 2023

Spatial Distribution Analysis

The spatial distribution patterns revealed that the lighter to darker color of the regions can be defined as the pattern of lowest to highest value of maps, except map (f) and (g) in Figure 3. The map (f) was illustrated as the graduated symbol of the pattern, showing the biggest circle of a huge number of hospitals and smallest circle directing the minimum number of hospitals. And the map (g) was described the classification of landuse; agriculture with yellow color, forest showing green color, miscellaneous referring brown color, urban highlighting with red color and water body with blue color. As result of the analysis, the distribution pattern of coronary heart diseases, hypertension and diabetes showed that a significant number of patients were highlighted with the darkest color, suggesting regions with greater prevalence of NCDs. The highest severe affected NCDs have been widespread in Mueang Nonthaburi District with 4,015 coronary heart diseases patients and Mueang Samut Prakan District with 42,690 patients and 23,049 patients who suffered hypertension and diabetes respectively. Among 3 diseases, the high prevalence rate of hypertension and diabetes were nearly identical in shown in map (b) and (c), especially in these provinces: Nonthaburi Province in Zone 4, Ratchaburi, Samut Sakhon and Nakhon Pathom Provinces in Zone 5 and Chonburi, Samut Prakan and Rayong Provinces in Zone 6. Combined with landuse applications, the red color of urban areas mostly occurred in these provinces. It proved that the provinces in Thai Health 2023 report [3] as having the highest levels of hazardous industrial waste were definitely same with the provinces of highest prevalence NCDs rate in Zone 6. When the lowest prevalence rate of NCDs across the provinces and districts were analyzed, Ko Kut District in Trat Province is the lowest patients for all 3 diseases, showing the coastal regions suffering low incidence case of NCDs. And the findings from the urban density and total population maps were that the dark red regions of urban density absolutely aligned with the some of the dark green regions of total population, showing that areas with high total population occupied high urban-density area. The significant volume of total population was found in Mueang Nonthaburi District with 371,899 people having the highest urban area density. Land use patterns play a significant role in shaping the spatial distribution of non-communicable diseases. Urbanization often leads to reduced physical activity, increased air pollution, and limited access to green spaces, all of which are linked to higher risks of hypertension and diabetes. Similarly, lack of forest areas around BMR may limit opportunities for recreation areas and stress reduction, contributing to adverse health outcomes. For hospital mapping, larger circles represented the districts with more hospitals including rural and sub-district areas. The highest number of hospitals with 37 hospitals in total can be found in Mueang Nakhon Pathom District, indicating most hospitals were found in places where NCDs were most prevalent. For the social factors, the highest income level was in Khao Khitchakut District, Chanthaburi Province with 501,573 baht annually, showing a low prevalence rate of NCDs in high-income region. From the environmental point of view, another indicator of 2023 $PM_{2.5}$ pattern highlighted regions with high $PM_{2.5}$ concentrations, particularly in Phraphutthabat District, Saraburi Province with the highest level of 30.686 $\mu g/m^3$, where transportation and agricultural burning can be contributed to poor air quality. The lowest $PM_{2.5}$ levels with 16.325 $\mu g/m^3$ was observed in Mueang Trat District which is near coastal areas, resulting in fewer pollution sources. Finally, the spatial distribution patterns of NCDs and risk factors can be pointed out that the most widespread distribution pattern mostly happened in Mueang (City) of the districts and Nonthaburi, Ratchaburi, Samut Sakhon, Nakhon Pathom, Chonburi, Samut Prakan, Rayong and Saraburi provinces should be focused on handling of NCDs controlling process based on the results of spatial distribution pattern.

Additionally, $PM_{2.5}$ is one of the critical environmental factors influencing the patterns of NCDs. According to the air pollution concentration equivalent to Air Quality Index (AQI) defined by PCD, the range of $PM_{2.5}$ (0 to 15 $\mu g/m^3$) defined with blue color code which is showing excellent level of very good air quality, followed by 15.1 to 25 $\mu g/m^3$ with green color of defining satisfactory for good air quality, 25.1 to 37.5 $\mu g/m^3$ with yellow color with moderate level of air quality, 37.6 to 75

µg/m^3 with orange color of indicating unhealthy air quality and above 75.1 µg/m^3 with red color which is mentioned to avoid outdoor activities and wear masks due to very unhealthy air conditions [10]. The monthly distribution pattern of $PM_{2.5}$ value in 2023 showed the same defined value of AQI value in Figure 4. It revealed that the $PM_{2.5}$ value captured during January, February, March, April and December in 2023 exceeded the standard value of 37.5 µg/m^3, covering the orange color in most districts in the maps. In the remaining months, monthly $PM_{2.5}$ value captured the low value which was below the standard number of 37.5 µg/m^3. Therefore, further analysis was carried out in 5 months which were over the standard limit of AQI.

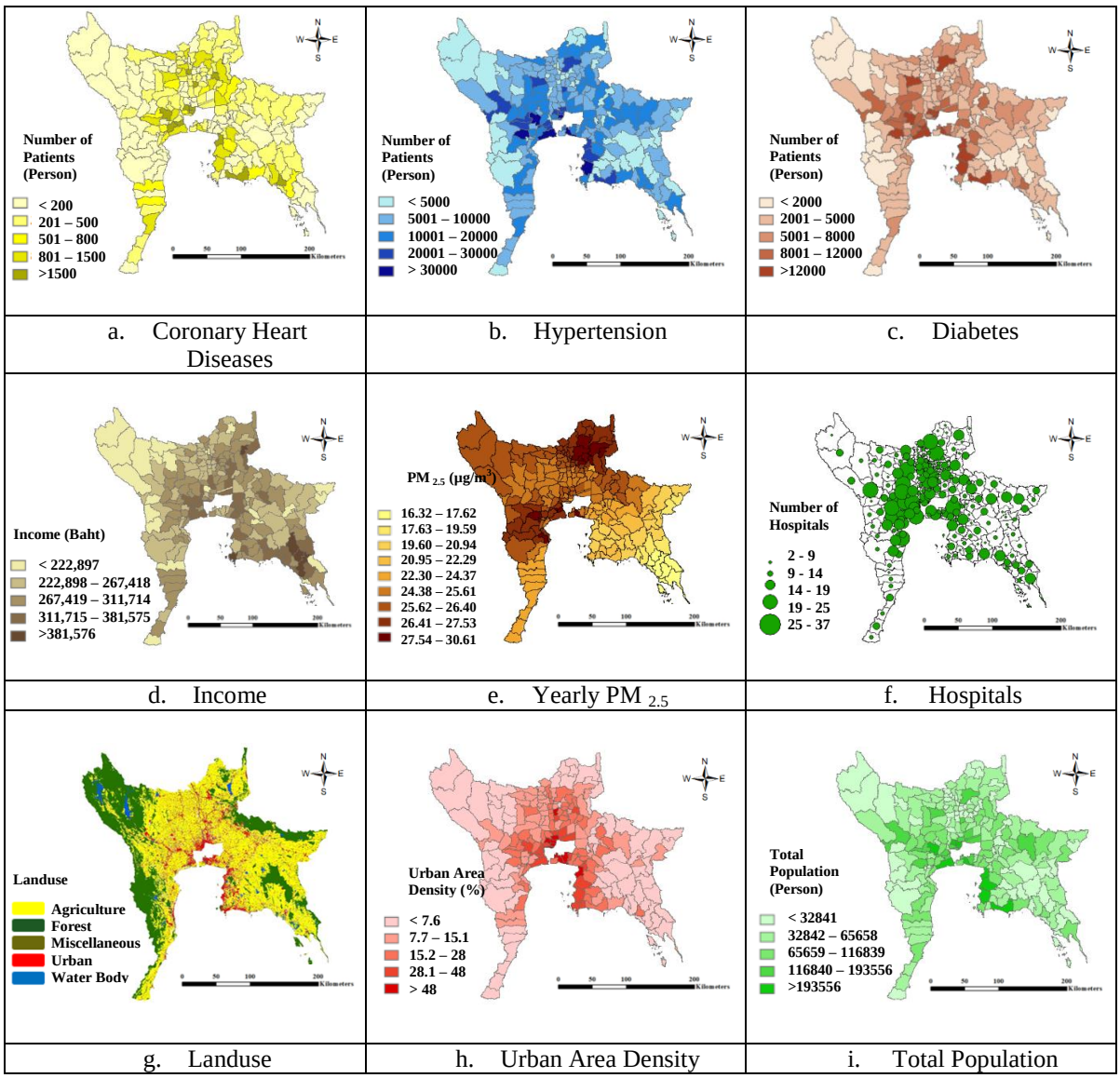

Figure 3 Maps of Spatial Distribution Patterns of NCDs and related Factors in 2023

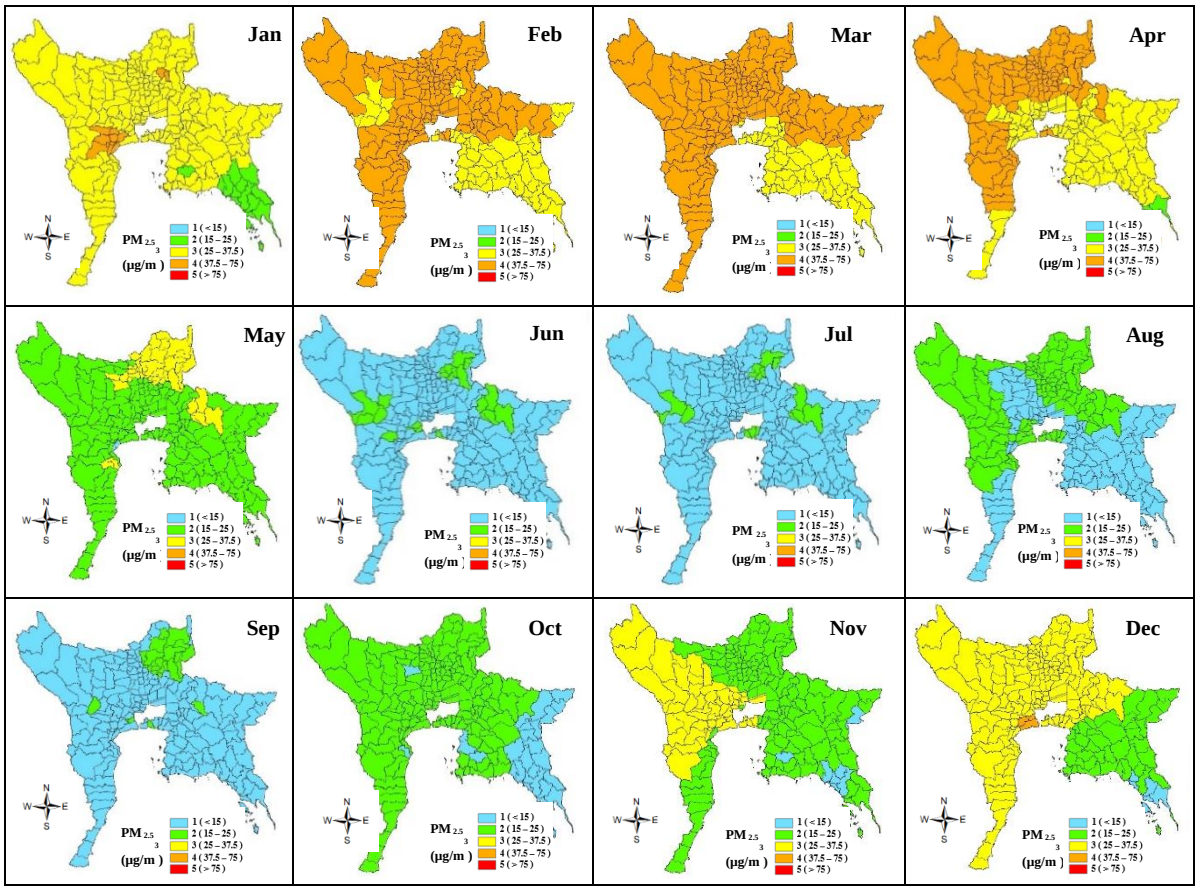

Figure 4 Maps of Spatial Distribution Patterns of Monthly $PM_{2.5}$ Value in 2023 according to AQI of PCD

The maps of spatial distribution patterns of $PM_{2.5}$ across (January, February, March, April and December) in 2023 by using IDW method were illustrated in map (a). High concentrations of $PM_{2.5}$ were shown in red while low concentrations were displayed in blue color. From IDW mapping, the worse air quality with red color occurred in some specific regions. The highest concentrations of $PM_{2.5}$ were observed in Ratchaburi, Phetchaburi, and Saraburi provinces during January to March, as indicated by red and orange pollution levels. In April, pollution levels shifted toward Suphanburi, Phetchaburi, and Kanchanaburi provinces, while in December, $PM_{2.5}$ concentrations were predominantly concentrated in Samut Sakhon, Kanchanaburi, and Ratchaburi provinces. When the months which received severe air contamination were identified, the air pollution levels which are above the standard limit of 37.5 µg/m^3 mostly happened in the months of February, March and April. In addition, the $PM_{2.5}$ values were classified into 9 classes (from 19 to 55 µg/m^3) to highlight the specific regions where suffered the worst air pollution across the months as shown in image (b). When the spatial distribution patterns of $PM_{2.5}$ in January were analyzed, it was observed that the hazardous air pollution level over 37.5 µg/m^3 was recorded in Mueang Samut Songkhram District at 45.27 µg/m^3. In February, Mueang Ratchaburi District obtained the highest polluted level of 49.55 µg/m^3. Notably, Mueang Phetchaburi District recorded the highest values in March with 58.13 µg/m^3 and in April, the highest air quality of 51.51 µg/m^3 was reached in Mueang Supanburi District. In December, Mueang Samut Sakhon District experienced the region which affected the most air pollution with 41.29 µg/m^3. Therefore, the peak air pollution which causes unhealthy conditions for the community mostly occurred in winter season and Mueang Districts of Samut Songkhram, Ratchaburi, Phetchaburi, Supanburi and Samut Sakhon in Zone 5 were significantly polluted the worse air concentrations among districts as illustrated in Figure 5.

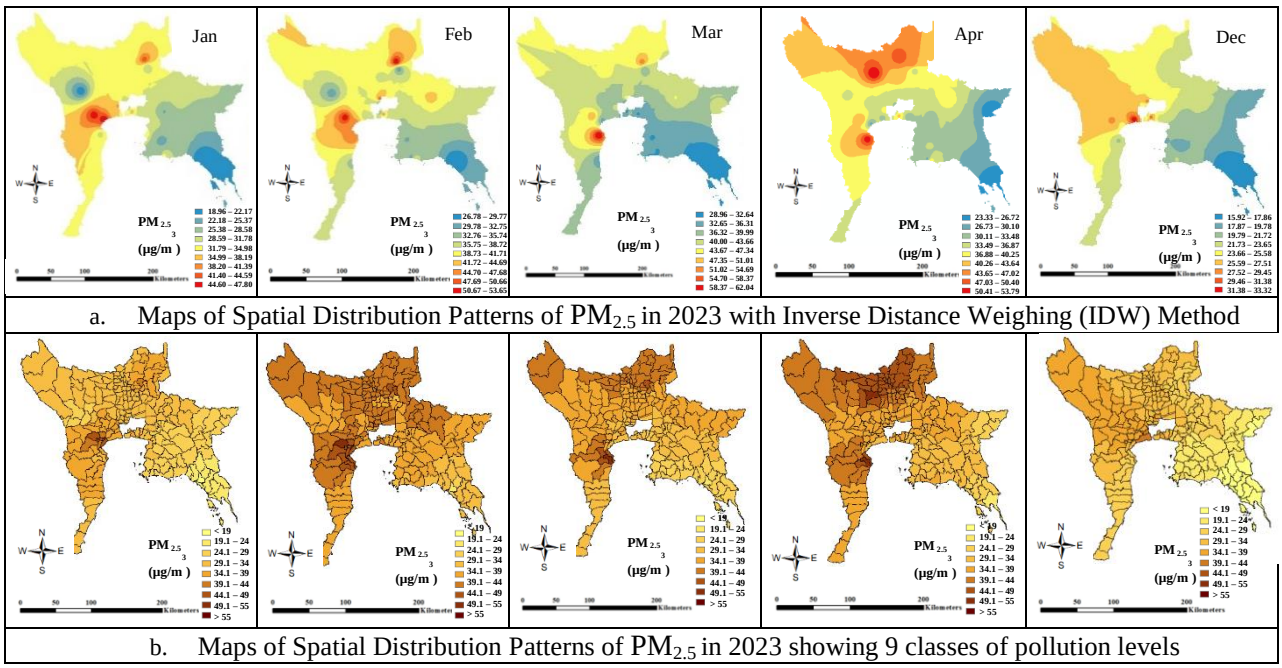

a. Maps of Spatial Distribution Patterns of $PM_{2.5}$ in 2023 with Inverse Distance Weighing (IDW) Method

b. Maps of Spatial Distribution Patterns of $PM_{2.5}$ in 2023 showing 9 classes of pollution levels

Figure 5 Maps of Spatial Distribution Patterns of $PM_{2.5}$ in 2023 showing the months which are over standard value (37.5 µg/m^3)

Correlation Analysis

Once the spatial distribution pattern of NCDs and risk factors was accomplished, the specific provinces to be focused on controlling NCDs were pointed out. Continuously, the correlation analysis was conducted to analyze the range of influence and relationship between factors. Pearson's correlation coefficient was used to assess the strength and direction of linear relationships between prevalence of NCDs and variables such as urban, aging population, $PM_{2.5}$ concentrations, income and number of hospitals. The result, with 99% confidence level with p-values less than 0.01 were considered statistically significant. The sign of correlation coefficient showed the direction of the relationship between variables and the magnitude of correlation indicated the strength of relationship. If the range is between 0.1 and 0.3, it means weak correlation. The value is from 0.3 to 0.5 which indicates moderate correlation and if it is greater than 0.5, it directs strong correlation [11]. Another study analyzed that NCDs were statistically correlated with unmodifiable risk factors which were affecting the prevalence of NCDs by surveying local population [5]. Due to this fact, a correlation analysis was carried out to understand the influence of factors statistically. According to Table 1, the number of patients who suffered hypertension exhibited a strong and statistically significant correlation with all factors (All Age Group, Number of Hospitals and Urban Area), except 2023 $PM_{2.5}$ pollution levels and income. Diabetes was high in correction with factors except $PM_{2.5}$ and income also while coronary heart diseases were highly correlated with only the working age and elderly age group. According to the detailed analysis of pollution patterns, the relationship between $PM_{2.5}$ and NCD prevalence was defined through visual spatial comparison rather than statistical analysis. Although $PM_{2.5}$ did not show a statistically significant correlation with NCD rates in this analysis, it is recommended to consider other influenced factors such as transportation-related emissions, industries, crop burning and wind direction which may impact on the pattern of air pollution. Future research should analyze multi-year air quality data and urban traffic metrics to better capture NCDs exposure patterns and environmental health implications of NCD clustering. One of the social factors –

income was low correlated with diseases, showing that income is not a strong indicator for NCDs. The observed correlation between hypertension and diabetes with both urbanization and aging experienced the role of sedentary lifestyles, unhealthy diets, and lack of green space area which tends to increase physical vulnerability among older adults in urban areas. In contrast, the weak correlation between NCD prevalence, $PM_{2.5}$ concentrations and income levels may reflect limitations in data availability and temporal assessment. As a conclude, Hypertension and Diabetes have the highest correlations across multiple factors, indicating their strong association with both population growth and aging demographics, emphasizing the need for targeted healthcare policies in urban and aging populations.

Clustered Analysis

The clustered analysis described the spatial clustering pattern that indicated the relationship of NCDs and risk factors in the study area. The cluster mapping illustrated that High-High was specifically defined as the areas surrounded by other high value. Similarly, the areas with low values surrounded by low value were described as Low-Low. High-Low means the high areas surrounded by other low values and Low-High means the low areas surrounded by high values. In this study, High-High and Low-Low clusters were considered to define the groups of regions which were affected by NCDs and risk factors. As illustrated in Figure 6, the high-high clusters of coronary heart diseases, hypertension and diabetes predominantly happened in the Bangkok Metropolitan Regions (BMR) - Nakhon Pathom, Samut Sakhon, Samut Prakan and Nonthaburi regions, demonstrating areas of a high prevalence of NCDs with similar spatial patterns while low-low cluster of diseases mostly occurred in And Thong, Ayutthaya, Chanthaburi, Chachoengsao and Kanchanaburi regions.

Compared to all diseases, the high-high clustered regions of hypertension and diabetes were more widespread than those of coronary heart diseases. Analyzing the factors, the clustered risk factors described that urban areas were predominantly concentrated in the BMR, Chonburi and Rayong, which corresponded to densely populated areas. Clustered populations who are less than 60 years were also similar pattern of urban density, but the High-High cluster pattern of elderly people was not found in Chonburi and Rayong. Therefore, the NCDs pattern was mostly influenced by the older people group. While certain red colors of $PM_{2.5}$ concentrations overlapped with urbanized and highly populated regions, one of the highly clustered groups of income – Chanthaburi province was found in the regions of low prevalence of NCDs, pollution and good air quality. When examining the link between diseases and risk factors, the high-high clustered pattern of NCDs (a, b and c) correlated with urban density (d) and aging communities (g, h and i) regions.

Table 1 Correlation of NCDs and Factors

Factors	Coronary Heart Diseases	Hypertension	Diabetes
Less than 16 years	0.495**	0.88**	0.89**
16 – 60 years	0.646**	0.929**	0.936**
Greater than 60 years	0.704**	0.951**	0.951**
No. of Hospitals	0.367**	0.708**	0.676**
Urban Areas	0.392**	0.742**	0.743**
2023 $PM_{2.5}$ Pollution Levels	-0.12	0.125	0.119
Income	0.223**	0.168*	0.174*

** Correlation is significant at the 0.01 level (2-tailed).

* Correlation is significant at the 0.05 level (2-tailed).

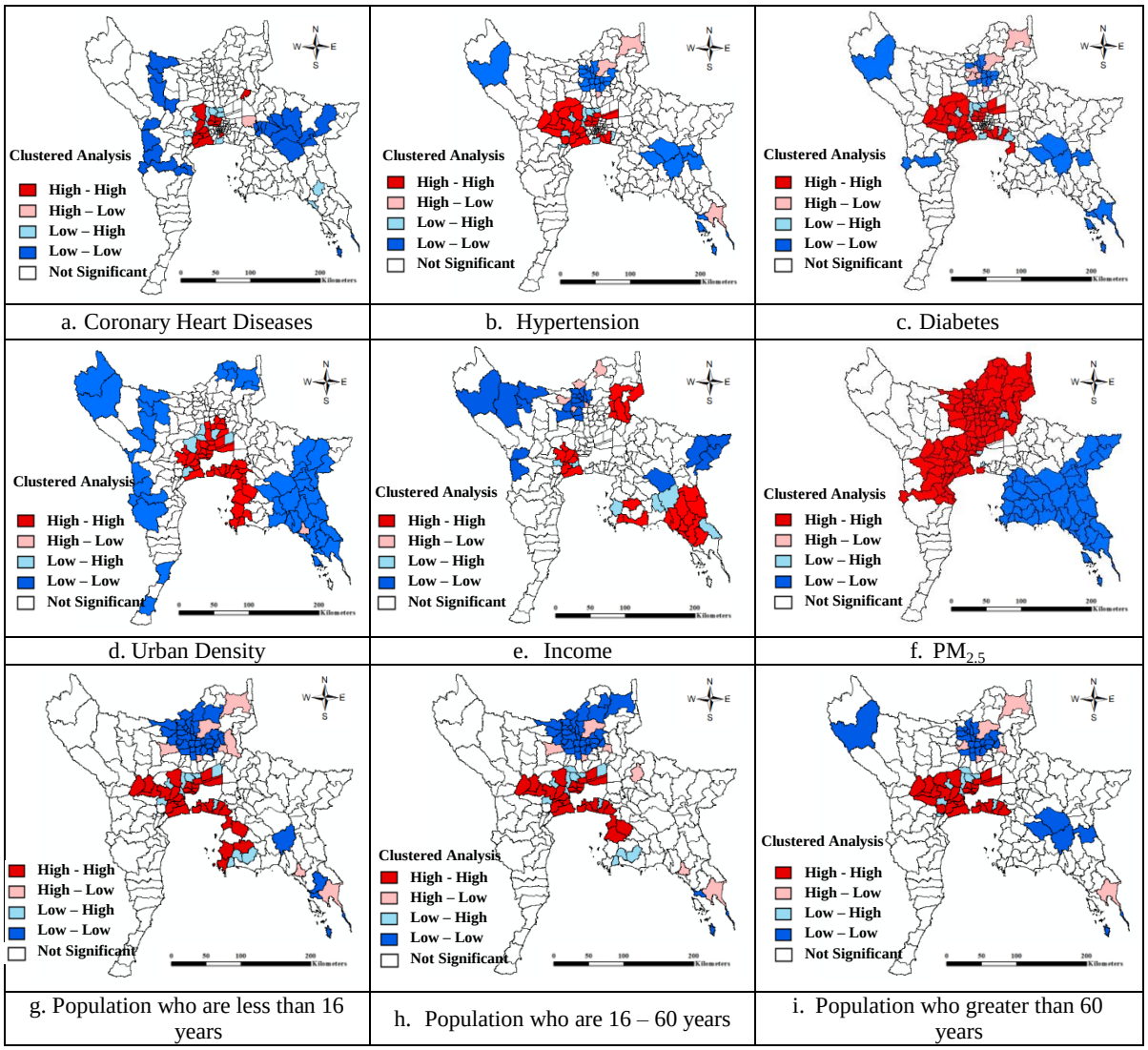

Figure 6 Maps of Cluster Analysis of NCDs and Risk Factors

Conclusions

The trend of prevalence rate of NCDs was gradually increasing so the prioritized provinces should be tackled and controlled to reduce the causes of NCDs. From this study, social factors and urban areas were mostly influenced by prevalence of NCDs and air pollution was hazardous in winter season of the year. From the findings from spatial and clustered analysis, urbanization around BMR tends to restrict green space area, leading to inadequate physical activity for aging populations which is associated with high incidence of hypertension and diabetes, therefore BMR and industrial zones should be prioritized to support the effective action plan environmentally, socially and economically. Although the study faced limitation in temporal changes between environmental and social datasets, as well as in correlation analysis, the study highlighted the utility of GIS for identifying regions at high risk of NCDs prevalence due to intense urbanization and dense populations. By integrating spatial epidemiology with environmental and demographic data, this research provided decision-support analysis for more targeted public health strategies and reinforces the importance of spatial planning in addressing the growing burden of NCDs.

Acknowledgements

The researcher would like to express gratitude to Faculty of Engineering, Mahidol University to support the precious guidance and encouragement through the journey of the research. And the author thanks the Office of the Permanent Secretary, Ministry of Natural Resources and Environment for providing GIS data and information.

References

[1] WHO. 2016. Noncommunicable Diseases. Available: https://www.who.int/news-room/fact-sheets/detail/noncommunicable-diseases. [Accessed 20 July 2024].

[2] Ministry of Public Health of Thailand, WHO, the United Nations Development Programme (UNDP), and the United Nations Inter-Agency Task Force (UNIATF). 2021. Prevention and Control of Noncommunicable Diseases in Thailand: The Case for Investment.

[3] Institute for Population and Social Research. 2023. Thai Health 2023: Thailand's Commitment in COP (Conference of Parties) & Responses to Climate Change Mahidol University. Nakhon Pathom. 14-27.

[4] WHO. 2017. Noncommunicable Diseases. Available: https://www.who.int/health-topics/noncommunicable-diseases#tab=tab. [Accessed 20 July 2024].

[5] Nawamawat, J., Prasittichok, W., Prompradit, T., et.al. 2020. Prevalence and characteristics of risk factors for non-communicable diseases in semi-urban communities: Nakhonsawan, Thailand. Journal of Health Research. 34(4): 295-303.

[6] Laohasiriwong, W., Puttanapong, N., Singsalasang, A. 2018. Prevalence of hypertension in Thailand: Hotspot clustering detected by spatial analysis. Geospatial Health. 13(1): 20-27.

[7] ESRI, Spatial Analysis in Arcgis Pro. Available: https://pro.arcgis.com/en/pro-app/latest/help/analysis/introduction/spatial-analysis-in-arcgis-pro.htm. [Accessed December 2024].

[8] HDC. Health and Medical Data Center. Available: https://hdc.moph.go.th/center/public/standard-report/3e9b22afedc152096c7caf484c7d9629/6a1fdf282fd28180eed7d1cfe0155e11. [Accessed 10 September 2024].

[9] LDD. Soil and Landuse Information Service. Available: https://dinonline.ldd.go.th/Default.aspx. [Accessed 20 October 2024].

[10] Air4Thai. Air4Thai. Available: http://air4thai.pcd.go.th/webV3/#/History. [Accessed January 2025].

[11] Kent State University. 2021. Pearson Correlation. Available: https://libguides.library.kent.edu/SPSS/PearsonCorr. [Accessed 3 Jan 2025].

Thai Environmental Engineering Journal Vol. 39 No. 1 (2025) : 81-91
www.eeat.or.th

Influence of Carbon Nanotube on Physical and Mechanical Properties of Vetiver Root Fiber-Reinforced Bioplastic Composites

Pongsathorn Kongkeaw[1*], Peerawit Pasangtiyo[2], Pichapa Lumpai[2] and Onkanya Panjumlong[2]

[1]Program of Physics, Faculty of Science and Technology, Rajabhat Maha Sarakham University, Maha Sarakham 44000, Thailand
[2]Program of Science, Faculty of Education, Rajabhat Maha Sarakham University, Maha Sarakham 44000, Thailand
[*]E-mail : pongsathorn.ko@rmu.ac.th

Article History; *Received: 31 March 2025, Accepted: 21 April 2025, Published: 30 April 2025*

Abstract

Development of sustainable bio-based materials from agricultural by-products represents a critical direction for addressing environmental challenges while supporting circular economy initiatives. This research investigates the influence of carbon nanotubes (CNTs) on the physical and mechanical properties of vetiver root fiber-reinforced polylactic acid (PLA) bio composites. A composite formulation with a 90:10 ratio of PLA to vetiver root fibers was prepared with varying concentrations of CNTs (2, 4, 6, 8, and 10% by weight). Control samples of pure PLA, PLA with vetiver fibers only, and PLA with CNTs only were also fabricated for comparative analysis. The samples were characterized by tensile strength, flexural strength, density, water absorption, thickness swelling, and thermal stability. Results revealed that pure PLA exhibited the highest tensile strength (10.37±0.88 MPa), which decreased with increasing CNT content, reaching a minimum at 6% CNTs before slightly recovering at higher concentrations. This behavior was attributed to CNT agglomeration and interfacial incompatibility between hydrophobic CNTs and hydrophilic natural fibers. Similarly, flexural properties followed comparable trends, with lowest values at 6% CNTs. Physical properties showed that density increased with CNT content, while water absorption and thickness swelling peaked at 6% CNTs before decreasing at higher concentrations. Thermogravimetric analysis demonstrated enhanced thermal stability at higher CNT loadings due to the barrier effect and improved heat distribution. This research demonstrates the potential of CNT-reinforced vetiver root fiber bio composites as environmentally friendly materials with tailorable properties for various applications.

Keywords : Composites; Carbon Nanotubes; Vetiver Root Fibers; Mechanical Properties; Thermal Stability

Introduction

Vetiver grass has a deep, strong root system that grows vertically and branches into a dense network, effectively anchoring soil, preventing erosion, and maintaining soil moisture [1, 2]. Studies on the mechanical properties of vetiver roots have shown they are strong, resistant to tensile forces and bending, highly flexible, and can withstand curvature stress well [3, 4]. These properties give vetiver roots high potential for use as reinforcement material in various composite materials, especially in the development of bio-hybrid composites that integrate natural materials with biopolymers to enhance impact resistance, reduce brittleness, and improve biodegradability while maintaining adequate mechanical strength.

Polylactic Acid (PLA) is a widely popular biopolymer used in bioplastic production, as it is made from renewable resources such as plant starch or sugar from corn, cassava, or sugarcane [5, 6]. PLA has good mechanical properties, such as high stiffness and tensile strength [7, 8]. However, PLA has significant limitations, including high brittleness, low impact resistance, and insufficient moisture resistance for use in harsh environments [9] such as temperature fluctuations [10], moisture resistance is limited [11] and UV radiation [12]. These exceptional properties make CNTs ideal reinforcement agents for addressing the inherent limitations of PLA when combined with natural fibers.

Carbon Nanotubes (CNTs) are nanomaterials with outstanding mechanical and electrical properties, extremely high strength, excellent flexibility, light weight, and good thermal and electrical conductivity [13]. Adding even a small amount of CNTs (0.1-5% by weight) to polymer composite systems can significantly improve the mechanical properties of materials [14]. CNTs function as a network for distributing forces within composite materials, reducing crack formation and propagation, and increasing the ability to withstand various forces such as tensile, compressive, and bending forces [15, 16].

The combination of natural fibers from vetiver roots with CNTs in a PLA matrix represents an innovative approach to developing eco-friendly high-performance bio composites. Literature reviews have shown that reinforcement with appropriate amounts of CNTs can increase tensile strength by up to 30-45% and elastic modulus by 15-60% compared to neat polymers [15, 17], while natural fibers help increase toughness and impact resistance of the materials [18].

This research specifically aims to develop environmentally friendly bio-hybrid composite materials. This focused application directs our research parameters and analytical approaches, allowing for more targeted investigation of the material properties required for flooring applications. By developing a composite specifically for flooring, we can establish clear performance benchmarks for mechanical strength, water resistance, and microstructure that directly inform our experimental design and manufacturing processes.

For environmentally friendly bio-hybrid composite flooring, the material must demonstrate excellent flexural properties to withstand foot traffic, low water absorption to maintain dimensional stability in varying humidity conditions, and adequate thermal stability for diverse installation environments including areas with underfloor heating systems. This application-specific development model guides our selection of CNT concentrations (2-10% by weight) and testing methodologies to optimize performance for flooring applications while maintaining environmental sustainability. This focused approach aligns with Thailand's Bio-Circular-Green Economy (BCG Model) initiative [19] and provides a clear pathway from laboratory research to commercial application in the sustainable building materials sector, promoting the utilization of local resources according to the royal initiative while offering an eco-friendly alternative to conventional flooring materials that often contain harmful chemicals and non-renewable resources.

Materials and Methods

Raw materials

(a) (b)

Figure 1 Raw materials (a) vetiver root fibers (b) SEM micrograph of CNTs

The raw materials prepared for this research included upland vetiver grass (*Vetiveria Nemoralis A. Camus*), Roi-Et variety, collected from Ban Pla Bu village, Nong Saeng sub-district, Wapi Pathum district, Maha Sarakham province, Thailand. These vetiver grasses are selected from mature plants that are approximately 3 years old, with the most suitable strength and flexibility of the fibers. The root section of the vetiver grass was used in this study as shown in Figure 1(a). The first step involved preparing and separating the vetiver root fibers by washing them with distilled water to remove soil and impurities, followed by sun-drying for 8 hours. Subsequently, the dried roots were cut using a precision cutting machine to obtain fibers with diameters ranging between 200-300 µm, widths of approximately 1-2 mm, and lengths of about 20-40 mm. The cutting process was carefully controlled to ensure consistent fiber dimensions, as larger fibers can significantly impair mechanical properties, processing efficiency, and final product quality. This precise size control is critical for achieving optimal dispersion of fibers within the polymer matrix and maintaining consistent performance in the application. In the next step, the fiber surface was modified by soaking in 0.5% by volume concentration of sodium hydroxide solution for 2 h at room temperature. The fibers were then washed with distilled water, and the water condition was verified to have a neutral pH using a pH meter. Afterward, the fibers were dried in a hot air oven at 60°C for 24 h to achieve an average moisture content of 4-13%. Meanwhile, the matrix was prepared from Polylactic Acid (PLA) supplied by GLOBAL BIOPOLYMERS, Bangkok, Thailand. The multi-walled carbon nanotubes (MWCNTs) utilized in this experimental study were of high purity (>95 wt%) with inner diameters ranging from 3-5 nm and outer diameters of 8-15 nm as shown in Figure 1(b). These nanotubes were synthesized using the Chemical Vapor Deposition (CVD) method, which is recognized for producing high-quality carbon nanostructures with controlled dimensions and properties. The MWCNTs were commercially procured from AliExpress, China, and were selected based on their dimensional consistency and high purity to ensure reliable experimental outcomes.

Preparation of Bioplastic Composite Materials

For this research, a base formulation with a ratio of 90:10 %wt between PLA and dry vetiver root fibers (moisture content 4-13%) was established. Carbon nanotubes (CNTs) were subsequently incorporated into this base mixture at varying concentrations of 2, 4, 6, 8, and 10 %wt according to the experimental conditions. Additionally, control samples were prepared for comparative analysis, consisting of pure PLA (100 %wt), PLA reinforced only with vetiver root fibers, and PLA reinforced only with CNTs, to serve as standards for comparing various properties of the composite materials. The composite materials were processed using a closed-system mixer at a temperature of 200°C for 6 min. These temperature and time parameters were optimized to ensure uniform distribution of the constituent materials, particularly the dispersion of carbon nanotubes within the polymer matrix. The selected temperature was appropriate for the melting of PLA while preventing thermal degradation of the natural fibers and carbon nanotubes. Following the mixing process, all samples were finely ground using a material grinder to produce uniform, small plastic granules suitable for subsequent injection molding.

Specimen Fabrication and Testing

The finely ground composite granules were then injection molded using an injection molding machine at 180°C to produce test specimens according to ASTM standard dimensions. The injection molding temperature was optimized to ensure proper melting and flow of the composite material without causing degradation of the components. The fabricated specimens were subjected to mechanical property testing, including tensile strength tests according to ASTM D638 standard and flexural strength tests according to ASTM D790 standard, using a universal testing machine. For physical property testing, evaluate density (ASTM D792), thickness swelling (ASTM D570), and water absorption (ASTM D1037),

which are key parameters indicating dimensional stability and moisture resistance critical for flooring materials that may be exposed to varying environmental conditions. To ensure statistical reliability, five replicate specimens were tested for each experimental condition in all mechanical and physical property tests. Thermal property testing to determine the decomposition temperature of the composite materials was conducted using Thermogravimetric Analysis (TGA), with testing temperatures ranging from 30 to 850°C to encompass the thermal decomposition range of all components in the composite materials.

Microstructural Analysis

The microstructural study of the composite materials was performed using Scanning Electron Microscopy (SEM) to analyze the adhesion characteristics between the polymer matrix and reinforcing materials, the distribution of vetiver root fibers, and the quality of carbon nanotube dispersion within the composite structure. This morphological analysis provided important information regarding the relationship between microstructural features and the observed mechanical and physical properties.

Statistical Analysis

All test data were presented as mean values with standard deviations and analyzed for statistical differences using one-way Analysis of Variance (ANOVA) at a 95 percent confidence level ($\alpha = 0.05$). One-way ANOVA was selected because our design compared multiple CNT concentration groups on single dependent variables. Data normality and variance homogeneity were verified before analysis to ensure ANOVA assumptions were met to assess the statistical significance of differences observed between experimental groups. The significance criterion was established at $p < 0.05$, which enables accurate and reliable interpretation of the influence of carbon nanotube concentration on various properties of the vetiver root fiber-reinforced bioplastic composites. Additionally, Pearson correlation analysis was performed to quantify relationships between different mechanical and physical properties.

Table 1 Physical and mechanical average values of tests performed

Sample	Density (g/cm^3)	Water absorption (%)	Thickness Swilling (%)	Tensile strength (MPa)	Tensile modulus (MPa)	Flexural strength (MPa)	Flexural modulus (MPa)
PLA 100%	0.435±0.03	4.31±0.99	4.13±0.91	10.37±0.88	208.33±8.96	0.50±0.010	5.33±0.76
PLA+ Fiber	0.543±0.05	2.06±0.09	5.18±1.05	4.55±0.73	195.50±5.63	0.16±0.046	5.00±1.32
PLA+ CNTs	0.560±0.06	5.92±1.20	7.55±1.35	9.93±0.57	202.50±6.5	0.44±0.04	5.67±0.29
CNTs 2% wt	0.424±0.07	5.00±1.07	3.23±0.63	2.27±0.51	192.83±3.51	0.15±0.02	5.17±0.58
CNTs 4% wt	0.400±0.03	4.32±1.37	5.25±0.37	1.03±0.21	196.00±8.79	0.10±0.07	3.17±1.26
CNTs 6% wt	0.691±0.11	7.3±1.05	6.34±1.69	0.88±0.06	142.50±11.5	0.04±0.00	1.83±0.76
CNTs 8% wt	0.623±0.07	3.43±0.91	3.64±0.75	2.00±0.21	151.83±16.6	0.13±0.06	5.00±0.50
CNTs 10% wt	0.740±0.18	3.74±0.45	3.11±1.28	2.21±0.18	198.33±5.03	0.11±0.01	4.50±0.87
p-value	0.002*	0.000*	0.001*	0.000*	0.000*	0.000*	0.001*

where *is significantly difference at $p<0.05$

Results and Discussion

Mechanical properties

1. Tensile test

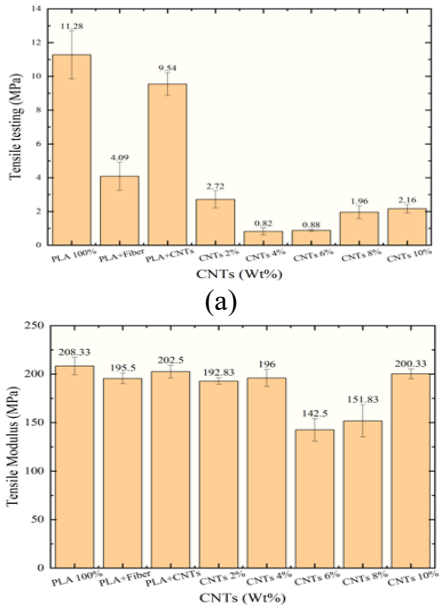

Figure 2 Tensile properties of Bioplastic composites (a) Tensile strength (b) Tensile modulus

Figure 2(a) illustrates the relationship between CNT content and tensile strength, showing a significant decreasing trend as carbon nanotube concentration increases in the composite material. Pure PLA (100%) exhibited the highest tensile strength at 11.28 MPa, followed by PLA+CNTs at 9.54 MPa. The vetiver root fiber and carbon nanotube composite (PLA+Fiber+CNTs) demonstrated a continuous decline in tensile strength with increasing carbon nanotube content, reaching its lowest value of 0.58 MPa at 6% wt CNTs. Subsequently, the tensile strength slightly increased to 1.96 MPa and 2.16 MPa at CNT concentrations of 8% wt and 10% wt, respectively. This phenomenon can be explained by the theory of carbon nanotube dispersion in polymer matrices. As described by [20], at lower CNT concentrations, nanotube dispersion in the matrix is more uniform. However, as CNT content increases, agglomeration occurs, creating defect sites within the composite structure that serve as failure initiation points when subjected to tensile forces [21]. Additionally, the reduction in tensile strength may result from the incompatibility between hydrophobic carbon nanotubes and hydrophilic vetiver root fibers, leading to interfacial voids and reduced load transfer efficiency between the matrix and reinforcing materials [22]. Nevertheless, the slight increase in tensile strength at 8% and 10% CNT content may be attributed to the formation of an interconnected network at higher concentrations, enhancing load-bearing capacity, which aligns with findings by [23] that high-concentration CNTs can form continuous networks and increase strength. Figure 2(b) demonstrates the relationship between carbon nanotube content and tensile modulus, revealing a non-linear variation with CNT concentration. Pure PLA exhibited a high tensile modulus of 208.33 MPa, while the composite materials showed relatively stable or slightly decreased modulus values at 2% and 4% CNT content (192.83 MPa and 196 MPa, respectively). However, a significant decrease occurred at 6% and 8% CNT concentrations (142.5 MPa and 151.83 MPa), before increasing again at 10% CNTs (198.33 MPa). This pattern aligns with percolation threshold theory, which explains that at a critical concentration of carbon nanotubes, significant changes in composite material behavior occur [24]. In this case, 6% CNT content may represent the percolation threshold causing structural changes within the composite, possibly due to excessive CNT agglomeration resulting in matrix discontinuity. The increase in modulus at 10% CNTs corresponds with research by [25], which found that at very high CNT concentrations, a percolated network forms throughout the matrix, improving force absorption and distribution, thereby increasing the modulus. Statistical analysis of the data in Table 1 reveals p-values less than 0.05 ($p<0.05$) for all experimental conditions, indicating statistically significant differences between group means at a 95% confidence level. The analysis confirms that pure PLA has the highest tensile strength (10.37±0.88 MPa), significantly different from all composite types. The addition of vetiver root fibers alone significantly reduced tensile strength (4.55±0.73 MPa). Furthermore, incorporating CNTs into the PLA/vetiver root

fiber system resulted in significantly lower tensile strength compared to pure PLA, though slight increases were observed at 8% and 10% CNTs concentrations.

2. Flexural test

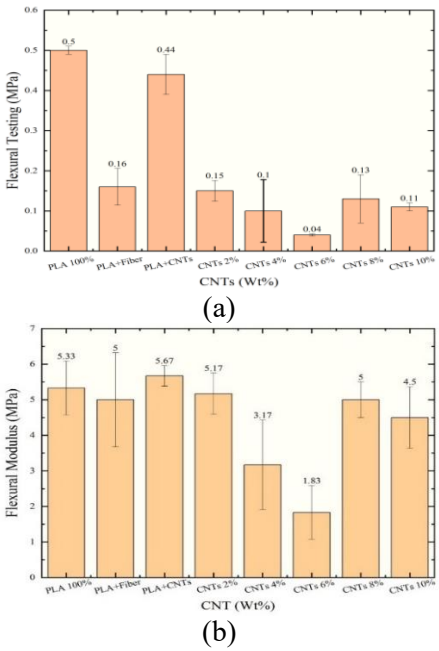

Figure 3 Flexural properties of Bioplastic composites (a) Flexural strength (b) Tensile modulus

Figure 3(a) illustrates the relationship between CNTs content and flexural strength, demonstrating a declining trend as CNTs concentration increases in the composite material. Pure PLA (100%) exhibited the highest flexural strength at 0.50 MPa, followed by PLA+CNTs at 0.44 MPa, while the composite material containing only vetiver root fibers (PLA+Fiber) showed a significantly reduced flexural strength of 0.16 MPa compared to pure PLA. When examining composite materials with various CNTs concentrations, the flexural strength showed a continuous decrease from 0.15 MPa at 2% wt CNTs to 0.10 MPa at 4% wt CNTs, reaching its lowest value of 0.04 MPa at 6% wt CNTs. Subsequently, the flexural strength slightly increased to 0.13 MPa and 0.11 MPa at CNTs concentrations of 8% wt and 10% wt, respectively. This phenomenon can be explained by theories of dispersion and interaction between component materials in composites. As [26] described, the reinforcement efficiency of carbon nanotubes depends on their dispersion and adhesion to the polymer matrix. When CNTs content increases, the likelihood of agglomeration also increases, creating stress concentration points and reducing load transfer efficiency [27].

Figure 3(b) depicts the relationship between CNTs content and flexural modulus, revealing an interesting pattern. The PLA+CNTs composite shows the highest modulus at 5.67 MPa, slightly higher than pure PLA at 5.33 MPa, while PLA+Fiber exhibits a lower modulus of 5.00 MPa compared to pure PLA. When analyzing composite materials with varying CNTs concentrations, the flexural modulus demonstrates a decreasing trend as CNT content increases from 5.17 MPa at 2% wt CNTs to 3.17 MPa at 4% wt CNTs, reaching its lowest value of 1.83 MPa at 6% wt CNTs. Subsequently, the modulus increases significantly to 5.00 MPa and 4.50 MPa at CNTs concentrations of 8% wt and 10% wt, respectively. This non-linear relationship between CNTs content and flexural modulus aligns with critical loading theory, which explains that there is critical filler content that significantly affects the mechanical properties of composite materials [28]. The increase in modulus at CNTs concentrations of 8% and 10% compared to 6% corresponds with research by [25], who found that at the percolation threshold of carbon nanotubes, an interconnected network forms throughout the matrix, enhancing the composite material's resistance to deformation, which is reflected in the increased modulus values. The mean values and standard deviations of flexural strength and flexural modulus, as shown in Table 1, reveal that the p-value for all experimental conditions is less than 0.05 ($p<0.05$), indicating that the differences between the mean values of each group are statistically significant at the 95% confidence level.

For flooring applications, flexural properties directly indicate performance under distributed loads from foot traffic and furniture. At 8-10% wt, the composites showed flexural values suitable for residential flooring applications, with recovery in properties that suggest optimization potential. The mechanical

profile at these concentrations' balances strength requirements with other beneficial properties critical for flooring performance.

Physical properties test

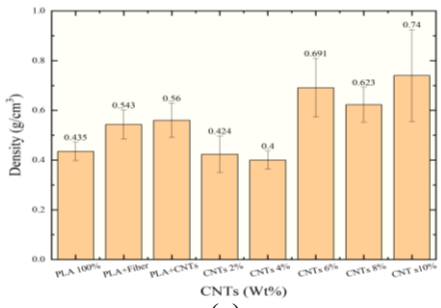

(a)

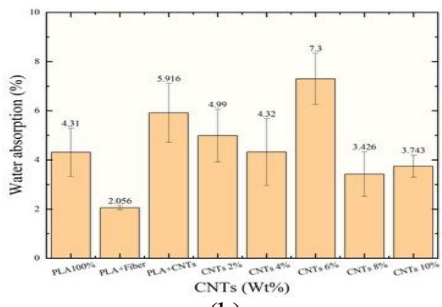

(b)

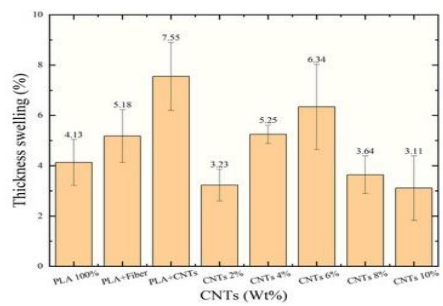

(c)

Figure 4 Physical properties of Bioplastic composites (a) Density (b) Water absorption and (c) Thickness swelling

Thermal properties test

Figure 5 presents the thermal decomposition profiles of various bioplastic composites analyzed using Thermogravimetric Analysis (TGA). All samples exhibit similar decomposition patterns, with the primary weight loss occurring in the temperature range of approximately 300-400°C, corresponding to the degradation of the PLA matrix as evidenced by the sharp drops in the weight curves and corresponding peaks in the derivative weight curves. Pure PLA (Figure 5a) shows a single-step decomposition with maximum degradation at approximately 350°C, consistent with the thermal breakdown of PLA. The PLA+Fiber composite (Figure 5b) demonstrates a slightly more complex degradation pattern, with the fiber component likely contributing to a minor secondary decomposition process. The addition of CNTs to PLA (Figure 5c) appears to maintain a thermal profile similar to pure PLA, indicating minimal interference with the polymer's thermal degradation mechanisms. When examining various CNT concentrations (Figures 5d-h), a trend emerges where higher CNT content (particularly at 8 %wt and 10 %wt, Figures 5g-h) results in slightly enhanced thermal stability, as indicated by the shifted decomposition temperatures. This improvement can be attributed to the barrier effect of well-dispersed CNTs, which impede the release of volatile degradation products and retard mass loss during heating [32]. Additionally, the high thermal conductivity of CNTs facilitates more efficient heat distribution throughout the composite, potentially delaying localized thermal degradation [33]. These results demonstrate that carbon nanotube materials can enhance the thermal stability of polymer composites.

Enhanced thermal stability at 8-10% CNT loadings is particularly beneficial for flooring installed over radiant heating systems or in areas receiving direct sunlight. The improved heat distribution properties of these composites may contribute to more comfortable walking surfaces while reducing the risk of thermal deformation. This thermal profile complements the dimensional stability advantages, creating a material well-suited to the variable environmental conditions flooring materials must withstand.

Microstructural analysis of tensile fracture surfaces provides critical insights into these mechanical behavior patterns. Figure 6 presents SEM micrographs of tensile fracture surfaces for (a) PLA+Fiber, (b) 6% CNT, and (c) 10% CNT composites. The PLA+Fiber sample shows relatively good fiber-matrix adhesion with minimal pull-out. In contrast,

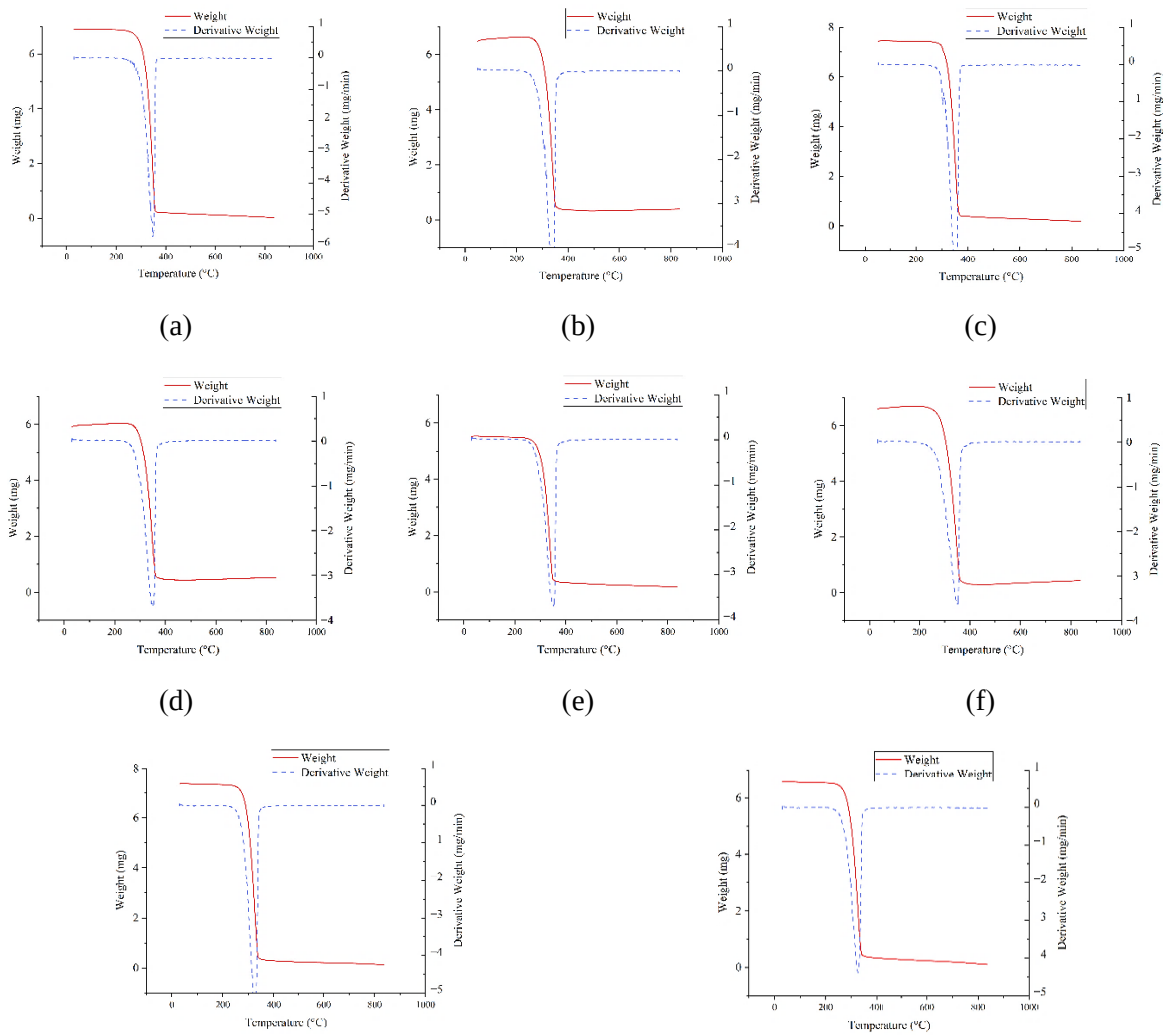

Figure 5 Decomposition temperature of Bioplastic composites (a) PLA100% wt (b) PLA+Fiber (c) PLA+CNT (d)CNT 2% wt (e) CNT4% wt (f) CNT6% wt (g) CNT8% wt (h) CNT10% wt

the 6% CNT sample exhibits significant CNT agglomeration and interfacial voids between fibers and matrix, explaining the observed mechanical property minimum. The 10% CNT sample reveals formation of a continuous CNT network bridging between fibers and matrix with improved interfacial adhesion, corresponding to the recovery in tensile properties. Similar structural features are observed in flexural fracture surfaces, confirming that CNT dispersion quality and network formation directly determine mechanical performance in these composites. Based on our comprehensive analysis, 8-10% CNT formulations provide the optimal balance for flooring applications with superior dimensional stability and thermal performance. Pure PLA and 2% CNT formulations, with higher mechanical strength, are better suited for packaging applications, while intermediate concentrations (4-6%) are not recommended for structural uses.

Microstructural analysis

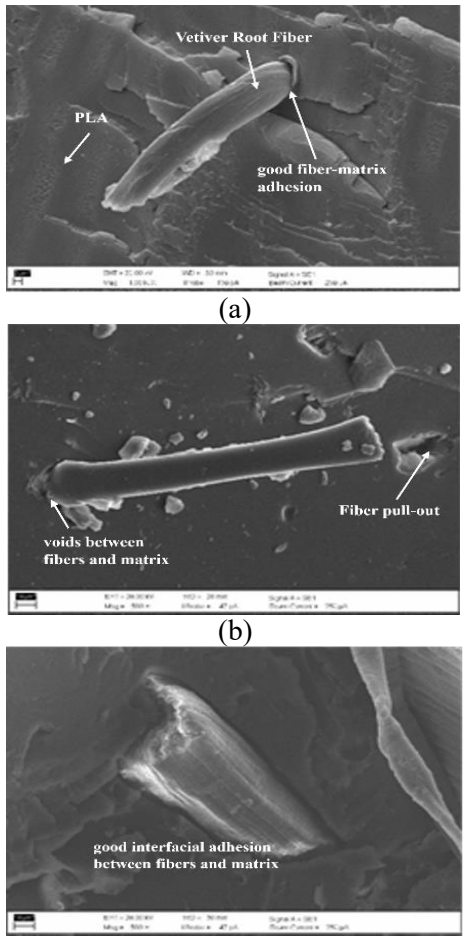

Figure 6 SEM micrographs (a) PLA+fiber at 1000x (b) PLA + fiber with 6 wt% CNT at 500x and (c) PLA + fiber with 10 wt% CNT at 500x

Conclusions

This study demonstrates that CNTs content significantly influences the properties of vetiver root fiber-reinforced PLA bio-composites developed for environmentally friendly flooring applications. The research revealed a non-linear relationship between CNTs concentration and material performance, with 6% wt CNTs representing a critical threshold where properties reached minimum values before improving at higher concentrations. Composites with 8-10% wt CNT content demonstrated the most balanced performance profile for flooring applications. While mechanical strengths were lower than pure PLA, these formulations exhibited superior dimensional stability with reduced water absorption (3.43-3.74%) and thickness swelling (3.64-3.11%), critical factors for flooring durability. The results establish specific formulation guidelines for developing sustainable bio-hybrid composite flooring from vetiver roots and CNTs that align with Thailand's Bio-Circular-Green Economy model.

Future work will expand on these findings to include electrical conductivity characterization, as the conductive nature of CNTs could provide additional functional properties such as antistatic behavior beneficial for specialty flooring applications. Preliminary testing suggests a correlation between the mechanical property threshold and electrical percolation threshold, which warrants comprehensive investigation.

Acknowledgements

The authors would like to acknowledge the financial support provided by the Science, Research and Innovation Fund, Fundamental Fund (FF.) for the fiscal year 2025.

References

[1] Gnansounou, E and Raman, J. K. 2018. A review on bioremediation potential of vetiver grass. In E. Gnansounou (Ed.), Springer Singapore: 127-140.

[2] Islam, Md. A., Islam, M. S and Elahi, T. E. 2020. Effectiveness of Vetiver Grass on Stabilizing Hill Slopes: A Numerical Approach. Geo-Congress 2020. 106-115.

[3] Jandyal, T and Shah, M. Y. 2024. An experimental investigation on the effect of vetiver grass root system on the engineering properties of soil. Life Cycle Reliability and Safety Engineering. 13(3): 335-350.

[4] Pattnaik, S. S., Behera, D., Nanda, D., Das, N and et. *al.* 2025. Green Chemistry approaches in materials science: physico-mechanical properties

and sustainable applications of grass fiber-reinforced composites. Green Chemistry. 27(10): 2629-2660.

[5] Kumari, S. V. G., Pakshirajan, K and Pugazhenthi, G. 2022. Recent advances and future prospects of cellulose, starch, chitosan, polylactic acid and polyhydroxyalkanoates for sustainable food packaging applications. International Journal of Biological Macromolecules. 221: 163-182.

[6] Taib, N.-A. A. B and et al. 2023. A review on poly lactic acid (PLA) as a biodegradable polymer. Polymer Bulletin. 80(2): 1179-1213.

[7] Bledzki, A. K., Jaszkiewicz, A and Scherzer, D. 2009. Mechanical properties of PLA composites with man-made cellulose and abaca fibres. Composites Part A: Applied Science and Manufacturing. 40(4): 404-412.

[8] Graupner, N., Herrmann, A. S and Müssig, J. 2009. Natural and man-made cellulose fibre-reinforced poly (lactic acid) (PLA) composites: An overview about mechanical characteristics and application areas. Composites Part A: Applied Science and Manufacturing. 40(6-7): 810-821.

[9] Zhao, X., Liu, J., Li, J and *et. al*. 2022. Strategies and techniques for improving heat resistance and mechanical performances of poly (lactic acid) (PLA) biodegradable materials. International Journal of Biological Macromolecules. 218: 115-134.

[10] Jiang, Y., Yan, C., Wang, K. and *et. al*. 2019. Super-Toughed PLA Blown Film with Enhanced Gas Barrier Property Available for Packaging and Agricultural Applications. Materials. 12(10): 1663.

[11] Sonjui, T and Jiratumnukul, N. (n.d.). 2014. Poly (lactic acid) organoclay nano composites for paper coating applications. In Songklanakarin J. Sci. Technol. 5(36): 535-540.

[12] Rapa, M., Darie Nita, R. N and Vasile, C. 2017. Influence of Plasticizers Over Some Physico-chemical Properties of PLA. Materiale Plastice. 54(1): 73-78.

[13] Syduzzaman, M., Islam Saad, M. S., Piam, M. F and *et. al*. 2025. Carbon nanotubes: Structure, properties and applications in the aerospace industry. Results in Materials. 25: 100654.

[14] Al-Maharma, A. Y., Sendur, P and Al-Huniti, N. 2018. Critical review of the factors dominating the fracture toughness of CNT reinforced polymer composites. Materials Research Express. 6(1): 012003.

[15] Ali, A., Koloor, S. S. R., Alshehri, A. H and *et. al*. 2023. Carbon nanotube characteristics and enhancement effects on the mechanical features of polymer-based materials and structures–A review. Journal of Materials Research and Technology. 24: 6495-6521.

[16] Mendoza Reales, O. and Dias Toledo Filho, R. 2017. A review on the chemical, mechanical and microstructural characterization of carbon nanotubes-cement based composites. Construction and Building Materials. 154: 697-710.

[17] Shan, L. 2023. The effects of nano-additives on the mechanical, impact, vibration, and buckling/post-buckling properties of composites: A review. Journal of Materials Research and Technology. 24: 7570-7598.

[18] Al-Maharma, A. Y and Sendur, P. 2018. Review of the main factors controlling the fracture toughness and impact strength properties of natural composites. Materials Research Express. 6(2): 022001.

[19] T. National Science and Technology Development Agency. Bio-Circular-Green Economy to be declared a national agenda. https://www.nstda.or.th/thaibioeconomy/138-bio-circular-green-economy-to-be-declared-a-national-agenda.html. [Accessed 31 March 2025].

[20] Ma, P.-C., Siddiqui, N. A., Marom, G and Kim, J.-K. 2010. Dispersion and functionalization of carbon nanotubes for polymer-based nanocomposites: A review. Composites Part A: Applied Science and Manufacturing. 41(10): 1345-1367.

[21] Spitalsky, Z., Tasis, D., Papagelis, K and Galiotis, C. 2010. Carbon nanotube–polymer composites: Chemistry, processing, mechanical and electrical properties. Progress in Polymer Science. 35(3): 357-401.

[22] Nurazzi, N. M., Asyraf, M. R. M., Fatimah Athiyah, S and *et.al*. 2021. A Review on Mechanical Performance of Hybrid Natural Fiber Polymer Composites for Structural Applications. Polymers. 13(13): 2170.

[23] Papageorgiou, D. G., Li, Z., Liu, M and *et.al*. 2020. Mechanisms of mechanical reinforcement by graphene and carbon nanotubes in polymer nanocomposites. Nanoscale. 12(4): 2228-2267.

[24] Sarikhani, N., Arabshahi, Z. S., Saberi, A. and *et.al*. 2022. Unified modeling and experimental realization of electrical and thermal percolation in polymer composites. Applied Physics Reviews. 9(4).

[25] Fiedler, B., Gojny, F. H., Wichmann, M. H. G and *et.al*. 2006. Fundamental aspects of nano-reinforced composites. Composites Science and Technology. 66(16): 3115-3125.

[26] Fu, S.-Y., Feng, X.-Q., Lauke, B. and Mai, Y.-W. 2008. Effects of particle size, particle/matrix interface adhesion and particle loading on mechanical properties of particulate–polymer composites. Composites Part B: Engineering. 39(6): 933-961.

[27] Thostenson, E., Li, C and Chou, T. 2005. Nanocomposites in context. Composites Science and Technology. 65(3-4): 491-516.

[28] Coleman, J. N., Khan, U., Blau, W. J and Gun'Ko, Y. K. 2006. Small but strong: A review of the mechanical properties of carbon nanotube–polymer composites. Carbon. 44(9): 1624-1652.

[29] Nilagiri Balasubramanian, K. B and Ramesh, T. 2018. Role, effect, and influences of micro and nano-fillers on various properties of polymer matrix composites for microelectronics: A review. Polymers for Advanced Technologies. 29(6): 1568-1585.

[30] Arora, B and Attri, P. 2020. Carbon Nanotubes (CNTs): A Potential Nanomaterial for Water Purification. Journal of Composites Science. 4(3): 135.

[31] Ashori, A., Sheshmani, S and Farhani, F. 2013. Preparation and characterization of bagasse/HDPE composites using multi-walled carbon nanotubes. Carbohydrate Polymers. 92(1): 865-871.

[32] Su, S. P., Xu, Y. H., China, P. R and *et. al*. 2011. Thermal degradation of polymer–carbon nanotube composites. In Polymer–Carbon Nanotube Composites: 482-510.

[33] Mohd Nurazzi, N., Asyraf, M. R. M., Khalina, A and *et.al*. 2021. Fabrication, Functionalization, and Application of Carbon Nanotube-Reinforced Polymer Composite: An Overview. Polymers. 13(7): 1047.

Thai Environmental Engineering Journal

Aims and Scope

Thai Environmental Engineering Journal is published 3 times a year by Environmental Engineering Association of Thailand in aims of provide an interdisciplinary platform for the disseminating recent research work in Environmental field. The journal's scope includes:

- Treatment Processes for Water and Wastewater
- Air Pollution and Control
- Solids and Hazardous Wastes Management
- Site Remediation Technology
- Water Resource Management; Surface water and Groundwater
- Environmental Management Protection and Conservation
- Impact Assessment of Pollution and Pollutants
- All areas of Environmental Engineering and Sciences

Frequency; 3 issues per year, every four months at April, August and December

Information for Authors

Manuscript submitted for publication should be of high academic merit and have never before, in whole or in part, been published elsewhere and will not be published elsewhere, except in abstract form. Manuscripts, parts of which have been previously published in conference proceeding, may be accepted if they contain additional material not previously published and not currently under consideration for publication elsewhere.

Submission of Manuscripts

All manuscripts should be submitted in https://www.tci-thaijo.org/index.php/teej/index

Manuscript Format and Style

Text format

Manuscript should be prepared using a text processing software such as Microsoft Word for windows. A4 size paper is conventionally accepted. Margins set up (in Page set up Menu) are outlined as follow.

Top Margin 3.0 cm., Bottom Margin 3.0 cm.
Left margin 2.5 cm., Right Margin 2.5 cm.

Title, author co-authors, address of correspondence and abstract are included in the first section while the remainder of paper is to appear in the second section. The total pages including figures, tables and references should not exceed 10 pages.

Font, font size & typeface

Times New Roman font type is required for Thai text and English text. Font size [Pica] for various text function are tabulated as follow.

Text functions	Font = Times New Roman	
	Pica Size**	Typeface
Title [English]	16 [CT]	Bold
Author & Co-authors	11 [CT]	Bold
Address of correspondence	11 [CT]	Normal
Abstract heading	12 [LRJ]	Bold
Abstract & Main Texts	11 [LJ]	Normal
Section Heading & Number*	12 [LJ]	Bold
Subsection Heading & Number	11 [LJ]	Bold

* Including "Abstract" "Acknowledgement" and "References"

** CT = Centre Text, LJ = Left Justified, LRJ = Left & Right Justified

Title

All titles of manuscript should be short and precise; long title should be condensed whenever possible (not more than 42 characters). Title should be printed with every first letter of every word capitalized, excluding prepositions and articles. Directly below the title, author should print their full names (first name then family name), address and institution. E-mail of corresponding author and between 3-5 key words should also be provided.

Abstract

Abstract should be provided on separate sheets and be not more than 300 words. International contributor who are unable to provide an abstract in Thai may submit an English abstract alone.

Style Guidelines

Units of measurement should be indicated in SI units throughout.

Tables

Tables and figures should be numbered with Arabic numerals, in order in which they are cited in the text. The table's titular heading should concisely detail the content of the table and include units of measure for all numerical data.

Format of Research Paper

The format of research paper is listed as follows:

1) Title
2) Author
3) Abstract
4) Introduction
5) Materials and Methods
6) Results and Discussion
7) Conclusions
8) References

References

The references section at the end of the manuscript should list all and only the references cited in the text in numberical order, with references given in Thai first and those in English following. In this section, the names of all authors should be provided if more than six, or the first three followed by *et. al.*

Reference to a journal article:

List all authors when six or fewer; when seven or more list only the first three (3) and add *et. al.* Titles of articles from academic journals should be listed in full and begin with a capital letter.

[1] Inthorn, D., Sidtitoon, N., Silapanuntakul, S. and Incharoensakdi, A. 2002. Sorption of mercury, cadmium and lead in aqueous solution by the use of microalgae. Science Asia. 28(3): 253-261.

Reference to article or abstract in a conference proceedings:

[1] Inthorn, D., Singhakarn, C. and Khan, E. Decolorization of reactive dyes by pre-treated Flute reed (phargmites karka (Retz)). At 34th Mid-Atlantic Industrial & Hazardous Conference, Annual Mid Atlantic Industrial and Hazardous Waste Conference at Rugers University, New Jersey, USA on September 20-21, 2002.

Reference to a book:

[1] Polprasert, C. 1996. Organic Waste Recycles. John Wiley & Sons Inc., New York.

Reference to article in a conference proceedings:

[1] Inthorn, D. Heavy metal removal. In: Kojima, H. and Lee, Y.K. Photosynthetic Microorganisms in Environmental Biotechnology, Springer-Verlag, 2001; 111-135.

Reference to an electronic data source:

Use the above format and supply the complete URL as well as the access date.

Subscription Form
Thai Environmental Engineering Journal

Date_____

Name_____

Address_____

_____

_____

_____

_____

Tel:_____ Fax:_____E-mail:_____

A subscription to the Thai Environmental Engineering Journal is request for_____year
(1,000 Baht/year for 3 Volume)

Signature_____

(_____)

Payment by "Environmental Engineering Association of Thailand"

- ❍ Bank Transfer: Savings Account No. 053-1-24040-3, Bank of Ayudhya Plc., Klong Prapa Branch
- ❍ Bank Transfer: Savings Account No. 056-2-32298-0, Siam Commercial Bank Plc., Aree Sampan Branch

Environmental Engineering Association of Thailand
122/4 Soi Rawadee, Rama VI Rd., Phayathai,
Phayathai, Bangkok 10400
Tel: +66 (0) 2617-1530-1 Fax: +66 (0) 2279-9720
E-mail: teej@eeat.or.th Website: http://www.eeat.or.th

THAI
ENVIRONMENTAL ENGINEERING JOURNAL
Environmental Engineering Association of Thailand (EEAT)

ISSN (PRINT) : 1686 - 2961
ISSN (ONLINE) : 2673 - 0359

Vol. 39 No. 1 January – April 2025